Allelic Insufficiency of Zinc Transporter 8 (*Znt8*) In Mice and Its Effect on T2D Prevention

By

YIMENG CAI
DISSERTATION

Submitted in partial satisfaction of the requirements for the degree of

DOCTOR OF PHILOSOPHY

in

Nutritional Biology

in the

OFFICE OF GRADUATE STUDIES

of the

UNIVERSITY OF CALIFORNIA

DAVIS

Approved:

_____

Liping Huang, Chair

_____

Gerardo G Mackenzie

_____

Helen Raybould

Committee in Charge

2021

Allelic Insufficiency of Zinc Transporter 8 (*Znt8*) In Mice and Its Effect on T2D Prevention

Abstract

Zinc transporter 8 (ZNT8) transports zinc from the cytoplasm into the secretory vesicle for insulin crystallization and storage in pancreatic beta-cells. Individuals with *ZNT8* allelic insufficiency have reduced risk of type 2 diabetes. However, the underlying mechanism of this protective effect is not well understood. ZNT1-10 in pancreatic islets and in β-cell lines derived from human and mice were examined using immunohistochemistry and immunofluorescence microscopic analysis. The data suggests that there are functional conservations of the ZNT proteins between humans and mice and mouse models of zinc transporters can be used for studying mechanisms of zinc-associated risks of T2D in humans. When fed a high-fat diet (45% kcal fat) for 17 weeks, male *Znt8*$^{+/-}$ mice had an improved glucose tolerance compared to the wild type mice during glucose challenge. Importantly, the total glucagon secretion assessed by the area under the curve during glucose challenge was significantly lower (~40%) in male *Znt8*$^{+/-}$ mice than the control mice. Furthermore, quantitative RT-PCR results suggested that *Znt8* mRNA expression was strongly and positively correlated with the expression of glucagon (R^2=0.75, p=2.43*10^{-4}) and *Sst* (R^2=0.8788, p=6.78*10^{-6}) in pancreatic islets. Most importantly, ZNT8 was found to colocalize with somatostatin in the mouse pylorus mucosa, but not with ghrelin, GIP, GLP1, and CCK. *Znt8* heterozygotes may be protected from high-fat-induced glucose intolerance or type 2 diabetes due to enhanced suppression of glucagon levels leading to better glycemic control. Colocalized expression of ZNT8 and somatostatin suggest a role of ZNT8 in regulating SST production and secretion, which may have an indirect impact on the rate of digestion and absorption of foods in the gut as well as the secretions of pancreatic hormones after meals. These findings would provide new research targets to uncover the role of ZNT8 in T2D development.

Contents

Chapter 1 - Zinc, zinc homeostasis and endocrine hormones as well as their influences on peripheral tissues in the pathogenesis of Type-2 diabetes

1. Introduction

Insulin resistance in peripheral tissues and dysfunction of pancreatic beta-cell are two factors which characterize Type 2 Diabetes (T2D). Additionally, dysfunction of other related hormones, for example, glucagon, growth hormone, and thyroid hormone are involved in the pathogenesis of T2D (1). Zinc is associated with insulin resistance and functions of these metabolic hormones mentioned above (2). Therefore, zinc homeostasis which is largely maintained by zinc transporters has been a research target for decades for its role in T2D development as well as in T2D prevention. In the following sections, I describe the roles of zinc and zinc transporters on production, secretion as well as function of hormones in the aspects of glucose and lipid metabolism, and satiety. In addition, I summarize the importance of zinc homeostasis in insulin sensitivity and glucose tolerance of peripheral tissues.

2. Zinc status in diabetic patients

Zinc concentration in the human pancreas is in the range of 4- 17 μM (3). However, compared to the normal pancreas, zinc levels in the diabetic pancreas reduced by 65% (4). Patients with diabetes also have reduced serum zinc concentration (5, 6), likely caused by increased zinc loss in urine (7). Higher urinary zinc loss is associated hyperglycemia which might lead to reduced tubular zinc reabsorption (8). As such, dietary zinc supplementation is thought to be beneficial for reducing risks for T2D development. Several large human cohort studies have provided scientific evidence supporting this theory, which suggest that higher zinc intake or higher plasma zinc concentration

is associated with decreased risk T2D (9, 10). Moreover, zinc supplementation has been shown to lower fasting glucose and insulin levels induced by obesity and insulin resistance in *ob*/*ob* and *db*/*db* animal models (11, 12). In diabetic patients, oral zinc supplementation can reduce blood HbA1c, total cholesterol, and low-density lipoprotein cholesterol (LDL-C) levels reducing risks of T2D- associated complications (13).

3. Zinc and endocrine hormones

3.1 Zinc functions like a hormone

Zinc has an insulin-mimetic effect on the insulin signaling pathway (Fig.1) via inhibition of protein tyrosine phosphatase (PTP1B), an enzyme which inhibits the autophosphorylation of the insulin receptor beta subunits (14, 15). PTP1B catalyzes dephosphorylation in a "ping-pong" pattern. First it binds and then quickly dephosphorylates the substrate. The enzyme is then bound by a water molecule to release the phosphate. Zinc ions binds to the region where the second step of the enzymatic reaction takes place, thus lowering the enzymatic activity of PTP1B (14). Zinc can also downregulate the phosphatase and tensin homolog protein (PTEN) gene expression probably through SALL4, a zinc-finger transcription factor, as well as causes PTEN degradation through a mechanism involving ubiquitin (16, 17). PTEN functions like a phosphatidylinositol-3,4,5-triphosphate (PIP3) phosphatase and inhibits the P13K/AKT activity, a key step in the insulin signaling pathway that regulates glucose uptake in response to insulin stimulation (18). Moreover, zinc can lower blood glucose levels by inhibiting gluconeogenesis via downregulating the gene transcription of phosphoenolpyruvate carboxykinase (PEPCK) and glucose-6-phosphatase (G6Pase) through FOXO1a transcription factor (19). PEPCK catalyzes the conversion from oxalate to phosphoenolpyruvate while G6Pase converts glucose-6-phosphate into glucose. Both

are key steps in gluconeogenesis. Furthermore, zinc can reduce blood glucose levels by enhancing glycogen synthesis via inhibition of the activities of glycogen synthase kinase beta which inactivates glycogen synthase (20). Finally, in adipocytes, zinc can suppress lipolysis in adipocytes by inactivating protein kinase A (PKA), a kinase phosphorylates and activates hormone-sensitive lipase (HSL), secondary to potentiating the insulin signaling pathway (21). Free fatty acids (FFA) are released by HSL from triaclyglycerides and are sent to other tissues for energy. It is worth noting that it is still unclear whether zinc exerts an insulin-mimetic effect independently or whether this is dependent on the presence of insulin (22).

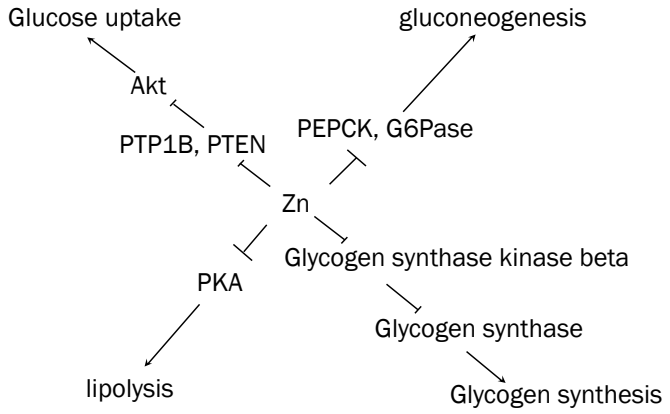

Figure 1. Zinc and its insulin-mimic effects

3.2 Zinc and insulin

Insulin is an anabolic peptide hormone secreted by pancreatic beta-cells. It promotes glucose absorption by muscle, fat and liver cells to convert to either glycogen or triaclyglycerides. It also inhibits glucose production. When insulin resistance develops, muscle, fat and liver cells have limited ability to uptake glucose, resulting in glucose accumulation in blood, which can lead to T2D. The majority of zinc (~70%) in the beta-cell is located in the insulin-containing secretory vesicles (23, 24) where two zinc molecules are bound to 6 insulin monomers forming a crystalized

structure that increases the insulin storage capacity in beta-cells (25). Zinc is secreted along with insulin into the interstitial space from beta-cells upon glucose stimulation. The secreted zinc has an autocrine effect that decreases subsequent insulin secretion (26). Subsequently, zinc is quickly reabsorbed into beta-cells by the ZIP (SLC39A) family of zinc transporters, such as ZIP6, ZIP8 and ZIP14 (27).

3.3 Zinc and glucagon

Glucagon is a catabolic peptide hormone secreted by alpha-cells of pancreas. When blood glucose is low, glucagon is secreted to signal the liver to produce glucose from glycogen, lipid and amino acids. Both fasting and glucose or arginine-induced suppression of glucagon secretion are inappropriately elevated in diabetic patients (28). Zinc is suggested to trigger glucagon secretion by co-secreting with insulin during hypoglycemia (29).

3.4 Zinc and somatostatin

Somatostatin is a peptide hormone in the digestive system (also in brain) secreted by δ-cell in the pancreas and in the gastrointestinal (GI) tract (30). In pancreas, somatostatin inhibits both insulin and glucagon secretion (31). In the GI tract, somatostatin inhibits secretion of an array of endocrine hormones including gastrin, ghrelin, GIP, GLP-1 and CCK leading to inhibited gastric acid secretion, and a decreased rate of nutrient absorption and intestinal motility (32, 33). Administration of somatostatin analogs can increase insulin sensitivity in insulin-dependent diabetic patients (34).

Bolkent et al. reported the effects of zinc supplementation in normal and diabetic rats on somatostatin cell density and oxidative stress in the gut (35). Compared to non-diabetic rats,

diabetic rats had significantly higher lipid peroxidation, lower level of glutathione GSH and more non-enzymatic glycosylation (NEG) in the stomach and the duodenum. Somatostatin-secreting cell density was higher in the stomach of diabetic than control rats. Oral gavage feeding zinc for 60 days reversed all these effects mentioned above in diabetic rats, suggesting that zinc may play a role in δ-cell function. Martin et al. investigated the effect of somatostatin combined with zinc on the regulation of glucose metabolism in diabetic dogs by somatostatin analog injections. The purpose of the study was to find out whether somatostatin with or without zinc could be a long-lasting agent to use as an adjunct to insulin for control of postprandial glucose and triglycerides (TG) levels (36). They found that when the somatostatin analog solution was supplemented with zinc, there was a 2-3-fold longer-lasting effect to decrease plasma glucose, TG, xylose and glucagon levels compared with the analog alone. It suggests that zinc has a synergic effect with somatostatin to slow the absorption of fat and carbohydrates.

3.5 Zinc and melatonin and serotonin

Melatonin is secreted by pineal gland in brain to regulate sleep-wake rhythm (37). Melatonin plays a role in glucose metabolism by binding to its receptors MT1 and MT2 in peripheral tissues, such as liver and muscle, to potentiate the insulin signaling pathway leading to increased glucose uptake and blood glucose clearance (38). Melatonin also decreases insulin secretion in beta-cells and increase glucagon secretion in alpha-cells via binding to MT1 and MT2 (39). Reduced melatonin biosynthesis in the brain induced by aging or sleep-wake inversion can cause insulin resistance and glucose intolerance (38).

Zinc correlates with serotonin secretion (40). Zinc may work as a cofactor for arylalkylamine-N-acetyltransferase (AANAT) to enhance the binding of serotonin to this enzyme

(41). AANAT is involved in the conversion of serotonin to melatonin. The acetylation of serotonin by AANAT is a key step in melatonin production. Thus, zinc is important in both serotonin and melatonin production (42).

3.6 Zinc, growth hormone and insulin-like growth factor-1 (IGF-1)

Growth hormone is secreted from the pituitary gland and can stimulate the liver to secrete IGF-1. Both hormones play a role in glucose control and insulin sensitivity. Growth hormone counteracts insulin in glucose and lipid metabolism by decreasing glucose uptake in adipose tissue, increasing gluconeogenesis and glycogenolysis as well as stimulating lipolysis (43, 44). However, in skeletal muscle tissue, growth hormone increases free fatty acids uptake by increasing the activity of lipoprotein lipase. During re-esterification, skeletal muscle cells then accumulates diacylglycerides and ceramides which potently hinder insulin-signaling pathway, which may lead to insulin resistance (45). On the other hand, IGF-1 has a hypoglycemic effect. Secreted IGF-1 can bind insulin receptor with low affinity and thus can increase insulin sensitivity in muscle (46). It has been shown that patients with T2D have reduced serum IGF-1 and increased serum growth hormone levels (47, 48).

Zinc deficiency is associated with both reduced serum growth hormone and IGF-1 levels (49, 50). In normal conditions, zinc stimulates the activity of growth hormone by binding and promoting its dimerization. This dimerization is important for hormone stability, cellular storage capacity of the hormone-secretory vesicles (51, 52). It also inhibits growth hormone to bind proximal pituitary so that growth hormone can reach peripheral targets (53). Moreover, zinc supplementation has been shown to increase serum IGF-1 levels (50). Therefore, zinc may play an

important role in modulating insulin sensitivity in the peripheral tissues through regulation of the secretion and activities of growth hormone and IGF-1.

3.7 Zinc and thyroid hormone

The thyroid hormone plays important roles in glucose and lipid metabolism. Dysregulation of thyroid hormone production and its activity is associated with risk factors of T2D (54). In general, thyroid hormone increases gluconeogenesis, lipogenesis and decreases glycogen synthesis in the liver resulting in the increase of glucose output (54). On the other hand, thyroid hormone increases glucose uptake, glycolysis, lipolysis as well as mitochondrial function in peripheral tissues leading to more energy expenditure (54). Therefore, both hyperthyroidism and hypothyroidism are risk factors for insulin resistance and T2D (54).

Zinc affects thyroid hormone level in many ways. First, it protects the structure of the follicles in the thyroid gland (55). Thyroid hormones (thyroxine T4 and triiodothyronine T3) are produced by the follicular cells that involves production of hydrogen peroxide. Cu/Zn superoxide dismutase (SOD1) is a zinc-containing enzyme which plays an important role in modulating reactive oxygen species (ROS) to help avoid oxidative stress and destruction of follicular cells (56). Second, zinc is required for the function of Type I-5' deiodinase, an enzyme responsible for the conversion of T4 to a more active form of thyroid hormone T3 in liver and kidney (57). Finally, zinc seems to maintain the active form of T3 receptor in nucleus by binding to it which indirectly increases the function of thyroid hormones (58, 59). However, the correlation between zinc and thyroid hormone is not unidirectional. There is evidence to suggest that the increased activity of thyroid hormones can upregulate the expression of ZIP10, a zinc transporter involved in zinc uptake of small intestine and kidney resulting in increased zinc absorption as well as decreased

zinc urinary excretion (60). Taken together, the data suggest that zinc is important for normal production and functions of thyroid hormones to maintain a balanced glucose and lipid metabolism.

3.8 Zinc and leptin

Leptin is produced by white adipose tissue and functions through the central nervous system (CNS) to regulate food intake and energy expenditure (61). Leptin can also modulate glucose metabolism by suppressing the glucose output from the liver, increasing glucose uptake independent of insulin, and inhibiting glucose-stimulated insulin secretion in the pancreas (61). Studies have been shown that serum zinc levels are often reduced in obese and T2D patients while blood leptin levels are high (62). It has been shown that zinc deficiency promotes leptin production in the adipose tissue (63) and high serum leptin levels are positively correlated to fasting insulin levels and insulin resistance (64).

4. Zinc transporters and endocrine hormones

Zinc homeostasis is maintained primarily by two transporter families, namely the zinc importers (ZRT- and IRT-like proteins or ZIPs) and the zinc transporters (ZNTs). ZIPs (ZIP1-14) which are responsible for zinc uptake to increase zinc concentrations in the cytosol (65), while ZNTs (ZNT1-10) are involved in zinc export or cellular sequestration leading to a decrease in zinc concentrations in the cytoplasm (66). Additionally, zinc can bind to small molecular proteins, such as metallothioneins (MTs), to chelate free zinc to avoid zinc toxicity and meanwhile to serve as a reservoir for zinc in the cytosol (67). Moreover, it has been shown that the voltage-gated calcium

channels (VGCCs) can transport zinc intracellularly along with calcium under glucose stimulation that triggers insulin secretion in beta-cells (68).

4.1 Zinc transporter 8 (ZNT8) and insulin

ZNT8 is predominantly expressed in the beta-cells of the pancreas. It is localized on the membrane of the secretory vesicles which transports zinc from the cytoplasm to the insulin-secreting vesicles (69). ZNT8 has six transmembrane domains with its N- and C-terminus both located in the cytosolic side of the secretory vesicle (69). Several genome-wide association studies (GWAS) have identified a single nucleotide polymorphism (SNP) in the C-terminus of ZNT8 (R325W) confers to a risk of T2D (70). The R325 risk allele is associated with ~18% increase in risk of T2D. It is found that R325 carriers have increased proinsulin to insulin conversion during oral glucose tolerance test (71, 72). Oral as well as intravenous glucose-stimulated insulin secretion are decreased along with higher fasting glucose and impaired beta-cell function assessed by homeostasis model on beta-cell function (HOMA-B) in R325 carriers (72, 73). A study conducted by Merriman et al. suggests the R325 variant, the risk allele of ZNT8, is more active than the W325 variant (74) resulting in an unbalanced cellular zinc distribution in human islets (75).

Interestingly, subsequent GWAS studies have identified 12 nonsense mutations in ZNT8 that lead to variants of ZNT8 truncated in different lengths (76). People who carry one allele of the nonsense mutation are 65% less likely to have T2D than those with two alleles of wild type ZNT8 (76). Since the finding of the association of the ZNT8 SNP and mutations with T2D risks, *Znt8* KO mouse models have been established, including global and beta-cell-specific KO mice, to study the metabolic link between ZNT8 and beta-cell function in glucose control (77–82). Since zinc is a key mineral for insulin crystallization and ZNT8 is the major zinc transporter for the secretory vesicles in beta-cells, one would expect that the null-mutations of *Znt8* in mice could

negatively affect insulin crystallization in the insulin-containing vesicle. As expected, electron microscopy reveals abnormal 'rod-shaped' or gray cores instead of dense cores in the insulin-secreting vesicles of *Znt8* KO mice (77, 81, 82). However, the abnormality in the insulin crystallization seems to have limited effect on glucose metabolism when mice are maintained on regular chow diets. Instead, risk in development of glucose intolerance in *Znt8* KO mice is highly dependent on the environmental or genetic factors, such as fat percentage in diets, mouse strains or knockout strategy (cell-specific or global) (77–80, 82, 83). In summary, both global and beta-cell-specific *Znt8* KO can result in decreased zinc concentrations in the islets or the beta-cell as well as a reduced insulin secretion after glucose stimulation (78, 79, 81, 82).

It has been suggested that the amyloid precursor protein (IAPP) may play a role in mediating the protective phenotypes of ZNT8 allelic insufficiency in humans (84). Unlike rodent IAPP, human IAPP is prone to form oligomers which could trigger beta-cell apoptosis (85). In the beta-cells with ZNT8 allelic insufficiency or the W325 allele, more insulin monomers are expected in the cell due to less expression of ZNT8 or less transporter activity of the protein. With more insulin monomers available to bind to IAPP in the lower zinc concentration condition, IAPP is less prone to form toxic oligomers and beta-cell death leading to lower risk of T2D (86).

It has been shown in mice that the zinc secretion accompanied with insulin after glucose stimulation can subsequently decrease insulin clearance from the liver via inhibition of insulin endocytosis mediated by clathrin (87). Thus, reduced zinc secretion induced by *Znt8*KO in beta-cells indirectly enhances the insulin clearance after glucose stimulation, which might be the causal factor for the reduced peripheral insulin level despite augmented insulin secretion from beta-cells (83). In these *Znt8* beta-cell specific KO mice, c-peptide/insulin ratio is increased and glucose tolerance is mildly impaired (83).

4.2 Other zinc transporters related to beta-cell health, insulin secretion and its function

Although ZNT8 is predominantly expressed in the beta-cells, other ZNT proteins have also been detected. For example, ZNT5 and ZNT7. ZNT5 is expressed in the insulin-secretory vesicles suggesting a role in transporting zinc from the cytoplasm into the vesicles (88). ZNT7 resides on the membrane of the Golgi apparatus of the beta-cells and is found to regulate basal insulin secretion possibly by modulating insulin gene transcription by MTF1 (metal-responsible transcription factor 1) (89). Other zinc transporters, especially the ZIP family of zinc transporters, are also expressed in the beta-cells. ZIP6 and ZIP7 function to uptake zinc under basal condition and reuptake zinc after glucose stimulation (90). They are involved in insulin secretion via positively affecting insulin exocytosis and controlling oxidative stress in islet cells by regulating cellular zinc levels in both the cytosolic and specific subcellular compartments (90). ZIP7 can serve as a 'gatekeeper' for zinc release from the endoplasmic reticulum (ER) and Golgi apparatus to the cytosol (91). Lack of ZIP7 leads to accumulation of zinc in the ER causing ER stress leading to pancreatic beta-cells which is a key etiological reason of T2D (92, 93). In addition, ZIP7 expression is positively correlated to levels of insulin receptor and its substrates 1 and 2 (IRS1 and IRS2) as well as activation of GLUT4 and the glycogen branching enzyme leading to increased blood glucose clearance (94).

4.3 ZNT8 and glucagon

ZNT8 is also expressed in the pancreatic alpha-cells and may play a role in regulation of glucagon secretion (95). The biological effect of ZNT8 on glucagon secretion has been studied using knockout mice, including both alpha-cell-specific and global knockouts, as well as transgenic mice (95, 96). Solomou et. al. reported that mice with a fractional alpha-cell-specific depletion of Znt8

expression (~15%, αZnt8KO) had normal glucose tolerance compared to the control when mice were fed a regular laboratory chow diet (95). However, these mice had enhanced glucagon secretion during hypoglycemic clamps. Likewise, islets isolated from αZnt8KO mice secreted more glucagon than the control when stimulated at a lower glucose concentration (1 mM) without a change in the total alpha-cell-associated glucagon contents. Correspondingly, mice over-expressing human ZNT8 in alpha-cells (αZnT8Tg) had unchanged alpha-cell-associated glucagon contents, but glucagon secretion was reduced (96). *In vitro* studies using isolated islets from αZnT8Tg mice showed a decrease in glucagon secretion at 1 mM of glucose but no changes in glucagon secretion was observed in the presence of a high glucose level at 17 mM. Collectively, these results highlight an important physiological role of ZnT8 in the regulation of glucagon secretion from alpha-cells during fasting.

5. Zinc, zinc homeostasis and peripheral tissues

5.1 Adipose tissues

ZIP14 can inhibit the Janus Kinases-signal transducer and activator of transcription proteins (JAK-STAT) signaling pathway and nuclear factor-Kappa B (NF-κB) signaling pathway (97). Activations of these pathways are associated with upregulated cytokine production like interleukin-6 (IL-6) and tumor necrosis factor-alpha (TNF-α). Leptin production and secretion is also upregulated by the JAK-STAT activation. Prolonged inflammation and enhanced leptin production in the adipose tissues are known contributors to insulin resistance and T2D development.

A beneficial role of ZIP14 has also been noted in a human study. It is found that obese subjects have significantly less *ZIP14* gene expression in fat tissue than non-obese individuals and

its level is significantly increased after weight loss (98). ZIP14 is also associated with adipocyte differentiation possibly through regulation of the PPARγ gene (98, 99).

Beige adipocytes are originated from the beige precursors or white adipocytes which are induced by certain external factors like chronic cold temperature exposure, exercise or PPARγ agonists in humans (100). Beige adipocytes are similar to the brown adipocytes which are thermogenic. ZIP13 is found to inhibit beige adipocyte differentiation by inhibiting CCAAT/enhancer binding protein-β (C/EBP-beta) function, a transcription factor that works with PRDM16 (PR domain containing 16), to determine the browning of adipocytes (101). *Zip13* KO mice are resistant to diet-induced glucose and insulin tolerance possibly by increased energy expenditure (101). Thus, ZIP13 might be a potential target for fighting against obesity-induced diabetes.

ZNT7 expression is positively associated with differentiation of adipocytes and may mediate lipogenesis through activating Akt and Erk1/2 (102). *Znt7* KO mice has lean phenotype and affects lipogenesis in fat tissue also by inhibiting basal and insulin-stimulated glucose uptake (103).

5.2 Muscle

Glucose uptake in muscle has been shown to be related with both ZIP7 (104) and ZNT7 (105). Both zinc transporters can affect the expression of the insulin receptor and insulin receptor substrate genes as well as the activation of AKT, the key components in the insulin signaling pathway (104, 105). Therefore, the expression or activation of ZIP7 and ZNT7 influence glucose uptake upon insulin stimulation and is linked to risks of insulin resistance in muscle and T2D.

5.3 Liver

Pancreatic A2 phospholipase (PLA2) is a zinc-dependent enzyme that is involved in the absorption of essential fatty acids, alpha linolenic acid (ALA) and linoleic acid (LA), in the small intestine (106, 107). Zinc binds to PLA2 and activates it (106). ALA and LA can then be desaturated by the delta 6 desaturase (FADS6) to produce long-chain polyunsaturated fatty acids 9 (PUFAs), a biosynthetic step that requires zinc works as a cofactor (108). Zinc deficiency lowers the expression of FADS6 (109). Low levels of PUFA is related to an increased triglycerides secretion in the liver leading to dyslipidemia (110).

In the hepatocytes, zinc can bring up lipolysis, lipophagy and beta-oxidation resulting in reduced lipid deposition (111). Increased cytosolic free zinc concentrations in the hepatocyte promotes the activity of the Ca^{2+}/CaMKKβ/AMPK signaling pathway that upregulates autophagy and lipid turnover (111). Moreover, zinc can also stimulate the activity of MTF-1 which in turn bind to the promoter of PPARα to induce the expression of PPARα (111). Subsequently, PPARα activates the transcriptional expression of its target genes related to autophagy and lipolysis (111).

ZIP14 could suppress phosphodiesterase (PDE) activity which is important for cAMP level and subsequent gene expression important for gluconeogenesis such as G6pase (112). *ZIP14* KO mice show hyperinsulinemia and greater fat deposit partly due to impaired gluconeogenesis and glycolysis as well as increased glycogen synthesis in the liver (113).

6. Conclusion

Given the fact that lower serum zinc levels are present in T2D patients and zinc deficiency negatively affects production of many metabolically related hormones and their actions, one would predict that zinc plays a crucial role in the development of metabolic diseases, including T2D.

Indeed, zinc is related to metabolically related hormones in many ways ultimately affecting insulin levels and glucose metabolism related to development of T2D. For example, zinc itself has an insulin-mimic effects which lowers blood glucose level. Zinc is involved in normal secretion of the pancreatic hormones, insulin and glucagon, which are two major endocrine hormones in the glycemic control. Zinc play roles in melatonin production, growth hormone stability, as well as thyroid hormone production and function. Moreover, zinc is also correlated with somatostatin in gut delta-cells, NPY transcription and leptin production. Abnormalities in production, secretion and function of these hormones can lead to glucose intolerance and insulin resistance.

Cellular zinc concentration is tightly regulated by the zinc transporter families. Zinc transporters ZNT5, ZNT7, ZNT8 and zinc importers ZIP6 and ZIP7 are either linked to beta-cell health, or basal and glucose-stimulated insulin secretion. ZNT8 is also found to regulate glucagon secretion.

Zinc homeostasis in fat, muscle and liver is crucial in maintaining glucose tolerance and insulin sensitivity. In fat tissues, ZIP14 can reduce prolonged inflammation and leptin production in adipocytes. ZIP13 negatively impacts differentiation of beige adipocytes which are a type of thermogenic adipocyte. Moreover, ZNT7 is positively related to differentiation of white adipocytes and affects lipogenesis. In muscle, both ZIP7 and ZNT7 enhance insulin stimulated glucose uptake. In the liver, zinc can reduce lipid deposition. ZIP14 in the liver can mediate gluconeogenesis and glycolysis.

Therefore, maintaining zinc homeostasis is a critical research target in preventing and treatment of T2D for its role in normal hormonal function and their influences on peripheral tissues.

References

1. Alrefai, H., Allababidi, H., Levy, S., and Levy, J. (2002) The endocrine system in diabetes mellitus. *Endocrine*. **18**, 105–119
2. Kasim Baltaci, A., Mogulkoc, R., and Bugra Baltaci, S. (2019) *The role of zinc in the endocrine system*
3. Raimondo, M., Pungpapong, S., Scolapio, J. S., Woodward, T. A., and Wallace, M. B. Is Zinc Concentration in Pancreatic Fluid a Marker for Pancreatic Diseases? *JOP. J. Pancreas*
4. Scott, D. A., and Fisher, A. M. (1938) The insulin and the zinc content of normal and diabetic pancreas. *J. Clin. Invest.* **17**, 725–728
5. Garg, V. K., Gupta, R., and Goyal, R. K. (1994) Hypozincemia in diabetes mellitus. *J. Assoc. Physicians India*. **42**, 720–721
6. Basaki, M., Saeb, M., Nazifi, S., and Shamsaei, H. A. (2012) Zinc, copper, iron, and chromium concentrations in young patients with type 2 diabetes mellitus. *Biol. Trace Elem. Res.* **148**, 161–164
7. el-Yazigi, A., Hannan, N., and Raines, D. A. (1993) Effect of diabetic state and related disorders on the urinary excretion of magnesium and zinc in patients. *Diabetes Res. (Edinburgh, Lothian)*. **22**, 67–75
8. Chausmer, A. B. (1998) Zinc, insulin and diabetes. *J. Am. Coll. Nutr.* **17**, 109–115
9. Sun, Q., Van Dam, R. M., Willett, W. C., and Hu, F. B. (2009) Prospective study of zinc intake and risk of type 2 diabetes in women. *Diabetes Care*. **32**, 629–634
10. Shan, Z., Bao, W., Zhang, Y., Rong, Y., Wang, X., Jin, Y., Song, Y., Yao, P., Sun, C., Hu,

F. B., and Liu, L. (2014) Interactions between zinc transporter-8 gene (SLC30A8) and plasma zinc concentrations for impaired glucose regulation and type 2 diabetes. *Diabetes*. **63**, 1796–1803

11. Begin-Heick, N., Dalpe-Scott, M., Rowe, J., and Heick, H. M. C. (1985) Zinc supplementation attenuates insulin secretory activity in pancreatic islets of the ob/ob mouse. *Diabetes*. **34**, 179–184
12. Simon, S. F., and Taylor, C. G. (2001) Dietary Zinc Supplementation Attenuates Hyperglycemia in db/db Mice. *Exp. Biol. Med.* **226**, 43–51
13. Jayawardena, R., Ranasinghe, P., Galappatthy, P., Malkanthi, R. L. D. K., Constantine, G. R., and Katulanda, P. (2012) Effects of zinc supplementation on diabetes mellitus: A systematic review and meta-analysis. *Diabetol. Metab. Syndr.* **4**, 13
14. Bellomo, E., Massarotti, A., Hogstrand, C., and Maret, W. (2014) Zinc ions modulate protein tyrosine phosphatase 1B activity. *Metallomics*. **6**, 1229–1239
15. Seely, B. L., Staubs, P. A., Reichart, D. R., Berhanu, P., Milarski, K. L., Saltiel, A. R., Kusari, J., and Olefsky, J. M. (1996) Protein tyrosine phosphatase 1B interacts with the activated insulin receptor. *Diabetes*. **45**, 1379–1385
16. Wu, W., Wang, X., Zhang, W., Reed, W., Samet, J. M., Whang, Y. E., and Ghio, A. J. (2003) Zinc-induced PTEN protein degradation through the proteasome pathway in human airway epithelial cells. *J. Biol. Chem.* **278**, 28258–28263
17. Lu, J., Jeong, H., Kong, N., Yang, Y., Carroll, J., Luo, H. R., Silberstein, L. E., Ma, Y., and Chai, L. (2009) Stem cell factor SALL4 represses the transcriptions of PTEN and SALL1 through an epigenetic repressor complex. *PLoS One*. 10.1371/journal.pone.0005577

18. Maehama, T., and Dixon, J. E. (1998) The tumor suppressor, PTEN/MMAC1, dephosphorylates the lipid second messenger, phosphatidylinositol 3,4,5-trisphosphate. *J. Biol. Chem.* **273**, 13375–13378

19. Cameron, A. R., Anil, S., Sutherland, E., Harthill, J., and Rena, G. (2010) Zinc-dependent effects of small molecules on the insulin-sensitive transcription factor FOXO1a and gluconeogenic genes. *Metallomics*. **2**, 195–203

20. Ilouz, R., Kaidanovich, O., Gurwitz, D., and Eldar-Finkelman, H. (2002) Inhibition of glycogen synthase kinase-3β by bivalent zinc ions: Insight into the insulin-mimetic action of zinc. *Biochem. Biophys. Res. Commun.* **295**, 102–106

21. Nakayama, A., Hiromura, M., Adachi, Y., and Sakurai, H. (2008) Molecular mechanism of antidiabetic zinc-allixin complexes: Regulations of glucose utilization and lipid metabolism. *J. Biol. Inorg. Chem.* **13**, 675–684

22. Norouzi, S., Adulcikas, J., Sohal, S. S., and Myers, S. (2017) Zinc transporters and insulin resistance: Therapeutic implications for type 2 diabetes and metabolic disease. *J. Biomed. Sci.* 10.1186/s12929-017-0394-0

23. Hutton, J. C., Penn, E. J., and Peshavaria, M. (1983) Low-molecular-weight constituents of isolated insulin-secretory granules. Bivalent cations, adenine nucleotides and inorganic phosphate. *Biochem. J.* **210**, 297–305

24. Chabosseau, P., and Rutter, G. A. (2016) Zinc and diabetes. *Arch. Biochem. Biophys.* 10.1016/j.abb.2016.05.022

25. Dunn, M. F. (2005) Zinc-ligand interactions modulate assembly and stability of the insulin hexamer - A review. in *BioMetals*, pp. 295–303, **18**, 295–303

26. Ferrer, R., Soria, B., Dawson, C. M., Atwater, I., and Rojas, E. (1984) Effects of Zn2+ on

glucose-induced electrical activity and insulin release from mouse pancreatic islets. *Am. J. Physiol.* **246**, C520-7

27. Huang, L. (2014) Zinc and its transporters, pancreatic β-cells, and insulin metabolism. in *Vitamins and Hormones*, pp. 365–390, Academic Press Inc., **95**, 365–390
28. Unger, R. H., Aguilar-Parada, E., Müller, W. A., and Eisentraut, A. M. (1970) Studies of pancreatic alpha cell function in normal and diabetic subjects. *J. Clin. Invest.* **49**, 837–848
29. Zhou, H., Zhang, T., Harmon, J. S., Bryan, J., and Robertson, R. P. (2007) Zinc, not insulin, regulates the rat α-cell response to hypoglycemia in vivo. *Diabetes*. **56**, 1107–1112
30. Arimura, A., Sato, H., Dupont, A., Nishi, N., and Schally, A. V. (1975) Somatostatin: Abundance of immunoreactive hormone in rat stomach and pancreas. *Science (80-.).* **189**, 1007–1009
31. Koerker, D. J., Ruch, W., Chideckel, E., Palmer, J., Goodner, C. J., Ensinck, J., and Gale, C. C. (1974) Somatostatin: Hypothalamic inhibitor of the endocrine pancreas. *Science (80-.).* **184**, 482–484
32. Mani, B. K., and Zigman, J. M. (2015) A strong stomach for somatostatin. *Endocrinology*. **156**, 3876–3879
33. Krejs, G. J. (1986) Physiological role of somatostatin in the digestive tract: Gastric acid secretion, intestinal absorption, and motility. *Scand. J. Gastroenterol.* **21**, 47–53
34. Orskov, L., Møller, N., Bak, J. F., Pørksen, N., and Schmitz, O. (1996) Effects of the somatostatin analog, octreotide, on glucose metabolism and insulin sensitivity in insulin-dependent diabetes mellitus. *Metabolism.* **45**, 211–7
35. Bolkent, S., Bolkent, S., Yanardag, R., Mutlu, O., and Yildirim, S. (2006) Alterations in

somatostatin cells and biochemical parameters following zinc supplementation in gastrointestinal tissue of streptozotocin-induced diabetic rats. *Acta Histochem. Cytochem.* **39**, 9–15

36. Martin, C., Wallum, B., Krom, B., Hall, L., and Gerich, J. (1984) Effect of a zinc phosphate suspension of a long-acting somatostatin analog on postprandial plasma glucose, triglyceride and glucagon concentrations in alloxan diabetic dogs. *Life Sci.* **35**, 2627–2633

37. Brown, G. M. (1994) Light, melatonin and the sleep-wake cycle. *J. Psychiatry Neurosci.* **19**, 345

38. Dragoi, C. M., Arsene, A. L., Dinu-Pirvu, C. E., Dumitrescu, I. B., Popa, D. E., Burcea-Dragomiroiu, G. T. A., Udeanu, D. I., Timnea, O. C., Velescu, B. S., and Nicolae, A. C. (2017) Melatonin: A Silent Regulator of the Glucose Homeostasis. in *Carbohydrate*, InTech, 10.5772/66625

39. Peschke, E., Bähr, I., and Mühlbauer, E. (2013) Melatonin and pancreatic islets: Interrelationships between melatonin, insulin and glucagon. *Int. J. Mol. Sci.* **14**, 6981–7015

40. Gill, C. H., Peters, J. A., and Lambert, J. J. (1995) An electrophysiological investigation of the properties of a murine recombinant 5-HT3 receptor stably expressed in HEK 293 cells. *Br. J. Pharmacol.* **114**, 1211–1221

41. Peuhkuri, K., Sihvola, N., and Korpela, R. (2012) Dietary factors and fluctuating levels of melatonin. *Food Nutr. Res.* **56**, 17252

42. Turgut, M., Yenisey, C., Akyüz, O., Ozsunar, Y., Erkus, M., and Biçakçi, T. (2006) Correlation of serum trace elements and melatonin levels to radiological, biochemical, and

histological assessment of degeneration in patients with intervertebral disc herniation. *Biol. Trace Elem. Res.* **109**, 123–34

43. Möller, N., Jorgensen, L., Ahildgard, N., Orskov, L., Schmitz, O., and Christiansen, J. (1991) *Effects of Growth Hormone on Glucose Metabolism*

44. Kim, S.-H., and Park, M.-J. (2017) Effects of growth hormone on glucose metabolism and insulin resistance in human. *Ann. Pediatr. Endocrinol. Metab.* **22**, 145–152

45. Vijayakumar, A., Yakar, S., and LeRoith, D. (2011) The intricate role of growth hormone in metabolism. *Front. Endocrinol. (Lausanne).* **2**, 32

46. Clemmons, D. R. (2004) The relative roles of growth hormone and IGF-1 in controlling insulin sensitivity. *J. Clin. Invest.* **113**, 25–27

47. Teppala, S., and Shankar, A. (2010) Association between serum IGF-1 and diabetes among U.S. adults. *Diabetes Care*. **33**, 2257–2259

48. Holly, J. M. P., Amiel, S. A., Sandhu, R. R., Rees, L. H., and Wass, J. A. H. (1988) The role of growth hormone in diabetes mellitus. *J. Endocrinol.* **118**, 353–364

49. Root, A. W., Duckett, G., Sweetland, M., and Reiter, E. O. (1979) Effects of Zinc Deficiency Upon Pituitary Function in Sexually Mature and Immature Male Rats. *J. Nutr.* **109**, 958–964

50. Hamza, R. T., Hamed, A. I., and Sallam, M. T. (2012) Effect of zinc supplementation on growth Hormone Insulin growth factor axis in short Egyptian children with zinc deficiency. *Ital. J. Pediatr.* **38**, 21

51. Cunningham, B. C., Bass, S., Fuh, G., and Wells, J. A. (1990) Zinc mediation of the binding of human growth hormone to the human prolactin receptor. *Science (80-.).* **250**, 1709–1712

52. Petkovic, V., Miletta, M. C., Eblé, A., Iliev, D. I., Binder, G., Flück, C. E., and Mullis, P. E. (2013) Effect of Zinc Binding Residues in Growth Hormone (GH) and Altered Intracellular Zinc Content on Regulated GH Secretion. *Endocrinology*. **154**, 4215–4225

53. Macdonald, R. S. (2000) *Zinc and Health: Current Status and Future Directions The Role of Zinc in Growth and Cell Proliferation 1,2*, [online] https://academic.oup.com/jn/article-abstract/130/5/1500S/4686427 (Accessed April 29, 2020)

54. Wang, C. (2013) The Relationship between Type 2 Diabetes Mellitus and Related Thyroid Diseases. *J. Diabetes Res.* 10.1155/2013/390534

55. Gupta, R. P., Verma, P. C., and Garg, S. L. (1997) Effect of experimental zinc deficiency on thyroid gland in guinea-pigs. *Ann. Nutr. Metab.* **41**, 376–81

56. Campos, C., and Casado, Á. (2015) Oxidative stress, thyroid dysfunction & Down syndrome. *Indian J. Med. Res.* **142**, 113–119

57. Dhawan, D., Singh Baweja, M., Dani, V., and Dhawan, D. K. (2007) *Zinc sulphate following the administration of iodine-131 on the regulation of thyroid function, in rats*, [online] www.nuclmed.gr (Accessed June 6, 2020)

58. Miyamoto, T., Sakurai, A., and Degroot, L. J. (1991) Effects of zinc and other divalent metals on deoxyribonucleic acid binding and hormone-binding activity of human αl thyroid hormone receptor expressed in Escherichia coli. *Endocrinology*. **129**, 3027–3033

59. Freake, H. C., Govoni, K. E., Guda, K., Huang, C., and Zinn, S. A. (2001) *Biochemical and Molecular Action of Nutrients Actions and Interactions of Thyroid Hormone and Zinc Status in Growing Rats*, [online] https://academic.oup.com/jn/article-abstract/131/4/1135/4686944 (Accessed April 30, 2020)

60. Pawan, K., Neeraj, S., Sandeep, K., Kanta Ratho, R., and Rajendra, P. (2007)

Upregulation of Slc39a10 gene expression in response to thyroid hormones in intestine and kidney. *Biochim. Biophys. Acta - Gene Struct. Expr.* **1769**, 117–123

61. Meek, T. H., and Morton, G. J. Leptin, diabetes, and the brain. 10.4103/2230-8210.105568

62. Fischer, S., Hanefeld, M., Haffner, S. M., Fusch, C., Schwanebeck, U., Köhler, C., Fücker, K., and Julius, U. (2002) Insulin-resistant patients with type 2 diabetes mellitus have higher serum leptin levels independently of body fat mass. *Acta Diabetol.* **39**, 105–110

63. Liu, M.-J., Bao, S., Bolin, E. R., Burris, D. L., Xu, X., Sun, Q., Killilea, D. W., Shen, Q., Ziouzenkova, O., Belury, M. A., Failla, M. L., and Knoell, D. L. (2013) Zinc Deficiency Augments Leptin Production and Exacerbates Macrophage Infiltration into Adipose Tissue in Mice Fed a High-Fat Diet. *J. Nutr.* **143**, 1036–1045

64. Fischer, S., Hanefeld, M., Haffner, S. M., Fusch, C., Schwanebeck, U., Köhler, C., Fücker, K., and Julius, U. (2002) Insulin-resistant patients with type 2 diabetes mellitus have higher serum leptin levels independently of body fat mass. *Acta Diabetol.* **39**, 105–110

65. Jeong, J., and Eide, D. J. (2013) The SLC39 family of zinc transporters. *Mol. Aspects Med.* **34**, 612–619

66. Huang, L., and Tepaamorndech, S. (2013) The SLC30 family of zinc transporters-A review of current understanding of their biological and pathophysiological roles. *Mol. Aspects Med.* **34**, 548–560

67. Kimura, T., and Kambe, T. (2016) The functions of metallothionein and ZIP and ZnT transporters: An overview and perspective. *Int. J. Mol. Sci.* **17**, 336

68. Gyulkhandanyan, A. V., Lee, S. C., Bikopoulos, G., Dai, F., and Wheeler, M. B. (2006) The Zn2+-transporting pathways in pancreatic β-cells: A role for the L-type voltage-gated Ca2+ channel. *J. Biol. Chem.* **281**, 9361–9372

69. Chimienti, F., Devergnas, S., Favier, A., and Seve, M. (2004) Identification and cloning of a β-cell-specific zinc transporter, ZnT-8, localized into insulin secretory granules. *Diabetes*. **53**, 2330–2337

70. Sladek, R., Rocheleau, G., Rung, J., Dina, C., Shen, L., Serre, D., Boutin, P., Vincent, D., Belisle, A., Hadjadj, S., Balkau, B., Heude, B., Charpentier, G., Hudson, T. J., Montpetit, A., Pshezhetsky, A. V., Prentki, M., Posner, B. I., Balding, D. J., Meyre, D., Polychronakos, C., and Froguel, P. (2007) A genome-wide association study identifies novel risk loci for type 2 diabetes. *Nature*. **445**, 881–885

71. Kirchhoff, K., Machicao, F., Haupt, A., Schäfer, S. A., Tschritter, O., Staiger, H., Stefan, N., Häring, H. U., and Fritsche, A. (2008) Polymorphisms in the TCF7L2, CDKAL1 and SLC30A8 genes are associated with impaired proinsulin conversion. *Diabetologia*. **51**, 597–601

72. Dimas, A. S., Lagou, V., Barker, A., Knowles, J. W., Mägi, R., Hivert, M. F., Benazzo, A., Rybin, D., Jackson, A. U., Stringham, H. M., Song, C., Fischer-Rosinsky, A., Welløv Boesgaard, T., Grarup, N., Abbasi, F. A., Assimes, T. L., Hao, K., Yang, X., Lecoeur, C., Barroso, I., Bonnycastle, L. L., Böttcher, Y., Bumpstead, S., Chines, P. S., Erdos, M. R., Graessler, J., Kovacs, P., Morken, M. A., Narisu, N., Payne, F., Stancakova, A., Swift, A. J., Tönjes, A., Bornstein, S. R., Cauchi, S., Froguel, P., Meyre, D., Schwarz, P. E. H., Häring, H. U., Smith, U., Boehnke, M., Bergman, R. N., Collins, F. S., Mohlke, K. L., Tuomilehto, J., Quertemous, T., Lind, L., Hansen, T., Pedersen, O., Walker, M., Pfeiffer,

A. F. H., Spranger, J., Stumvoll, M., Meigs, J. B., Wareham, N. J., Kuusisto, J., Laakso, M., Langenberg, C., Dupuis, J., Watanabe, R. M., Florez, J. C., Ingelsson, E., McCarthy, M. I., and Prokopenko, I. (2014) Impact of type 2 diabetes susceptibility variants on quantitative glycemic traits reveals mechanistic heterogeneity. *Diabetes*. **63**, 2158–2171

73. Staiger, H., Machicao, F., Stefan, N., Tschritter, O., Thamer, C., Kantartzis, K., Schäfer, S. A., Kirchhoff, K., Fritsche, A., and Häring, H. U. (2007) Polymorphisms within novel risk loci for type 2 diabetes determine β-cell function. *PLoS One*. 10.1371/journal.pone.0000832

74. Merriman, C., Huang, Q., Rutter, G. A., and Fu, D. (2016) Lipid-tuned Zinc Transport Activity of Human ZnT8 Protein Correlates with Risk for Type-2 Diabetes. *J. Biol. Chem.* **291**, 26950–26957

75. Wong, W. P., Allen, N. B., Meyers, M. S., Link, E. O., Zhang, X., MacRenaris, K. W., and El Muayed, M. (2017) Exploring the Association between Demographics, SLC30A8 Genotype, and Human Islet Content of Zinc, Cadmium, Copper, Iron, Manganese and Nickel. *Sci. Rep.* **7**, 473

76. Flannick, J., Thorleifsson, G., Beer, N. L., Jacobs, S. B. R., Grarup, N., Burtt, N. P., Mahajan, A., Fuchsberger, C., Atzmon, G., Benediktsson, R., Blangero, J., Bowden, D. W., Brandslund, I., Brosnan, J., Burslem, F., Chambers, J., Cho, Y. S., Christensen, C., Douglas, D. A., Duggirala, R., Dymek, Z., Farjoun, Y., Fennell, T., Fontanillas, P., Forsén, T., Gabriel, S., Glaser, B., Gudbjartsson, D. F., Hanis, C., Hansen, T., Hreidarsson, A. B., Hveem, K., Ingelsson, E., Isomaa, B., Johansson, S., Jørgensen, T., Jørgensen, M. E., Kathiresan, S., Kong, A., Kooner, J., Kravic, J., Laakso, M., Lee, J.-Y., Lind, L., Lindgren, C. M., Linneberg, A., Masson, G., Meitinger, T., Mohlke, K. L.,

Molven, A., Morris, A. P., Potluri, S., Rauramaa, R., Ribel-Madsen, R., Richard, A.-M., Rolph, T., Salomaa, V., Segrè, A. V, Skärstrand, H., Steinthorsdottir, V., Stringham, H. M., Sulem, P., Tai, E. S., Teo, Y. Y., Teslovich, T., Thorsteinsdottir, U., Trimmer, J. K., Tuomi, T., Tuomilehto, J., Vaziri-Sani, F., Voight, B. F., Wilson, J. G., Boehnke, M., McCarthy, M. I., Njølstad, P. R., Pedersen, O., Consortium, G.-T., Consortium, T.-G., Groop, L., Cox, D. R., Stefansson, K., and Altshuler, D. (2014) Loss-of-function mutations in SLC30A8 protect against type 2 diabetes. *Nat. Genet.* **46**, 357–363

77. Hardy, A. B., Wijesekara, N., Genkin, I., Prentice, K. J., Bhattacharjee, A., Kong, D., Chimienti, F., and Wheeler, M. B. (2012) Effects of high-fat diet feeding on Znt8-null mice: Differences between β-cell and global knockout of Znt8. *Am. J. Physiol. - Endocrinol. Metab.* **302**, E1084-96

78. Wijesekara, N., Dai, F. F., Hardy, A. B., Giglou, P. R., Bhattacharjee, A., Koshkin, V., Chimienti, F., Gaisano, H. Y., Rutter, G. A., and Wheeler, M. B. (2010) Beta cell-specific Znt8 deletion in mice causes marked defects in insulin processing, crystallisation and secretion. *Diabetologia*. **53**, 1656–1668

79. Pound, L. D., Sarkar, S. A., Benninger, R. K. P., Wang, Y., Suwanichkul, A., Shadoan, M. K., Printz, R. L., Oeser, J. K., Lee, C. E., Piston, D. W., McGuinness, O. P., Hutton, J. C., Powell, D. R., and O'Brien, R. M. (2009) Deletion of the mouse Slc30a8 gene encoding zinc transporter-8 results in impaired insulin secretion. *Biochem. J.* **421**, 371–376

80. Lemaire, K., Ravier, M. A., Schraenen, A., Creemers, J. W. M., Van De Plas, R., Granvik, M., Van Lommel, L., Waelkens, E., Chimienti, F., Rutter, G. A., Gilon, P., In't Veld, P. A., and Schuit, F. C. (2009) Insulin crystallization depends on zinc transporter ZnT8 expression, but is not required for normal glucose homeostasis in mice. *Proc. Natl. Acad.*

Sci. U. S. A. **106**, 14872–14877

81. Mitchell, R. K., Hu, M., Chabosseau, P. L., Cane, M. C., Meur, G., Bellomo, E. A., Carzaniga, R., Collinson, L. M., Li, W.-H., Hodson, D. J., and Rutter, G. A. (2016) Molecular Genetic Regulation of Slc30a8/ZnT8 Reveals a Positive Association With Glucose Tolerance. *Mol. Endocrinol.* **30**, 77–91

82. Nicolson, T. J., Bellomo, E. A., Wijesekara, N., Loder, M. K., Baldwin, J. M., Gyulkhandanyan, A. V., Koshkin, V., Tarasov, A. I., Carzaniga, R., Kronenberger, K., Taneja, T. K., Da Silva Xavier, G., Libert, S., Froguel, P., Scharfmann, R., Stetsyuk, V., Ravassard, P., Parker, H., Gribble, F. M., Reimann, F., Sladek, R., Hughes, S. J., Johnson, P. R. V., Masseboeuf, M., Burcelin, R., Baldwin, S. A., Liu, M., Lara-Lemus, R., Arvan, P., Schuit, F. C., Wheeler, M. B., Chimienti, F., and Rutter, G. A. (2009) Insulin storage and glucose homeostasis in mice null for the granule zinc transporter ZnT8 and studies of the type 2 diabetes-associated variants. *Diabetes*. **58**, 2070–2083

83. Tamaki, M., Fujitani, Y., Hara, A., Uchida, T., Tamura, Y., Takeno, K., Kawaguchi, M., Watanabe, T., Ogihara, T., Fukunaka, A., Shimizu, T., Mita, T., Kanazawa, A., Imaizumi, M. O., Abe, T., Kiyonari, H., Hojyo, S., Fukada, T., Kawauchi, T., Nagamatsu, S., Hirano, T., Kawamori, R., and Watada, H. (2013) The diabetes-susceptible gene SLC30A8/ZnT8 regulates hepatic insulin clearance. *J. Clin. Invest.* **123**, 4513–4524

84. Fukunaka, A. F., and Fujitani, Y. (2018) Role of Zinc Homeostasis in the Pathogenesis of Diabetes and Obesity. *Int. J. Mol. Sci.* **19**, 476

85. Cao, P., Meng, F., Abedini, A., and Raleigh, D. P. (2010) The ability of rodent islet amyloid polypeptide to inhibit amyloid formation by human islet amyloid polypeptide has important implications for the mechanism of amyloid formation and the design of

inhibitors. *Biochemistry*. **49**, 872–881

86. Nedumpully-Govindan, P., and Ding, F. (2015) Inhibition of IAPP aggregation by insulin depends on the insulin oligomeric state regulated by zinc ion concentration. *Sci. Rep.* 10.1038/srep08240

87. Tamaki, M., Fujitani, Y., Hara, A., Uchida, T., Tamura, Y., Takeno, K., Kawaguchi, M., Watanabe, T., Ogihara, T., Fukunaka, A., Shimizu, T., Mita, T., Kanazawa, A., Imaizumi, M. O., Abe, T., Kiyonari, H., Hojyo, S., Fukada, T., Kawauchi, T., Nagamatsu, S., Hirano, T., Kawamori, R., and Watada, H. (2013) The diabetes-susceptible gene SLC30A8/ZnT8 regulates hepatic insulin clearance. *J. Clin. Invest.* **123**, 4513–4524

88. Kambe, T., Narita, H., Yamaguchi-Iwai, Y., Hirose, J., Amano, T., Sugiura, N., Sasaki, R., Mori, K., Iwanaga, T., and Nagao, M. (2002) Cloning and characterization of a novel mammalian zinc transporter, zinc transporter 5, abundantly expressed in pancreatic β cells. *J. Biol. Chem.* **277**, 19049–19055

89. Huang, L., Yan, M., and Kirschke, C. P. (2010) Over-expression of ZnT7 increases insulin synthesis and secretion in pancreatic β-cells by promoting insulin gene transcription. *Exp. Cell Res.* **316**, 2630–2643

90. Liu, Y., Batchuluun, B., Ho, L., Zhu, D., Prentice, K. J., Bhattacharjee, A., Zhang, M., Pourasgari, F., Hardy, A. B., Taylor, K. M., Gaisano, H., Dai, F. F., and Wheeler, M. B. (2015) Characterization of zinc influx transporters (ZIPs) in pancreatic β cells: Roles in regulating cytosolic zinc homeostasis and insulin secretion. *J. Biol. Chem.* **290**, 18757–18769

91. Taylor, K. M., Hiscox, S., Nicholson, R. I., Hogstrand, C., and Kille, P. (2012) Cell biology: Protein kinase CK2 triggers cytosolic zinc signaling pathways by

phosphorylation of zinc channel ZIP7. *Sci. Signal.* **5**, ra11

92. Bin, B. H., Bhin, J., Seo, J., Kim, S. Y., Lee, E., Park, K., Choi, D. H., Takagishi, T., Hara, T., Hwang, D., Koseki, H., Asada, Y., Shimoda, S., Mishima, K., and Fukada, T. (2017) Requirement of Zinc Transporter SLC39A7/ZIP7 for Dermal Development to Fine-Tune Endoplasmic Reticulum Function by Regulating Protein Disulfide Isomerase. *J. Invest. Dermatol.* **137**, 1682–1691

93. Cnop, M., Toivonen, S., Igoillo-Esteve, M., and Salpea, P. (2017) Endoplasmic reticulum stress and eIF2α phosphorylation: The Achilles heel of pancreatic β cells. *Mol. Metab.* **6**, 1024–1039

94. Myers, S. A., Nield, A., Chew, G.-S., and Myers, M. A. (2013) The Zinc Transporter, Slc39a7 (Zip7) Is Implicated in Glycaemic Control in Skeletal Muscle Cells. *PLoS One*. **8**, e79316

95. Solomou, A., Meur, G., Bellomo, E., Hodson, D. J., Tomas, A., Migrenne Li, S., Philippe, E., Herrera, P. L., Magnan, C., and Rutter, G. A. (2015) The Zinc Transporter Slc30a8/ZnT8 Is Required in a Subpopulation of Pancreatic α-Cells for Hypoglycemia-induced Glucagon Secretion. *J. Biol. Chem.* **290**, 21432–21442

96. Solomou, A., Philippe, E., Chabosseau, P., Migrenne-Li, S., Gaitan, J., Lang, J., Magnan, C., and Rutter, G. A. (2016) Over-expression of Slc30a8/ZnT8 selectively in the mouse α cell impairs glucagon release and responses to hypoglycemia. *Nutr. Metab. (Lond).* **13**, 46

97. Troche, C., Aydemir, T. B., and Cousins, R. J. (2016) Zinc transporter Slc39a14 regulates inflammatory signaling associated with hypertrophic adiposity. *Am. J. Physiol. - Endocrinol. Metab.* **310**, E258–E268

98. Maxel, T., Smidt, K., Larsen, A., Bennetzen, M., Cullberg, K., Fjeldborg, K., Lund, S.,

Pedersen, S. B., and Rungby, J. (2015) Gene expression of the zinc transporter ZIP14 (SLC39a14) is affected by weight loss and metabolic status and associates with PPARγ in human adipose tissue and 3T3-L1 pre-adipocytes. *BMC Obes.* 10.1186/s40608-015-0076-y

99. Tominaga, K., Kagata, T., Johmura, Y., Hishida, T., Nishizuka, M., and Imagawa, M. (2005) SLC39A14, a LZT protein, is induced in adipogenesis and transports zinc. *FEBS J.* **272**, 1590–1599

100. Sidossis, L., and Kajimura, S. (2015) Brown and beige fat in humans: Thermogenic adipocytes that control energy and glucose homeostasis. *J. Clin. Invest.* **125**, 478–486

101. Fukunaka, A., Fukada, T., Bhin, J., Suzuki, L., Tsuzuki, T., Takamine, Y., Bin, B. H., Yoshihara, T., Ichinoseki-Sekine, N., Naito, H., Miyatsuka, T., Takamiya, S., Sasaki, T., Inagaki, T., Kitamura, T., Kajimura, S., Watada, H., and Fujitani, Y. (2017) Zinc transporter ZIP13 suppresses beige adipocyte biogenesis and energy expenditure by regulating C/EBP-β expression. *PLoS Genet.* **13**, e1006950

102. Huang, L., Tepaamorndech, S., Kirschke, C. P., Pedersen, T. L., Keyes, W. R., and Newman, J. W. (2016) Zinc Transporter 7 (Znt7) Knockout in Mice Differentially Affects Lipid Metabolism in Adipose Tissues. *FASEB J.* **30**, 691.4-691.4

103. Tepaamorndech, S., Kirschke, C. P., Pedersen, T. L., Keyes, W. R., Newman, J. W., and Huang, L. (2016) Zinc transporter 7 deficiency affects lipid synthesis in adipocytes by inhibiting insulin-dependent Akt activation and glucose uptake. *FEBS J.* **283**, 378–394

104. Myers, S. A., Nield, A., Chew, G. S., and Myers, M. A. (2013) The zinc transporter, Slc39a7 (Zip7) is implicated in glycaemic control in skeletal muscle cells. *PLoS One*. **8**, e79316

105. Huang, L., Kirschke, C. P., Lay, Y. A. E., Levy, L. B., Lamirande, D. E., and Zhang, P. H. (2012) Znt7-null mice are more susceptible to diet-induced glucose intolerance and insulin resistance. *J. Biol. Chem.* **287**, 33883–33896

106. Lindahl, M., and Tagesson, C. (1996) Zinc (Zn2+) binds to and stimulates the activity of group I but not group II phospholipase A2. *Inflammation*. **20**, 599–611

107. Borgström, B. (1980) Importance of phospholipids, pancreatic phospholipase A2, and fatty acid for the digestion of dietary fat. In vitro experiments with the porcine enzymes. *Gastroenterology*. **78**, 954–962

108. Huang, Y. S., Cunnane, S. C., Horrobin, D. F., and Davignon, J. (1982) Most biological effects of zinc deficiency corrected by γ-linolenic acid (18: 3ω6) but not by linoleic acid (18: 2ω6). *Atherosclerosis*. **41**, 193–207

109. Reed, S., Qin, X., Ran-Ressler, R., Thomas Brenna, J., Glahn, R. P., and Tako, E. (2014) Dietary zinc deficiency affects blood linoleic acid: Dihomo-γ-linolenic acid (LA:DGLA) ratio; a sensitive physiological marker of zinc status in vivo (Gallus gallus). *Nutrients*. **6**, 1164–1180

110. Clejan, S., Castro-Magana, M., Collipp, P. J., Jonas, E., and Maddaiah, V. T. (1982) Effects of zinc deficiency and castration on fatty acid composition and desaturation in rats. *Lipids*. **17**, 129–35

111. Wei, C. C., Luo, Z., Hogstrand, C., Xu, Y. H., Wu, L. X., Chen, G. H., Pan, Y. X., and Song, Y. F. (2018) Zinc reduces hepatic lipid deposition and activates lipophagy via Zn2+/MTF-1/PPARa and Ca2+/CaMKKb/AMPK pathways. *FASEB J.* **32**, 6666–6680

112. Hojyo, S., Fukada, T., Shimoda, S., Ohashi, W., Bin, B. H., Koseki, H., and Hirano, T. (2011) The zinc transporter SLC39A14/ZIP14 controls G-protein coupled receptor-

mediated signaling required for systemic growth. *PLoS One*. **6**, e18059

113. Aydemir, T. B., Troche, C., Kim, M. H., and Cousins, R. J. (2016) Hepatic ZIP14-mediated zinc transport contributes to endosomal insulin receptor trafficking and glucose metabolism. *J. Biol. Chem.* **291**, 23939–23951

Chapter 2 - SLC30A family expression in the pancreatic islets of humans and mice: cellular localization in the β-cells

Abstract

Aims/hypothesis

Zinc is a vital co-factor for insulin metabolism in the pancreatic β-cell, involved in synthesis, maturation, and crystallization. Two families of zinc transporters, namely SLC30A (ZNT) and SLC39A (ZIP) are involved in maintaining cellular zinc homeostasis in mammalian cells. Single nuclear polymorphisms (SNPs) or mutations in zinc transporters have been associated with insulin resistance and risks of type 2 diabetes (T2D) in both humans and mice. Thus, mice can be useful for studying the underlying mechanisms of zinc-associated risks of T2D or T2D development. Therefore, it is important to identify potential differences in zinc transporter expression and cellular localization in the pancreatic β-cells between humans and mice.

Methods

We examined all members (ZNT1-10) of the ZNT family in pancreatic islets and in β-cell lines derived from both species using immunohistochemistry and immunofluorescence microscopic analysis.

Results

We found that there were no substantial differences in the expression of nine ZNT proteins in the human and mouse islets and β-cells. ZNT3 was only detected in human β-cells, but not in mouse β-cells. Moreover, we found that ZNT2 was localized on the cell surface of both human and mouse β-cells, suggesting a role of ZNT2 in direct export of zinc out of the β-cell.

Conclusions/interpretation

Our study demonstrates functional conservations of the ZNT proteins between humans and mice. The data suggests that mouse models of zinc transporters can be used for studying mechanisms of zinc-associated risks of T2D in humans.

Introduction

Cellular zinc homeostasis is largely maintained by two families of zinc transporters, namely SLC30A (ZNT) and SLC39A (ZIP) in humans and mice. The ZNT and ZIP zinc transporter families contain 10 and 14 members, respectively. The ZNT proteins function to maintain cellular zinc levels in a narrow physiological range by efflux of excess cytoplasmic zinc into the extracellular space or into intracellular organelles/vesicles when cellular zinc is high, whereas ZIPs move zinc in the opposite direction when cellular zinc is low.

Zinc co-resides with insulin in secretory granules in β-cells (1) where it is integrated into insulin molecules to form insulin-zinc crystals (2). The importance of zinc and its roles in insulin synthesis, processing, and secretion have been demonstrated by studying zinc transporters in insulin-secreting cell lines and in knockout animal models. For example, over-expressing ZnT7 in rat insulin-secreting cells stimulates insulin transcription leading to increase in basal insulin secretion (3). Consistent with the function of ZnT7 in basal insulin secretion, *Znt7* knockout (KO) mice have abnormalities in fasting insulin secretion (4). The process of proinsulin to insulin requires three zinc-dependent enzymes, including endopeptidases (PC1 and PC2) and carboxypeptidase E (5, 6). ZNT8 is associated with availability of zinc ions for these zinc-dependent enzymes (7). Additionally, in secretory granules, processed insulin is crystallized in the presence of zinc ions and stored before secretion (8). ZnT8 is required in this process by transporting zinc ions into these secretory granules (9).

As mouse knockout models have frequently been used for studying the underlying mechanisms by which zinc regulates insulin synthesis, maturation, and secretion in β-cells, and its impact on risks of T2D, identification of the degree of functional conservation of zinc transporters between humans and mice is important. The aim of this study was to establish a comprehensive

expression profile of the ZNT proteins (ZNT1-10) in human and mouse pancreatic islets, and to compare the diversity in cellular localization in human and mouse β-cell lines.

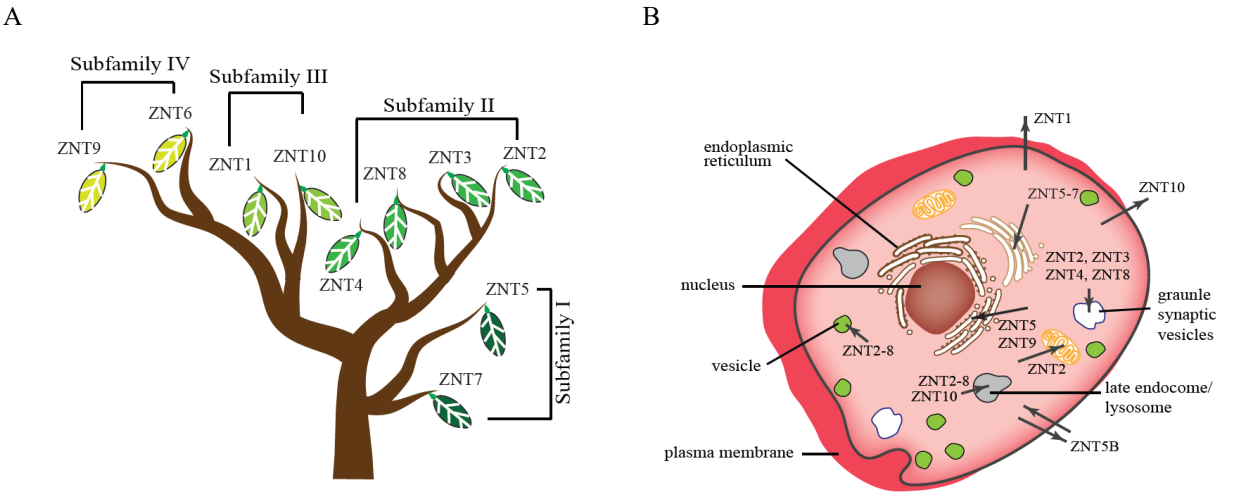

Figure 1. Summary of the ZNT family. A. phylogenetic tree of the ZNT family members. Amino acid sequences of the human ZNT proteins were used to generate the tree. The parsimony tree from the ZNT amino acid sequences was generated using an online Phylogenetic Tree Program at the ETH Zürich (http://www.cbrg.ethz.ch/services/PhylogeneticTree). The subfamilies of the ZNT proteins are displayed. B. Cellular localization of the mouse ZNT transporters in a generalized mammalian cell. Organelles of the cell are labeled in the panel. Arrows indicate the direction of transport of zinc ions across the cellular membrane by the ZNT proteins.

The ten ZNT proteins can be grouped into four subfamilies based on their protein sequence similarities (Fig. 1A). According to the phylogenetic tree of the mammalian ZNT family, ZNT5 ZNT7 can be grouped into the subfamily I, ZNT2-4 and ZNT8 into the subfamily II, ZNT1 and ZNT10 into the subfamily III, and ZNT6 and ZNT9 into the subfamily IV. The ZNT proteins in the same subfamily tend to reside in the cellular compartments with similar functions (Fig. 1B).

Our results demonstrate that most ZNT proteins were expressed in the islets of the human and mouse pancreas. In β-cells, most ZNTs were expressed intracellularly except for ZNT1 and ZNT2, which were also localized on the cell membrane of the human and mouse β-cells. Nevertheless, we did not detect ZNT3 in the mouse islets and cultured MIN6 β-cells although it was readily detectable in the human islets and cultured 1.1B4-KH5 β-cells. In addition, ZNT6 was

stained strongly in the human islets and presented in heterogeneous vesicles of different sizes. This staining pattern was not noticeable in the mouse islets. Taken together, our study suggests functional conservation of the ZNT proteins between humans and mice. These results are of interest for future studies in association of zinc metabolism with risks of T2D in humans using mouse models.

Materials and methods

Animals

C57Bl/6 mice were originally obtained from the Jackson Laboratory (Bar Harbor, MI), and the experimental mice were generated from in-house breeding. All mice were housed in a temperature-controlled room at 22-24^{o}C with a 12 h light-dark cycle, and were fed a standard laboratory chow diet (Laboratory Rodent Diet 5001, LabDiet, Brentwood, MO) and double-distilled water ad libitum. All animal experiments were conducted in accordance with National Institutes of Health Guidelines for the Care and Use of Experimental Animals and were approved by the Institutional Animal Care and Use Committee of the University of California, Davis.

Preparation of Mouse Pancreatic Tissue Sections

Whole pancreas was dissected from experimental mice at 7-10 weeks of age. Tissues were fixed, paraffin-embedded, and sectioned as described previously (10). Briefly, the mouse pancreas was dissected and placed in 4% paraformaldehyde solution or 10% buffered formalin (ThermoFisher Scientific, Waltham, MA) overnight. Tissues were then rinsed in 1 x PBS followed by dehydration in 80% FLEX (Richard-Allan Scientific, Kalamazoo, MI) and placed at 4^{o}C until processed. Dehydration steps consisted of 95% FLEX for 20 min twice, 100% FLEX 20 min twice, and Clear-

Rite 3 for 15 min twice were carried out in a STP 120 Spin Tissue Processor (Thermo Scientific™, ThermoFisher Scientific). Tissues were infiltrated and embedded in Type 9 paraffin (Richard-Allan Scientific) using a Epredia™ HistoStar™ Embedding Workstation (ThermoFisher Scientific). Tissue sections were cut in a 5-µm thickness using a Epredia™ HM 325 Rotary Microtome machine (ThermoFisher Scientific).

Human Pancreatic Tissue Sections

Paraffin embedded human pancreatic tissue sections were purchased from BioChain Inc. (Newark, CA). According to the manufacturer, the normal pancreatic tissue sections were prepared from the pancreases obtained from male donors at 66 or 71 years of age.

Antibodies

The primary polyclonal antibodies against ZNT1 and ZNT4-7 were affinity-purified against their specific peptides that the antibodies were raised against in rabbits. The synthetic peptides were: amino acids 495-507 of the human ZNT1, 93-110 of the mouse ZnT4, 750-762 of the human ZNT5, 446-460 of the mouse ZnT6, and 299-315 of the mouse ZnT7 (11–14). Peptides used in the generation of these antibodies are unique to the respective ZNT protein and have a high amino acid sequence similarities between humans and mice as determined by BLAST searches of the UniProtKB/Swiss-Prot (swissporot) database (https://blast.ncbi.nlm.nih.gov). The specificities of ZNT1 and ZNT4-7, including positive and negative controls in human and/or mouse tissues/cells, have been described previously (11–14).

Rabbit anti-ZNT2 polyclonal was kindly given by Dr. Shannon Kelleher (Pennsylvania State University). The specificity of this ZNT2 antibody was verified by peptide competition

analysis as described previously (15). Lack of non-specific reactivity of pre-immune sera was also reported (15).

Rabbit polyclonal anti-ZNT3, -ZNT9, and -ZNT10 antibody were purchased from Aviva Systems Biology (San Diego, CA). The anti-ZNT3 antibody was generated against a synthetic peptide derived from the amino acid sequences of the human ZNT3 (AMLLTASIAVCANLLMAFVLHQAGPPHSHGSRGAEYAPLEEGPEEPLPLG). According to the manufacture's datasheet, the affinity-purified ZNT3 antibody can react to ZNT3 from many species, including humans and mice. This antibody was validated to specifically recognize ZNT3 by Western blot analysis. The anti-ZNT9 antibody was generated against a synthetic peptide derived from the N-terminal end of the human ZNT9 (LKQEPLQVRVKAVLKKREYGSKYTQNNFITGVRAINEFCLKSSDLEQLR). The specificity of this affinity-purified ZNT9 antibody was validated by both Western blot analysis and immunohistochemistry (Aviva Systems Biology). It can recognize ZNT9 from multiple species, including humans and mice. Finally, the anti-ZNT10 antibody was generated against the C-terminal region of the human ZNT10. The specificity of this antibody was confirmed by Western blot analysis as described in the manufacture's datasheet. The positive and negative reactivates of the ZNT10 antibody was supported by the immunohistochemical staining of multiple human tissues illustrated in the Human Protein Atlas (https://www.proteinatlas.org).

Mouse monoclonal anti-ZNT8 antibody was purchased from R&D Systems (Minneapolis, MN). The anti-ZNT8 antibody was generated against a synthetic peptide derived from the amino acid sequences (Lys268-Pro359) of the human ZNT8 in mice. The purified ZNT8 antibody can react to both human and mouse ZnT8 (16). This antibody was also validated for immunohistochemistry according to the manufacture. The guinea pig polyclonal anti-ZnT8

antibody was generated against a synthetic peptide (ASPDSQVVRREIAKALSKSFTM) and was affinity-purified. This antibody was validated and described previously (16).

Secondary antibodies against the hosts that the primary antibodies raised from were purchased from either Vector Laboratories (Burlingame, CA) or ThermoFisher Scientific. We confirmed that secondary antibodies used in this study had no reactivates to proteins in the pancreas for immunohistochemistry (Fig. 2).

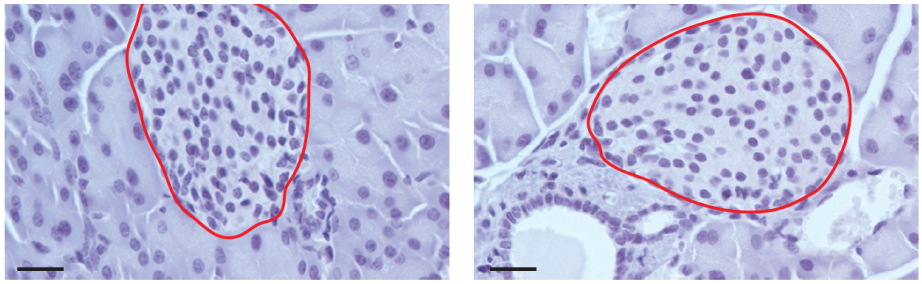

Figure 2. Representative images of negative controls for immunohistochemistry. The controls represent sections where no primary antibody was used while a goat anti-guinea pig secondary antibody (A) or a goat anti-rabbit secondary antibody was applied (B). Sections were counterstained with hematoxylin. The islet of Langerhans is encircled in red. Scale bar = 20 μm

Immunohistochemistry

Pancreatic tissues were deparaffinized with Xylene and rehydrated using FLEX alcohols. Tissue antigen retrieval was accomplished in either 10 mM sodium citrate, pH 6.0 or 20-100 mM Tris-Cl, pH 10, at the boiling point for 20 min. The endogenous peroxidase activity was abolished by treating sections with 5% H_2O_2 at room temperature for 15 min. The non-specific binding of biotin/avidin was blocked using an Avidin-Biotin Blocking kit (Vector Laboratories). Tissues were then treated with 3% goat serum to block non-specific protein bindings. Primary antibodies against ZNT1-10 were diluted in 1 x PBS containing 2% mouse and 2% goat sera as follows: ZNT1, 1:500; ZNT2, 1:250; ZNT3, 1:50; ZNT4, 1:25; ZNT5, 1:75; ZNT6, 1:25; ZNT7, 1:1,000; human ZNT8, 1:20; mouse ZnT8 1:1,000; ZNT9, 1:50; ZNT10, 1:50. Immunoperoxidase staining was

accomplished using a Vectastain ABC kit and DAB substrate (Vector Laboratories). Secondary biotinylated goat anti-rabbit or anti-mouse (Vector Labs) was diluted at 1:200-250 in 1 x PBS containing 2% goat serum. The immunoreactivity was developed in tissue sections using VECTASTAIN elite ABC and HRP substrate ImmPACT DAB kits (Vector Labs), which produced brown deposits in cells. Sections were counterstained with hematoxylin. Stained sections were viewed using a Nikon Eclipse 800 microscope (Nikon Instruments Inc., Melville, NY). Images were acquired using a SPOT RT3 digital camera (Diagnostic Instrument Inc., Sterling Heights, MI) with SPOT RT Software v3.0 via a Nikon Plan Apo 20X/0.75 or a Nikon Plan Fluor 40X/0.75 lens.

Culture of Mouse Insulin-secreting Cells

MIN6 β-cells were purchased from AddexBio (San Diego, CA). Cells were grown in DMEM containing 15% (v/v) Fetal Bovine Serum (FBS), 4.5 g/L glucose, 1.0 mM sodium pyruvate, 50 μM β-Mercaptoethanol (BME), 50 U/mL penicillin, and 50 μg/mL streptomycin (complete medium, ThermoFisher Scientific).

Culture of Human Insulin-secreting Cells (1.1B4) and Sub-cloning of an Insulin-secreting β-cell Line, 1.1B4-KH5

The 1.1B4 human insulin-secreting cell line (17) was purchased from Sigma-Aldrich (St. Louis, MO). Cells were cultured in a RPMI 1640 medium supplemented with 10% (v/v) fetal bovine serum (FBS) and 100 units/ml penicillin and 100 μg/ml streptomycin (complete medium with 11 mM glucose). Subcloning of 1.1B4-KH5 was achieved by limiting dilution method (18). The resulting individual clones were tested for the presence of high levels of insulin mRNA transcripts

by quantitative RT-PCR. Among the cloned cell lines, 1.1B4-KH5 expressed the most abundant insulin mRNA and was chosen for subsequent immunocytochemical analyses for the 10 ZNT proteins.

Immunocytochemical Analysis

1.1B4-KH5 or MIN6 β-cells were cultured in slide chambers for 24-48 h. Fresh medium containing 5 mM glucose was then replaced and incubated for another 24 h. Cells were then washed and fixed with 4% paraformaldehyde, permeabilized with 0.4% saponin, then blocked with 3% BSA in 1 x PBS. Primary antibodies were diluted in 1 x PBS containing 1% BSA as follows: ZNT1, 1:50; ZNT2, 1:200; ZNT3, 1:50; ZNT4, 1:10; ZNT5, 1:100; ZNT6, 1:25; ZNT7, 1:750; human ZNT8, 1:100; mouse ZnT8; ZNT9, 1:50, and ZNT10, 1:50. The ZNT proteins were detected by an Alexa 488-conjugated goat anti-rabbit or anti-guinea pig secondary antibody (1:250).

Results

Expression of ZNT1-10 in Human and Mouse Pancreatic Islets

To achieve a comprehensive view of the ZNT family in the human pancreatic islet, we examined protein expression of all members of the ZNT family (ZNT1-10) in paraffin-embedded pancreatic tissue sections by immunohistochemistry. Pancreas contains both the exocrine gland and endocrine islet of Langerhans (20). The islets are clumps of hormone-secreting cells scattered throughout the exocrine glandular acini. Islets consist of five types of endocrine cells, including the glucagon-secreting *a*-cell (~15-20%), the insulin-secreting β-cell (~70-80%), the somatostatin-secreting δ–cell (~5-10%), the pancreatic polypeptide-secreting PP cell (< 5%), and the ghrelin-secreting ε-

cell (< 1%) (21, 22). However, we did not include studies to determine expression of the ZNT proteins in the different types of endocrine cells.

In the human islet, the subfamily I ZNT proteins (ZNT5 and ZNT7) could be readily detected in both human and mouse islets (Fig. 3). Both ZNT proteins were expressed in the cytoplasm of the endocrine cells of the islet.

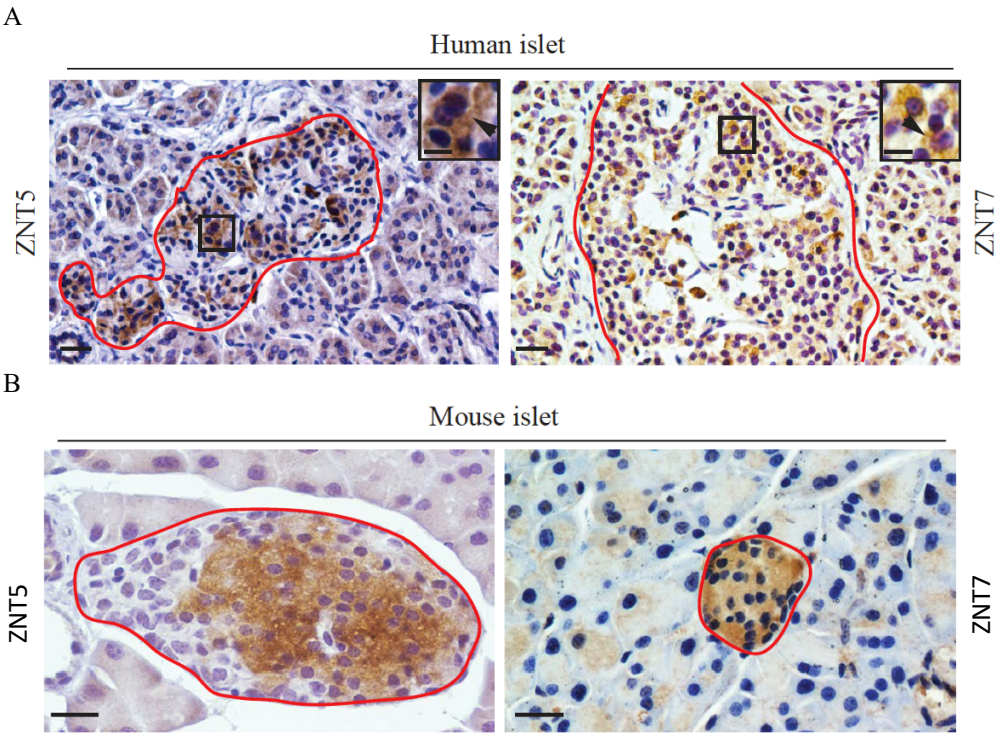

Figure 3. Expression of the subfamily I ZNT proteins in the human and mouse islets. A. Human ZNT5 and ZNT7. Immunohistochemical staining of ZNT5 and ZNT7 was carried out as described in Materials and Methods. Representative images are displayed. Scale bar = 20 μm. Inserts are higher magnifications of the marked areas (square boxes). Arrows in the inserts indicate the immunoreactivities. The scale bar in the insert = 10 μm. B. Mouse ZNT5 and ZNT7. Brown color shows immunoreactivities of ZNT5 and ZNT7 proteins. Sections were counterstained with hematoxylin. The islet of Langerhans is encircled in red. Scale bar = 20 μm.

For ZNT2-4 and ZNT8 in the subfamily II, positive immunostaining was seen in the cytoplasm of endocrine cells of the human islet (Fig. 4A), consistent with their expression patterns in other cell types of humans or rodents (7, 11, 23, 24). A Golgi staining pattern (perinuclear staining) was noticeable for ZNT2 and ZNT3. Moreover, ZNT4 and ZNT8 immunostaining displayed a punctate expression pattern in the human islets, which is in keeping with their

localization in secretory/vesicular compartments in mammalian cells (7, 12). However, the punctate expression pattern of ZnT4 and ZnT8 was not obviously seen in mouse islets (Fig. 4B). Rather, a constant and diffuse staining pattern was found for ZnT4, and ZnT8. Furthermore, in contrast to the human islet, we detected little ZNT3 expression in the endocrine cells of the mouse islet.

A

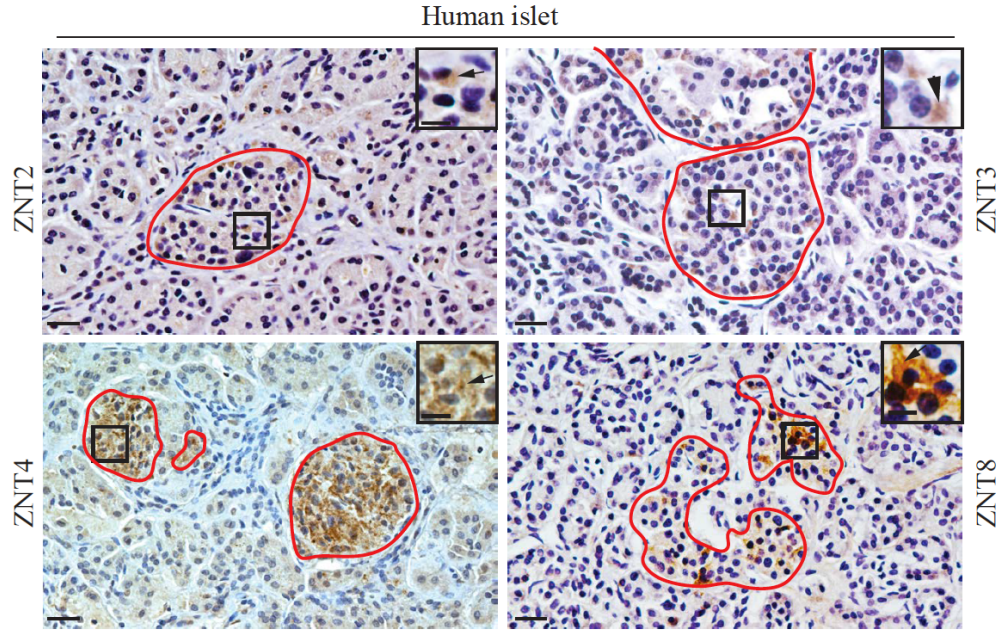

B

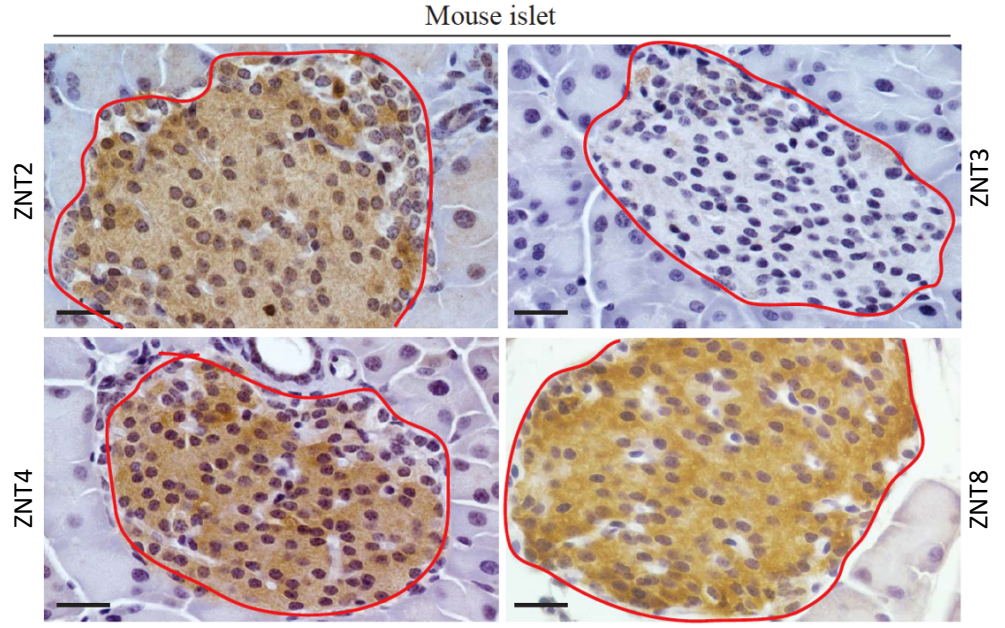

Figure 4. Expression of the subfamily II ZNT proteins in the human and mouse islets. A. Human ZNT2-4 and ZNT8. Immunohistochemical staining of these ZNT proteins in pancreatic tissue sections was carried out as described in Materials and Methods. Representative images are displayed. Scale bar = 20 μm. Inserts are higher magnifications of the marked areas (square boxes). Arrows in the inserts indicate the immunoreactivities. The scale bar in the insert = 10 μm. B. Mouse ZNT2-4 and ZNT8. Brown color shows immunoreactivities of the indicated ZNT proteins. Sections were counterstained with hematoxylin. The islet of Langerhans is encircled in red. Scale bar = 20 μm.

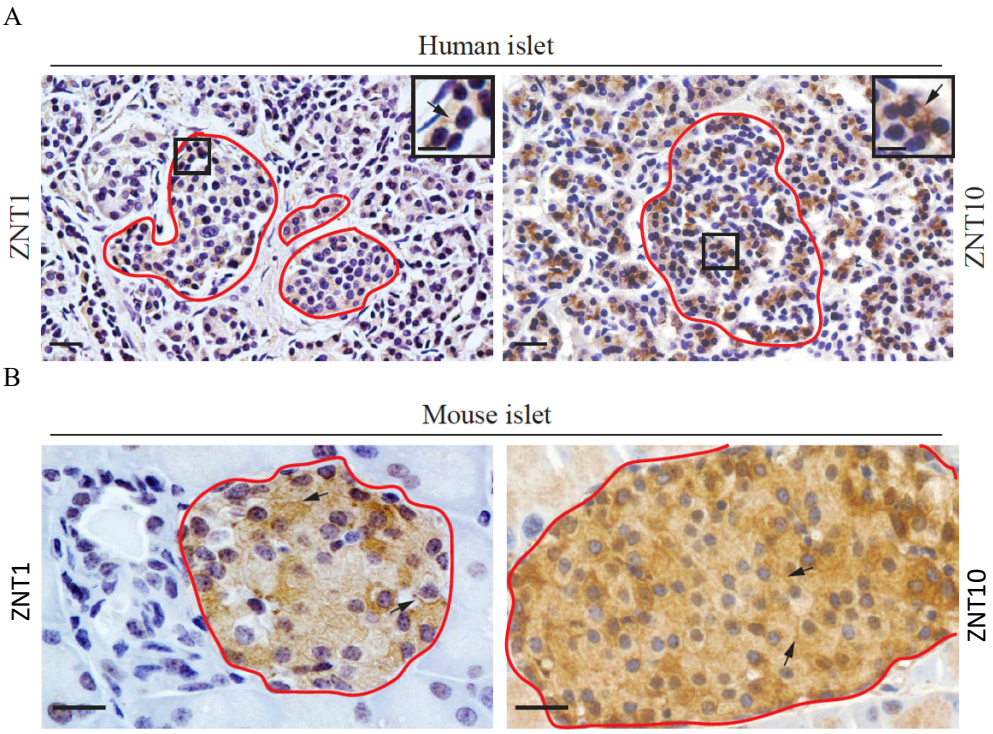

Figure 5. Expression of the subfamily III ZNT proteins in the human and mouse islets. A. Human ZNT1 and ZNT10. The immunoreactivities for ZNT1 and ZNT10 were examined in the pancreatic sections prepared from 66- and 71-year-old male donors. Representative images are displayed. Scale bar = 20 μm. Inserts are higher magnifications of the marked areas (square boxes). Arrows in the inserts indicate the immunoreactivities. The scale bar in the insert = 10 μm. B. Mouse ZNT1 and ZNT10. Brown color shows immunoreactivities of ZNT1 and ZNT10 proteins. Sections were counterstained with hematoxylin. The islet of Langerhans is encircled in red. Scale bar = 20 μm.

For ZNT1 and ZNT10 of the ZNT subfamily III, we showed that both zinc transporters were expressed in human and mouse islets and could be detected in the cytoplasm as well as on the cell membrane (Fig. 5). For ZNT6 and ZNT9 of the subfamily IV, strong immunoreactivities of ZNT6 were found in the human islets with a punctate pattern of heterogeneous vesicles of different sizes (Fig. 6A). It appeared that the ZNT6 immunoreactivity was enriched in large particles (Fig. 6A). In the mouse islet, heterogeneous staining was also observed for ZnT6 (Fig.

6B), but it was not as apparent as that observed in the human islets (Fig. 6A). ZNT9 was expressed in both human and mouse islets (Fig. 6). It was noticeable that the mouse ZnT9 staining (Fig. 6B) was more homogeneous than the human ZNT9 in the islets (Fig. 6A). Moreover, the human islet displayed different levels of staining activity for ZNT9 with some endocrine cells showing strong expression and others showing weak expression (Fig. 6A).

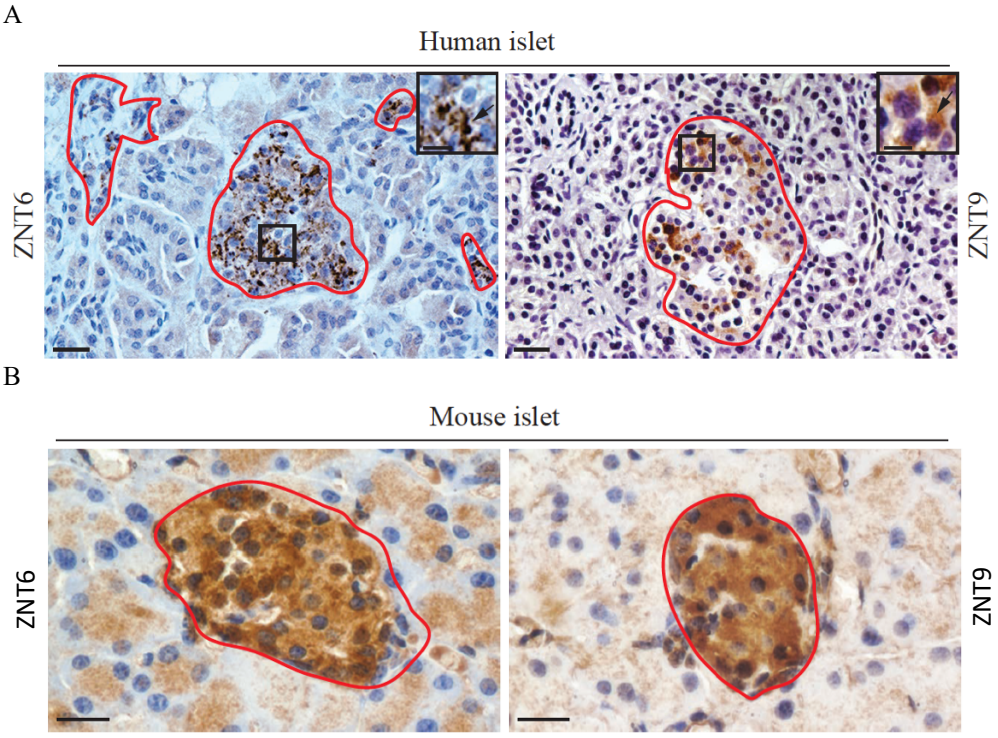

Figure 6. Expression of the subfamily IV ZNT proteins in the human and mouse islets. A. Human ZNT6 and ZNT9. Immunohistochemical staining of both ZNT proteins was carried out as described in Materials and Methods. Representative images are displayed. Scale bar = 20 μm. Inserts are higher magnifications of the marked areas (square boxes). Arrows in the inserts indicate the immunoreactivities. The scale bar in the insert = 10 μm. B. Mouse ZNT6 and ZNT9. Brown color shows immunoreactivities of ZNT5 and ZNT7. Sections were counterstained with hematoxylin. The islet of Langerhans is encircled in red. Scale bar = 20 μm.

Cellular Localization of ZNT1-10 in Human and Mouse Insulin-secreting β-cells

Our immunohistochemistry results in human and mouse pancreatic islets suggested that most ZNT proteins could be expressed in β-cells (Figs. 3-6). Therefore, we further investigated the expression of ZNT1-10 in a human β-cell line (1.1B4-KH5) and a mouse β-cell line (MIN6) by

immunofluorescence microscopic analysis. The human 1.1B4 β-cell line was originally developed by McCluskey et al (17). However, we detected heterogeneity for the expression of insulin in this cell line (data not shown). Thus, we decided to sub-clone the cell line for high insulin expression. The subline, 1.1B4-KH5, had an approximately 2-fold increase in insulin mRNA expression compared to the parental line and insulin was readily detectable in this line (data not shown). As shown in Figs 7-10, immunofluorescence microscopic analysis indicated that all ten ZNT proteins were expressed in this subcloned β-cell line. Eight of the ten ZNT proteins (ZNT3-10) resided exclusively in the cytoplasm of the human and mouse β-cells. The rest of two ZNT proteins, ZNT1 and ZNT2, were detected both in the cytoplasm and on the cytoplasmic membrane (Figs. 8 & 9). Among the intracellularly expressed ZNT proteins, ZNT4, ZNT6, and ZNT8 displayed a punctate staining pattern scattered in the cytoplasm with slight variations in particle sizes (Figs. 8 & 10). ZNT5 was detected in the cytoplasm of both human and mouse β-cells with a particulate/tubular punctate structure (Fig. 7), reminiscent of its Golgi and/or ER localization (25). The subcellular localization of ZNT7 was more concentrated in the perinuclear region (Fig. 7) in the human and mouse β-cells, consistent with its Golgi apparatus localization (13). Similar to ZNT7, the expression of ZNT9 and ZNT10 were mostly detected in the perinuclear region of the β-cells with a punctate staining pattern (Fig. 9 & 10). Moreover, in agreement with our immunohistochemistry results (Fig. 4B), ZNT3 was expressed in the human β-cells (with a scattered punctate staining pattern), but not in the mouse β-cells. Taken together, a majority of the ZNT proteins was expressed in the β-cells of the human or mouse origin with very similar cellular localization between the two species.

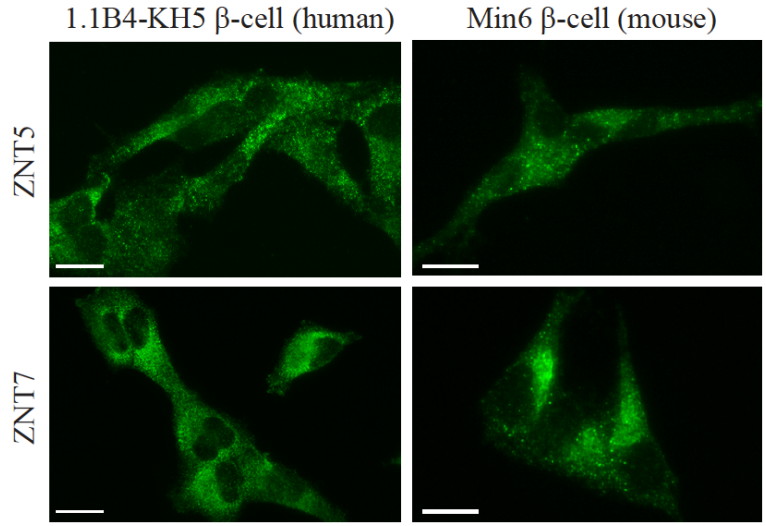

Figure 7. Micrographs of the immunofluorescently stained subfamily I ZNT proteins in human and mouse β-cells. a. Micrographs of ZNT5 and ZNT7 in human 1.1B4-KH5 β-cells. b. Micrographs of ZNT5 and ZNT7 in mouse MIN6 β-cells. Immunofluorescent staining was performed as described in Materials and Methods. Both ZNT5 and ZNT7 were detected intracellularly. Representative images are shown. Scale bar = 20 μm.

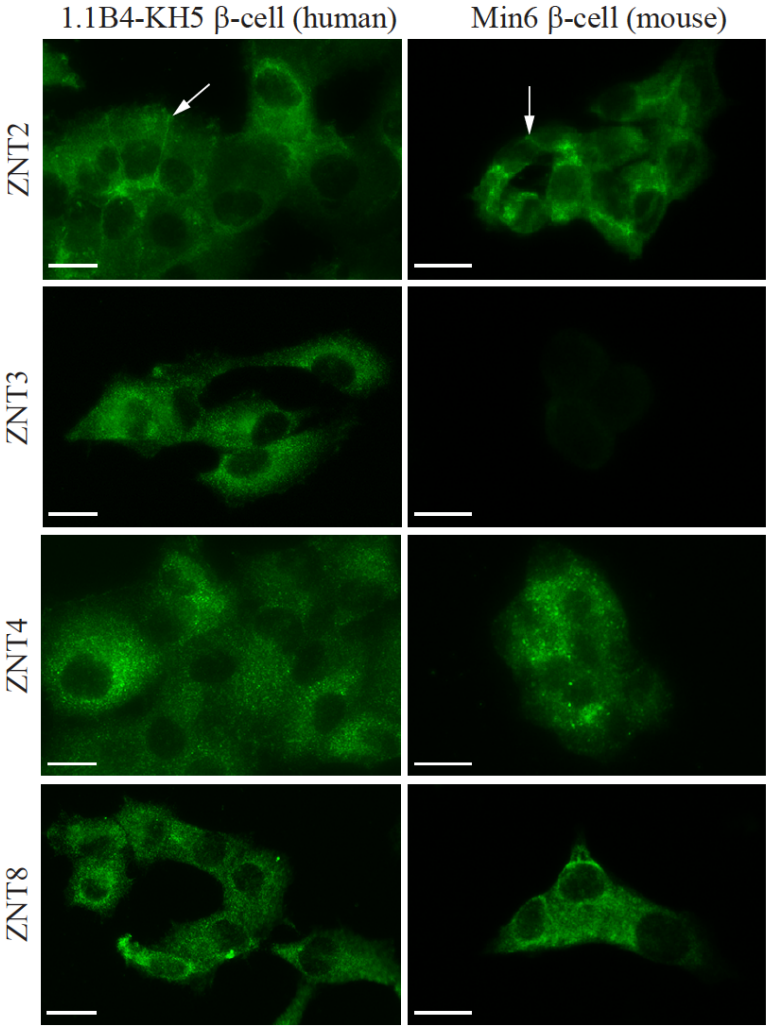

Figure 8. Micrographs of the immunofluorescently stained subfamily II ZNT proteins in human and mouse β-cells. a. Micrographs of ZNT2-4 and ZNT8 in human 1.1B4-KH5 β-cells. b. Micrographs of ZNT2-4 and ZNT8 in mouse MIN6 β-cells. Immunofluorescent staining was performed as described in Materials and Methods. ZNT2-4 and ZNT8 were all detected intracellularly. In addition to its cytoplasmic localization, ZNT2 was also localized on the cell surface of both human and mouse β-cells. Arrows indicate the cytoplasm membrane staining of ZNT2. Representative images are shown. Scale bar = 20 μm.

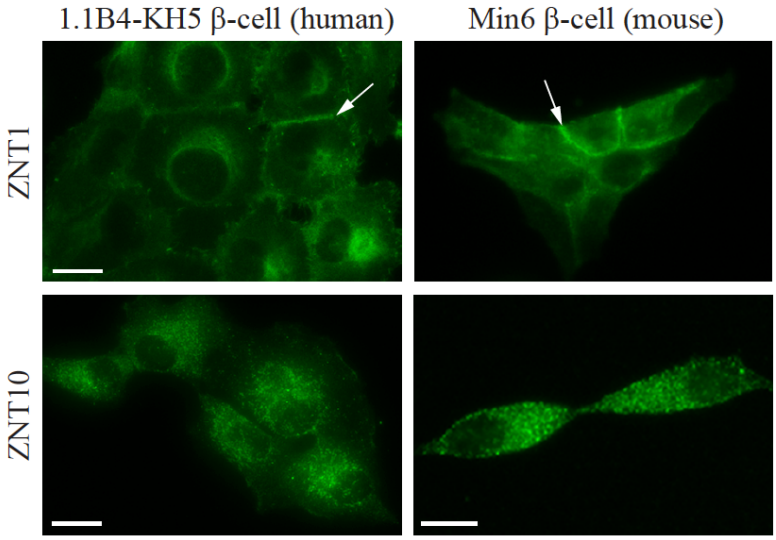

Figure 9. Micrographs of the immunofluorescently stained subfamily III ZNT proteins in human and mouse β-cells. a. Micrographs of ZNT1 and ZNT10 in human insulin-producing 1.1B4-KH5 β-cells. b. Micrographs of ZNT1 and ZNT10 in mouse MIN6 β-cells. Immunofluorescent staining was performed as described in Materials and Methods. ZNT1 was localized both in the cytoplasm and the plasma membrane of the human and mouse β-cells, while ZNT10 was only detected in the cytoplasm of the β-cells from humans and mice. Arrows indicate the cytoplasm membrane staining of ZNT1. Representative images are shown. Scale bar = 20 μm.

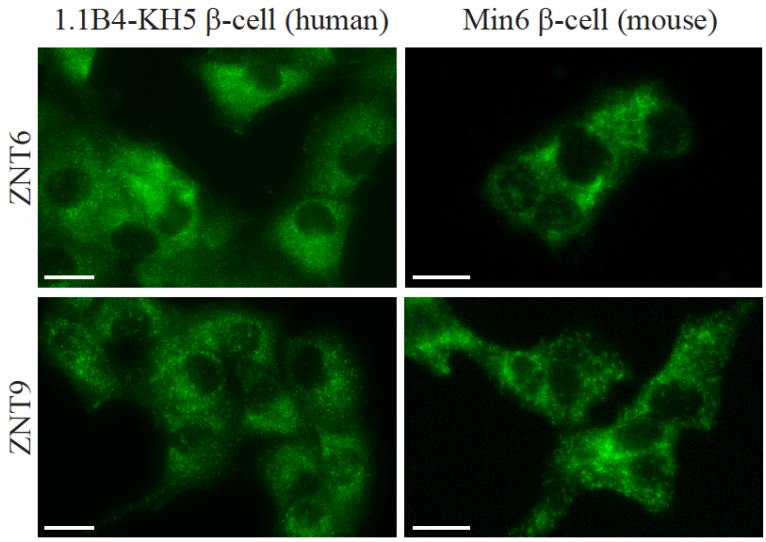

Figure 10. Micrographs of the immunofluorescently stained subfamily IV ZNT proteins in human and mouse β-cells. a. Micrographs of ZNT6 and ZNT9 in human 1.1B4-KH5 β-cells. b. Micrographs of ZNT6 and ZNT9 in

mouse MIN6 β-cells. Immunofluorescent staining was performed as described in Materials and Methods. Both ZNT6 and ZNT9 were detected intracellularly. Representative images are shown. Scale bar = 20 μm.

Discussion

We have investigated the expression and cellular localization of ten members of the ZNT family in human and mouse pancreatic islets and in cultured human and mouse β-cells by immunohistochemistry and immunofluorescence microscopic analysis, respectively. Our results revealed that all ten ZNT proteins were expressed in the human islets, while nine of them (except ZNT3) were detected in the mouse islets with similar expression patterns to their respective human counterparts. Our data have confirmed the expression and cellular localization of ZnT1 and ZnT4-8 reported previously in β-cells or other cell types in rodents (7, 12–14, 25).

An interesting finding in our study is the cell surface localization of ZNT2 in both human and mouse β-cells (Fig. 8). ZNT2 has been shown to be expressed on the membrane of vesicles, and is involved in zinc sequestration in secretory vesicles of lactating mammary gland (24). Human ZNT2, like mouse ZnT4 (11), is responsible for the deposition of zinc into the milk via exocytosis. Mutations or SNPs in the human *ZNT2* gene cause transient neonatal zinc deficiency (26, 27), whereas a null-mutation in the mouse *Znt4* gene (*lethal milk*) causes neonatal death (11). In the present study, we demonstrated that ZNT2 was localized on the cell surface of both human and mouse β-cells, suggesting that ZNT2 may have function in direct export of zinc out of the β-cell, a role similar to that of ZNT1. Although further studies are needed to confirm this assumption, it is conceivable that ZNT2 may carry out a different function in the β-cell compared to the mammary epithelial cell in regulation of cellular zinc homeostasis. Perhaps, β-cells are more sensitive to changes in cellular zinc concentrations than other cell types in the body. In fact, it has been demonstrated that elevations of vesicular zinc concentrations in β-cells by increased expression or

activity of ZNT8 can result in β-cell death, whereas down-regulation of ZNT8 promoters β-cell survival (16, 28). In addition, high concentrations of zinc (50 to 100 μM) has been shown to induce cell death in Burkitt lymphoma B cells (29). It may also be true for β-cells that an elevation of cellular zinc concentration can induce cell death. Therefore, an extra zinc exporter may be necessary for β-cell biology. Further studies are required to reveal how ZNT1 and ZNT2 can coordinate together to export zinc out the β-cell in both physiological and pathological conditions.

The expression of ZNT9 and ZNT10 has not been comprehensively studied in human and mouse islets or β-cells. We report here that both ZNT9 and ZNT10 are expressed in human and mouse islets as well as in β-cells. We found that ZNT9 was expressed intracellularly in endocrine cells of the islet and displayed perinuclear and vesicular staining patterns in both human and mouse β-cells. We also found that the expression of ZNT10 was readily detected on the cell surface of endocrine cells of the human and mouse islets. But this plasma membrane localization of ZNT10 was not observed in cultured human and mouse β-cells. Rather a punctate vesicular staining pattern was observed in these β-cells, which agrees with the endosome localization of ZNT10 found in neuroblastic PC12 cells (30). However, ZNT10 has been shown to be translocated to the plasma membrane of PC12 cells when extracellular zinc concentrations are high (31). The cell surface staining of ZNT10 in the endocrine cells of the human and mouse islets suggests that extracellular zinc concentrations may be high in the islets, leading to its plasma membrane translocation (32). Moreover, ZNT10 has been implicated in regulation of manganese homeostasis as a manganese transporter (33). The role of ZNT10 in zinc and/or manganese homeostasis in pancreatic endocrine cells, especially the β-cell, needs to be further explored based on our immunohistochemistry and cell staining data.

It has been shown that biological processes and genes are about 80% conserved between humans and mice (34). In this study, we report a similar degree of conservation of co-expression of the ZNT proteins in human and mouse islets as well as in β-cells. Although the pancreatic islets of humans and mice have structural differences, the islets have strong functional similarities between the two species. In both species, islets contain different types of endocrine cells where the majority of these cells (70-80%) are insulin-producing β-cells (22, 35). In the mouse islet, β-cells mainly reside in the core of the islet, while glucagon-producing α cells were at the periphery of the islet. Other endocrine cells are distributed between α and β cells in the mouse islet (36). This characteristic core β-cell staining pattern was clearly revealed in the mouse islet stained with ZnT5 in the current study (Fig. 5B), consistent with a previous report (37). Because endocrine cells in the human islet are randomly distributed throughout the islet compared to that of the mouse (36), this distinctive β-core staining was not observed in the human islet (Fig. 5A).

Association of zinc with risks of insulin resistance and development of T2D becomes strong after genome-wide association studies found a link of a risk allele of ZNT8 (R325; rs132663) to T2D in humans (38–40). Growing evidence has shown that ZNT8 plays a pivotal role in insulin crystallization, a process requires zinc. In humans, individuals carrying a ZNT8 R325 variant are likely to have abnormal glucose tolerance (41). A recent study has also demonstrated that ZNT8 with the R325 variant has higher zinc transport activity than the W325 variant, suggesting a link of high zinc transporter activity of the R325 variant to risks of T2D. We also reported that ZNT8 expression was higher in the human islets with T2D and mouse islets with diet-induced insulin resistance. It appears that increased ZNT8 expression or increased ZNT8 activity is harmful for the function of the β-cells. This notion is strongly supported by the observation that individuals who carry a null-mutation allele of ZNT8 are protected from T2D

(42). The mechanism underlying the high risk of the ZNT8 R325 variant for T2D is still not completely understood. Mouse models of *Znt8*-null or over-expression become important for dissection of the mechanisms. Mice with *Znt8*-null mutations (both global and β-cell specific KO) have significantly lower zinc content in the secretory granule of the β-cell, consistent with the function of ZNT8 in zinc transport into the secretory granule (43, 44). However, the physiological impact of the *Znt8*-null mutation on β-cell function and whole body glucose utilization varies in mice from none to mild effect (45). These data suggest that compensations of other ZNT proteins from the loss of *Znt8* in the β-cells or other endocrine cells cannot be excluded. Therefore, knowledge of particular species similarities and differences in the expression of the ZNT proteins between human and mouse islets and β-cells becomes a must in regard to the interpretation of data based on mouse studies to humans. Our study suggests that the expression of the ZNT proteins in the human islet was essentially similar to that of the mouse ZNTs, strongly indicating conservation of function between the two species. Similar expression and localization of the ZNT proteins observed in the β-cells between the two species also suggest that mice are suitable models for studying metabolic diseases associated with disrupted zinc metabolism due to mutations in zinc transporter genes or dietary zinc deficiency.

In this study, we showed that ZNT3 was expressed in the human islets and β-cells, while little to no expression of ZNT3 was detected in the mouse (Figs. 4 & 8). It has been shown that the expression of ZNT3 protein is primarily detected in synaptic vesicles of zinc-rich neurons in the brain, and it is responsible for synaptic vesicular zinc sequestration (46). A null mutation of *Znt3* in mice is dispensable for growth, reproduction, and sensorimotor functions (23). Although zinc content is depleted by the null mutation in the synaptic vesicles of neurons, the *Znt3* knockout mice do not show any neurological abnormalities, included learning deficit and memory loss, until

they age (47). ZNT3 has been demonstrated to be implicated in insulin production in mouse INS-1E β-cells and glucose control in *Znt3* KO mice. In INS-1E β-cells, elevated glucose levels stimulate *Znt3* mRNA expression, while knocking-down *Znt3* expression reduces insulin expression and secretion. Treatment of *Znt3* KO mice with a high-dosage of streptozotocin (200 mg/kg/day), a toxin to β-cells, results in slightly severe impaired glucose metabolism in the KO mice compared to the controls (48). However, it is worth noting that ZNT3 has not been detected previously in both *in silico* analysis (49) and in immunohistochemical analysis of the mouse pancreas (50).

In summary, we have demonstrated that all the members of the SLC30A family are expressed in the human islets and β-cells. We conclude that mice with or without genetic modifications can be suitable animal models to study mechanisms underlying zinc-insulin-associated glucose metabolism as a majority of the ZNT proteins were expressed in the mouse islets and β-cells with very similar expression patterns and localization to the human counterparts. In cultured human and mouse β-cells, all expressed ZNT proteins could be detected intracellularly, except for ZNT3 in mouse, while ZNT1 and ZNT2 were also detected on the plasma membrane of the β-cells. Our study suggests that zinc homeostasis is vital for the endocrine component of the pancreas evident by the extensive expression of the ZNT proteins. The results from the current study are critical for future studies to elucidate the factors that regulate zinc transporters and their association with β-cell function in the physiological and pathological conditions.

References

1. Sondergaard, L.G., Stoltenberg, M., Flyvbjerg, A., Brock, B., Schmitz, O., Danscher, G. and Rungby, J. (2003) Zinc ions in beta-cells of obese, insulin-resistant, and type 2 diabetic rats traced by autometallography. *APMIS*. **111**, 1147–1154
2. Wodak, S.J., Alard, P., Delhaise, P. and Renneboog-Squilbin ,C. (1985) Simulation of conformational changes in 2 Zn insulin. *J. Mol. Biol.* **181**, 317–322
3. Huang, L., Yan, M., Kirschke, C.P. (2010) Over-expression of ZnT7 increases insulin synthesis and secretion in pancreatic beta-cells by promoting insulin gene transcription. *Exp. Cell Res.* **316**, 2630–2643
4. Huang, L., Kirschke, C.P., Lay, Y.A., Levy, L.B., Lamirande, D.E. and Zhang, P.H. (2012) Znt7-null mice are more susceptible to diet-induced glucose intolerance and insulin resistance. *J. Biol. Chem.* **287**, 33883–33896
5. Davidson, H. W., Rhodes, C. J., and Hutton, J. C. (1988) Intraorganellar calcium and p H control proinsulin cleavage in the pancreatic β cell via two distinct site-specific endopeptidases. *Nat. 1988 3336168*. **333**, 93–96
6. Smeekens, S. P., Montag, A. G., Thomas, G., Albiges-Rizo, C., Carroll, R., Benig, M., Phillips, L. A., Martin, S., Ohagi, S., Gardner, P., et al. (1992) Proinsulin processing by the subtilisin-related proprotein convertases furin, PC2, and PC3. *Proc. Natl. Acad. Sci. U. S. A.* **89**, 8822
7. Wijesekara, N., Dai, F.F., Hardy, A.B., Giglou, P.R., Bhattacharjee, A., Koshkin,V., Chimienti, F., Gaisano, H.Y., Rutter, G.A. and Wheeler, M.B. (2010) Beta cell-specific Znt8 deletion in mice causes marked defects in insulin processing, crystallisation and secretion. *Diabetologia*. **53**, 1656–1668

8. Dunn, M.F. (2005) Zinc-ligand interactions modulate assembly and stability of the insulin hexamer -- a review. *Biometals*. **18**, 295–303

9. Lemaire, K., Ravier, M.A., Schraenen, A., Creemers, J.W., Van de Plas, R., Granvik, M., Van Lommel, L., Waelkens, E., Chimienti, F., Rutter, G.A., et al. (2009) Insulin crystallization depends on zinc transporter ZnT8 expression, but is not required for normal glucose homeostasis in mice. *Proc. Natl. Acad. Sci. U. S. A.* **106**, 14872–14877

10. Kirschke, C.P. and Huang, L. (2008) Expression of the ZNT (SLC30) family members in the epithelium of the mouse prostate during sexual maturation. *J. Mol. Histol.* **39**, 359–370

11. Huang, L. and Gitschier, J. (1997) A novel gene involved in zinc transport is deficient in the lethal milk mouse. *Nat. Genet.* **17**, 292–297

12. Huang, L., Kirschke, C.P. and Gitschier, J. (2002) Functional characterization of a novel mammalian zinc transporter, ZnT6. *J. Biol. Chem.* **277**, 26389–26395

13. Kirschke, C.P. and Huang, L. (2003) ZnT7, a novel mammalian zinc transporter, accumulates zinc in the Golgi apparatus. *J. Biol. Chem.* **278**, 4096–4102

14. Yu, Y.Y., Kirschke, C.P. and Huang, L. (2007) Immunohistochemical analysis of ZnT1, 4, 5, 6, and 7 in the mouse gastrointestinal tract. *J. Histochem. Cytochem.* **55**, 223–234

15. Kelleher, S. L., and Lönnerdal, B. (2002) Zinc Transporters in the Rat Mammary Gland Respond to Marginal Zinc and Vitamin A Intakes during Lactation. *J. Nutr.* **132**, 3280–3285

16. Huang, L., and Kirschke, C. P. (2016) Down-Regulation of Zinc Transporter 8 (SLC30A8) in Pancreatic Beta-Cells Promotes Cell Survival. *Austin J Endocrinol Diabetes*. **3**, 1037

17. McCluskey, J.T., Hamid, M., Guo-Parke, H., McClenaghan, N.H., Gomis, R. and Flatt, P.R. (2011) Development and functional characterization of insulin-releasing human pancreatic

beta cell lines produced by electrofusion. *J. Biol. Chem.* **286**, 21982–21992

18. Freshney, R.I. (2010). Culture of Animal Cells: A Manual of Basic Technique and Specialized Applications, 6th ed, Wiley-Blackwell

19. Petersen, A.B., Smidt, K., Magnusson, N.E., Moore, F., Egefjord, L. and Rungby, J. (2011) siRNA-mediated knock-down of ZnT3 and ZnT8 affects production and secretion of insulin and apoptosis in INS-1E cells. *APMIS*. **119**, 93–102

20. Beger, T. P. (2008) The pancreas : an integrated textbook of basic science, medicine, and surgery, 2ed, Blackwell Publishing Inc.

21. Brissova, M., Fowler, M. J., Nicholson, W. E., Chu, A., Hirshberg, B., Harlan, D. M., and Powers, A. C. (2005) Assessment of human pancreatic islet architecture and composition by laser scanning confocal microscopy. *J. Histochem. Cytochem.* **53**, 1087–1097

22. Wierup, N., Svensson, H., Mulder, H. and Sundler, F. (2002) The ghrelin cell: a novel developmentally regulated islet cell in the human pancreas. *Regul. Pept.* **107**, 63–69

23. Cole, T. B., Wenzel, H. J., Kafer, K. E., Schwartzkroin, P. A., and Palmiter, R. D. (1999) Elimination of zinc from synaptic vesicles in the intact mouse brain by disruption of the ZnT3 gene. *Proc. Natl. Acad. Sci.* **96**, 1716–1721

24. Lee, S., Hennigar, S. R., Alam, S., Nishida, K., and Kelleher, S. L. (2015) Essential Role for Zinc Transporter 2 (ZnT2)-mediated Zinc Transport in Mammary Gland Development and Function during Lactation. *J. Biol. Chem.* **290**, 13064

25. Thornton, J. K., Taylor, K. M., Ford, D., and Valentine, R. A. (2011) Differential Subcellular Localization of the Splice Variants of the Zinc Transporter ZnT5 Is Dictated by the Different C-Terminal Regions. *PLoS One*. **6**, e23878

26. Chowanadisai, W., Lonnerdal, B. and Kelleher, S.L. (2006) Identification of a mutation in

SLC30A2 (ZnT-2) in women with low milk zinc concentration that results in transient neonatal zinc deficiency. *J. Biol. Chem.* **281**, 39699–39707

27. Itsumura, N., Kibihara, Y., Fukue, K., Miyata, A., Fukushima, K., Tamagawa-Mineoka, R., Katoh, N., Nishito, Y., Ishida, R., Narita, H., et al. (2016) Novel mutations in SLC30A2 involved in the pathogenesis of transient neonatal zinc deficiency. *Pediatr. Res.* **80**, 586–594

28. Merriman, C., Huang, Q., Rutter, G.A. and Fu, D. (2016) Lipid-tuned Zinc Transport Activity of Human ZnT8 Protein Correlates with Risk for Type-2 Diabetes. *J. Biol. Chem.* **291**, 26950–26957

29. Schrantz, N., Auffredou, M.T., Bourgeade, M.F., Besnault, L., Leca, G. and Vazquez, A. (2001) Zinc-mediated regulation of caspases activity: dose-dependent inhibition or activation of caspase-3 in the human Burkitt lymphoma B cells (Ramos). *Cell Death Differ.* **8**, 152–161

30. Zhao, Y., Feresin, R.G., Falcon-Perez, J.M. and Salazar, G. (2016) Differential Targeting of SLC30A10/ZnT10 Heterodimers to Endolysosomal Compartments Modulates EGF-Induced MEK/ERK1/2 Activity. *Traffic*. **17**, 267–288

31. Bosomworth, H.J., Thornton, J.K., Coneyworth ,L.J., Ford, D. and Valentine, RA. (2012) Efflux function, tissue-specific expression and intracellular trafficking of the Zn transporter ZnT10 indicate roles in adult Zn homeostasis. *Metallomics*. **4**, 771–779

32. Zalewski, P.D, Millard, S.H, Forbes, I.J, Kapaniris, O., Slavotinek, A., Betts, W.H., Ward, A.D., Lincoln, S.F. and Mahadevan, I. (1994) Video image analysis of labile zinc in viable pancreatic islet cells using a specific fluorescent probe for zinc. *J. Histochem. Cytochem.* **42**, 877–884

33. Nishito, Y., Tsuji, N., Fujishiro, H., Takeda, T.A., Yamazaki, T., Teranishi, F., Okazaki, F., Matsunaga, A., Tuschl, K., Rao, R., et al. (2016) Direct Comparison of Manganese Detoxification/Efflux Proteins and Molecular Characterization of ZnT10 Protein as a Manganese Transporter. *J. Biol. Chem.* **291**, 14773–14787

34. Cox, B., Kotlyar, M., Evangelou, A.I., Ignatchenko, V., Ignatchenko, A., Whiteley, K., Jurisica, I., Adamson, S.L., Rossant, J. and Kislinger, T. (2009) Comparative systems biology of human and mouse as a tool to guide the modeling of human placental pathology. *Mol. Syst. Biol.* 10.1038/MSB.2009.37

35. Brissova, M., Fowler, M.J., Nicholson, W.E., Chu, A., Hirshberg, B., Harlan, D.M. and Powers, A.C. (2005) Assessment of human pancreatic islet architecture and composition by laser scanning confocal microscopy. *J. Histochem. Cytochem.* **53**, 1087–1097

36. Steiner, D.J., Kim, A., Miller, K. and Hara, M. (2010) Pancreatic islet plasticity: interspecies comparison of islet architecture and composition. *Islets*. 10.4161/ISL.2.3.11815

37. Kambe, T., Narita, H., Yamaguchi-Iwai, Y., Hirose, J., Amano, T., Sugiura, N., Sasaki, R., Mori, K., Iwanaga, T. and Nagao, M. (2002) Cloning and characterization of a novel mammalian zinc transporter, zinc transporter 5, abundantly expressed in pancreatic beta cells. *J. Biol. Chem.* **277**, 19049–19055

38. Saxena, R., Voight, B. F., Lyssenko, V., Burtt, N. P., De Bakker, P. I. W., Chen, H., Roix, J. J., Kathiresan, S., Hirschhorn, J. N., Daly, M. J., Hughes, T. E., Groop, L., and Altshuler, D. (2007) Genome-wide association analysis identifies loci for type 2 diabetes and triglyceride levels. *Science (80-.).* **316**, 1331–1336

39. Scott, L.J., Mohlke, K.L., Bonnycastle, L.L., Willer, C.J., Li, Y., Duren, W.L., Erdos, M.R., Stringham, H.M., Chines, P.S., Jackson, A.U., et al. (2007) A genome-wide association

study of type 2 diabetes in Finns detects multiple susceptibility variants. *Science*. **316**, 1341–1345

40. Sladek, R., Rocheleau, G., Rung, J., Dina, C., Shen, L., Serre, D., Boutin, P., Vincent, D., Belisle, A., Hadjadj, S., et al. (2007) A genome-wide association study identifies novel risk loci for type 2 diabetes. *Nature*. **445**, 881–885

41. Kirchhoff, K., Machicao, F., Haupt, A., Schäfer, S. A., Tschritter, O., Staiger, H., Stefan, N., Häring, H. U., and Fritsche, A. (2008) Polymorphisms in the TCF7L2, CDKAL1 and SLC30A8 genes are associated with impaired proinsulin conversion. *Diabetologia*. **51**, 597–601

42. Flannick, J., Thorleifsson, G., Beer, N. L., Jacobs, S. B. R., Grarup, N., Burtt, N. P., Mahajan, A., Fuchsberger, C., Atzmon, G., Benediktsson, R., Blangero, J., Bowden, D. W., Brandslund, I., Brosnan, J., Burslem, F., Chambers, J., Cho, Y. S., Christensen, C., Douglas, D. A., Duggirala, R., Dymek, Z., Farjoun, Y., Fennell, T., Fontanillas, P., Forsén, T., Gabriel, S., Glaser, B., Gudbjartsson, D. F., Hanis, C., Hansen, T., Hreidarsson, A. B., Hveem, K., Ingelsson, E., Isomaa, B., Johansson, S., Jørgensen, T., Jørgensen, M. E., Kathiresan, S., Kong, A., Kooner, J., Kravic, J., Laakso, M., Lee, J. Y., Lind, L., Lindgren, C. M., Linneberg, A., Masson, G., Meitinger, T., Mohlke, K. L., Molven, A., Morris, A. P., Potluri, S., Rauramaa, R., Ribel-Madsen, R., Richard, A. M., Rolph, T., Salomaa, V., Segrè, A. V., Skärstrand, H., Steinthorsdottir, V., Stringham, H. M., Sulem, P., Tai, E. S., Teo, Y. Y., Teslovich, T., Thorsteinsdottir, U., Trimmer, J. K., Tuomi, T., Tuomilehto, J., Vaziri-Sani, F., Voight, B. F., Wilson, J. G., Boehnke, M., McCarthy, M. I., Njølstad, P. R., Pedersen, O., Groop, L., Cox, D. R., Stefansson, K., and Altshuler, D. (2014) Loss-of-function mutations in SLC30A8 protect against type 2 diabetes. *Nat. Genet.* **46**, 357–363

43. Lemaire, K., Chimienti, F., and Schuit, F. (2012) Zinc transporters and their role in the pancreatic β-cell. *J. Diabetes Investig.* **3**, 202

44. Tamaki, M., Fujitani, Y., Hara, A., Uchida, T., Tamura, Y., Takeno, K., Kawaguchi, M., Watanabe, T., Ogihara, T., Fukunaka, A., Shimizu, T., Mita, T., Kanazawa, A., Imaizumi, M. O., Abe, T., Kiyonari, H., Hojyo, S., Fukada, T., Kawauchi, T., Nagamatsu, S., Hirano, T., Kawamori, R., and Watada, H. (2013) The diabetes-susceptible gene SLC30A8/ZnT8 regulates hepatic insulin clearance. *J. Clin. Invest.* **123**, 4513–4524

45. Davidson, H.W., Wenzlau, J.M. and O'Brien, R.M. (2014) Zinc transporter 8 (ZnT8) and β cell function. *Trends Endocrinol. Metab.* **25**, 415–424

46. Linkous, D. H., Flinn, J. M., Koh, J. Y., Lanzirotti, A., Bertsch, P. M., Jones, B. F., Giblin, L. J., and Frederickson, C. J. (2008) Evidence That the ZNT3 Protein Controls the Total Amount of Elemental Zinc in Synaptic Vesicles. *J. Histochem. Cytochem.* **56**, 3

47. Adlard, P.A., Parncutt, J.M., Finkelstein, D.I. and Bush, A.I. (2010) Cognitive loss in zinc transporter-3 knock-out mice: a phenocopy for the synaptic and memory deficits of Alzheimer's disease? *J. Neurosci.* **30**, 1631–1636

48. Smidt, K., Jessen, N., Petersen, A.B., Larsen, A., Magnusson, N., Jeppesen, J.B., Stoltenberg, M., Culvenor, J.G., Tsatsanis, A., Brock, B., et al. (2009) SLC30A3 responds to glucose- and zinc variations in beta-cells and is critical for insulin production and in vivo glucose-metabolism during beta-cell stress. *PLoS One*. 10.1371/JOURNAL.PONE.0005684

49. Seve, M., Chimienti, F., Devergnas, S., and Favier, A. (2004) In silico identification and expression of SLC30 family genes: An expressed sequence tag data mining strategy for the characterization of zinc transporters' tissue expression. *BMC Genomics*. **5**, 32

50. Zhong, M.L., Chi, Z.H., Shan, Z.Y., Teng, W.P. and Wang, Z.Y. (2012) Widespread expression of zinc transporter ZnT (SLC30) family members in mouse endocrine cells. *Histochem. Cell Biol.* **138**, 605–616

Chapter 3 - *Slc30a8 (Znt8)* allelic insufficiency reduces deleterious effect of high fat intake on lipid metabolism and glucose tolerance in mice

Abstract

Aims/hypothesis

Zinc transporter 8 (ZNT8) transports zinc from the cytoplasm into the secretory vesicle for insulin crystallization and storage in pancreatic beta-cells. Individuals with *ZNT8* allelic insufficiency have reduced risk of type 2 diabetes. However, the underlying mechanism of this protective effect is not well understood. We hypothesized that a reduction in insulin secretion induced by *ZNT8* allelic insufficiency could trigger compensatory reactions leading to reduced glucagon secretion from pancreatic alpha-cells. Thus, normoglycemia could be maintained.

Methods

Znt8$^{+/-}$ and wild type mice were fed a high-fat diet (45% kcal fat) for 17 weeks. The progress of diet-induced insulin resistance was monitored by body weight, fasting and non-fasting blood glucose levels, and insulin and glucose tolerance tests. Weight gain was monitored during the administration of the high-fat diet. Fat accumulation in the adipocytes and livers of experimental animals were determined. Liver glycogen contents and plasma glucagon levels were examined.

Results

Our study indicated that glucose-stimulated insulin secretion was reduced up to ~47% by *Znt8* allelic insufficiency in both genders. Female *Znt8*$^{+/-}$ mice had a tendency to gain less weight (~11%) and had less fat in the adipocytes (~50%) than the control-fed mice after the 17-weeks of dietary challenge (p<0.05). Moreover, female *Znt8*$^{+/-}$ mice displayed lower fasting triglyceride levels (~49%) than the control mice. On the other hand, male *Znt8*$^{+/-}$ mice had an improved glucose tolerance compared to the wild type mice during glucose challenge. Importantly, the total glucagon

secretion assessed by the area under the curve during glucose challenge was significantly lower (~40%) in male *Znt8*$^{+/-}$ mice than the control mice.

Conclusions/interpretation

Our results suggests that *Znt8* allelic insufficiency could provide protective effects on diet-induced glucose intolerance, possibly through regulation of glucagon secretion in male mice and lipid metabolism in female mice.

Introduction

Type 2 diabetes (T2D) affects about 26 million people in the U.S. according to the NIH AMP factsheet of T2D (1). Insulin resistance is a characteristic feature in T2D development (2) and it can trigger a compensatory increase in insulin secretion from pancreatic β-cells to maintain normal or near-normal blood glucose levels. This compensatory reaction leads to hyperinsulinemia. Continued elevations in peripheral insulin resistance, which demand more insulin to be secreted from β-cells eventually cause β-cell death leading to T2D (3).

Pancreatic β-cells contain high levels of zinc that is concentrated in the insulin-containing secretory vesicles (4–6), where zinc together with insulin forms dense core granules for insulin storage within the cell (5). Zinc is brought into these granular vesicles by ZNT8, a zinc transporter protein of the SLC30A family (7). The SLC30A family comprises 10 members (ZNT1-10) that facilitate cellular zinc homeostasis by reducing cytoplasmic zinc when cellular zinc level is high via export or organelle sequestration (8). Most of the ZNT family members are expressed in β-cells of humans and rodents. However, among these expressed ZNT transporters, ZNT8 is the only one that is primarily expressed and mainly responsive for zinc enrichment in the granules of the β-cell (7, 9). Genome-wide association studies (GWAS) have shown that individuals carrying a single nucleotide polymorphism (SNP) (R325W) (dbSNP ID: rs13266634) in the C-terminal end of the ZNT8 protein have increased risk of T2D (10). Moreover, this R allele of *ZNT8* is the predominant allele in human populations that is linked to the increased risk of T2D (11). It is reported that both basal and glucose-stimulated insulin secretion are negatively affected by the risk allele of *ZNT8* (12, 13), which is likely associated with impaired glucose tolerance in these carriers (14). In addition, the risk allele of *ZNT8* can act as an autoantigen in the development of type 1 diabetes (T1D) in children and young adults (15, 16).

While ZNT8 expression is greatly upregulated in the islets of the T2D pancreas in both humans and mice, this may have an undesirable consequence to β-cell functions and survival during insulin resistance and T2D development (17). Indeed, results from another GWAS suggest that *ZNT8* allelic insufficiency (individuals carrying a null allele of *ZNT8*) may be associated with reduced risk of T2D by more than 60% (18). This association challenges a widely accepted notion that a defect in the ZNT8-mediated insulin secretion is associated with T2D. In animal models of human T2D, the *Znt8*-null mutations in mice [both global and β-cell specific knockouts (KO)] significantly lowered the zinc content in the secretory granules of β-cells, which is consistent with the function of ZNT8 (19, 20). As such, *Znt8* KO mice had reduced numbers of insulin-containing granules as well as increased numbers of atypical granules in β-cells (9, 21). Nevertheless, it is worth noting that the physiological impact of these *Znt8*-null mutations on β-cell function and whole body glucose utilization are minimal and vary in mice, which is largely dependent on the genetic background of the KO mice (22). Finally, in humans, a small group of people who carries only one functional copy of *Znt8* were found to have reduced non-fasting glucose levels and a reduced blood glucose surge at 60 min after an oral glucose challenge, suggesting a beneficial effect of *ZNT8* allelic insufficiency on glucose homeostasis (18).

In the present study, we aimed to uncover the underlying mechanisms of the protective effect of *Znt8* allelic insufficiency on T2D using a $Znt8^{+/-}$ mouse model. We fed $Znt8^{+/-}$ and wild type (WT) control mice a moderately high-fat diet (45% kcal) for 17 weeks (3-20 weeks of age) to induce insulin resistance. The results indicated that glucose-stimulated insulin secretion was reduced by *Znt8* allelic insufficiency. We noticed that female $Znt8^{+/-}$ mice gained less weight than their WT littermates and had better lipid profiles. Moreover, we found that male $Znt8^{+/-}$ mice could handle blood glucose better than the control after glucose challenge. Fasting blood glucagon levels

in male *Znt8*$^{+/-}$ mice were significantly lower than that in the control-fed mice. The total glucagon secretion assessed by the area under the curve during glucose challenge was significantly lower in male *Znt8*$^{+/-}$ mice than the control mice. Our current study suggests that reduced expression of ZNT8 introduced by *ZNT8* allelic insufficiency may have a positive outcome for the control of whole-body glucose homeostasis in humans.

Materials and methods

Animals and diets

Mice (*Slc30a8*$^{tm1a(KOMP)Wtsi}$, herein *Znt8*$^{+/-}$, and WT littermates in the genetic background of C57BL/6N) were cryo-recovered from the KOMP Repository at the University of California, Davis. *Znt8*$^{+/-}$ male mice were mated to the WT female littermates for the mouse colony maintenance. The majority of experimental mice in the current study were generated by this breeding strategy. *Znt8*$^{-/-}$ mice were generated by *Znt8*$^{+/-}$ sibling mating. Mice were housed in a temperature-controlled room at 22-24^{o}C with a 12 h light-dark cycle. Breeder pairs were maintained on a regular laboratory chow diet (Laboratory Rodent Diet 5001, Lab-Diet, Brentwood, MO) and double-distilled water *ad libitum*. The experimental mice (male and female Znt8+/- and WT littermates, n=8-12/genotype/sex) were weaned at 3 weeks of age and then fed a moderately high-fat diet (45% kcal fat, D12451; Research Diets, New Brunswick, NJ) *ad labium* for 17 weeks. All animal experiments were conducted in accordance with National Institutes of Health Guidelines for the Care and Use of Experimental Animals and were approved by the Institutional Animal Care and Use Committee of the University of California, Davis.

Isolation of genomic DNA and genotyping

Genomic DNA was isolated from the mouse tail or ear clips using a DNeasy Tissue Kit (Qiagen, Valencia, CA). PCR was used for genotyping. PCR products of *Znt8*$^{+/-}$ mice yielded two distinct bands: a 573-bp DNA fragment (the *Znt8* knockout allele) and a 376-bp DNA fragment (the WT allele) according to the protocol provided by the KOMP repository at the University of California, Davis. PCR products were detected by agarose-gel electrophoresis. Primers were as follows: LoxP-forward (5'-GAGATGGCGCAACGCAATTAAT-3') and *Znt8* KO-reverse (5'-TGAATGTATGTGTGTGCATGTGTGGG-3'); *Znt8*-forward: 5'-TCAAGATTCAGAATCAGTGTCATCTGG-3' and *Znt8*-tt-reverse: 5'-AGACACCTGATCATGCATTTGCACC-3'.

Weight and blood glucose monitoring

Body weight was recorded weekly between 8:00 and 10:00 in the morning. Fasting blood glucose concentrations were determined at 10 and 18 weeks of age and non-fasting blood glucose levels at 11 and 19 weeks of age between 7:00 and 9:00 in the morning. Blood was collected from the tail vein and blood glucose levels were determined by a One-Touch UltraMini glucometer (LifeScan, Milpitas, CA).

Intraperitoneal insulin tolerance test (IPITT)

Mice at 17-week-old were fasted for 4 h (07:30-11:30) before the test. Drinking water was supplied during fasting. Blood samples were collected from the mouse tail vein and blood glucose levels were determined by a One-Touch UltraMini glucometer (LifeScan) during IPITT. After the baseline glucose levels were determined, mice were weighed and intraperitoneally injected with

Humulin® (100 mU/mL, 5.5 U/kg of body weight; Lilly, Indianapolis, IN). Blood glucose levels were then determined at 15, 30, 60, and 120 min after the insulin injection.

Intraperitoneal Glucose tolerance test (IPGTT), plasma insulin, and glucagon measurements

Mice at 18-week-old were fasted overnight (16-18 h) before the test. Drinking water was supplied during fasting. A baseline glucose level was determined by a glucometer using the blood sample collected from the tail vein. Mice were then weighed and intraperitoneally injected with sterile glucose solution (20%, 1.5 g/kg of body weight). Blood glucose, insulin and glucagon levels were then determined at 15, 30, 60, and 120 min after the injection of glucose. Insulin levels were determined by a mouse ultrasensitive insulin enzyme-linked immunosorbent assay (ELISA) kit (ALPCO, Salem, NH) and glucagon was measured by a mouse glucagon ELISA kit (Crystal Chem. Elk Grove village, IL).

Final blood collection, organ/tissue dissection, and fixation

Mice were anesthetized at 20-week-old by intraperitoneal injection of 100mg/kg ketamine (MWI Veterinary Supply, Boise, ID) plus 10 mg/kg xylazine (MWI Veterinary Supply). Final blood collection was performed via retro-orbital eye bleeding or cardiac puncture. Euthanasia was confirmed by cervical dislocation. Plasma was collected by centrifugation of blood samples at 960 g for 15 min at 4°C. Collected plasma was then snap frozen in liquid nitrogen and stored at -80ºC until use. Carcass weight, liver weight, and fat pad weight (epididymal, subcutaneous and retroperitoneal) were recorded at necropsy. Dissected tissues were snap-frozen in liquid nitrogen or fixed in 4% paraformaldehyde made in 1x PBS, pH 7.4 (PFA, ThermoFisher Scientific, Waltham, MA) overnight at room temperature (RT) with gentle shaking and then stored in 80%

ethanol at 4ºC until use. Subsequent tissue embedding and sectioning were carried out as described previously (23).

β-galactosidase staining

The pancreas was dissected at necropsy, rinsed in cold 1x PBS, and placed in 4% PFA. Samples were then transferred into ice-cold 30% (v/v) sucrose solution containing 2 mM $MgCl_2$ and incubated at 4ºC overnight. The solution was replaced with ice-cold OCT solution made in 30% sucrose (1:1, v/v) and incubated again at 4ºC overnight followed by embedding of the tissue in a cryo-cassette with OCT using a liquid nitrogen chilled isopentane bath. The OCT block was sectioned at 10 μm thickness and allowed to air dry at room temperature (RT) overnight. Before staining, the section was placed at 37ºC for 30 min and then washed in 1x PBS (pH 7.4)/2 mM $MgCl_2$ solution for 20 min at RT with gentle rocking. The washing step was repeated twice followed by incubation of the section in X-gal staining solution (1 mg/mL; ThermoFisher Scientific) at 37°C overnight. The section was then rinsed in 1x PBS for 10 min, washed twice in distilled water for 5 min, counter-stained with Nuclear Fast Red, mounted with Permount (Vector Laboratories, Burlingame, CA), and finally cover-slipped. Stained sections were viewed using a Nikon Eclipse 800 microscope (Nikon Instruments Inc., Melville, NY). Images were acquired via a Nikon Plan Apo 20X/0.75 or a Nikon Plan Fluor 40X/0.75 lens using a SPOT RT3 digital camera (Diagnostic Instrument Inc., Sterling Heights, MI) with SPOT RT Software v3.0.

Histology and immunohistochemistry

Paraffin embedded tissues (fat, liver and pancreas) were sectioned at 5 μm, deparaffinized and rehydrated as described previously (24). Hematoxylin & eosin (H&E) staining was performed

according to a published protocol (25). For immunohistochemistry, antigen retrieval was accomplished in 10 mM sodium citrate (pH 6.0) or 20-100 mM Tris-Cl (pH 10) for 20 min in boiling water. The endogenous peroxidase activity was abolished by treating the sections with 5% H_2O_2 at RT for 15 min. The non-specific binding of biotin/avidin was blocked using an Avidin-Biotin Blocking kit (Vector Laboratories). Tissues were then treated with 3% goat serum to block other non-specific protein bindings. A guinea pig primary anti-mouse ZnT8 polyclonal antibody (generated with the peptide sequence: CASRDSQVVRREIAKALSKSFTM by Genemed Synthesis, Inc., Texas, USA) was diluted 1:1000 in 1x PBS containing 2% mouse and 2% goat sera, applied to the section, and incubated at 4^{o}C overnight. A secondary biotinylated goat anti-guinea pig (Vector Laboratories) antibody was diluted at 1:200-250 in 1x PBS containing 2% goat sera. Immunoreactivities (brown deposits within cells) were detected using a Vectastain ABC kit and an ImmPACT DAB kit from Vector Laboratories. Sections were counterstained with hematoxylin and cover-slipped using permount. Stained sections were viewed using a Nikon Eclipse 800 microscope (Nikon Instruments). Images were acquired using a SPOT RT3 digital camera (Diagnostic Instrument Inc.) with SPOT RT Software v3.0.

Fat cell sizing

The H&E stained fat tissue sections were viewed at 10x magnification and images were taken in three different areas across a full section of the fat tissue. Adiposoft (https://imagej.net/Adiposoft) was used for cell counting and cell size measuring (26).

Measurements of triglycerides and non-esterified fatty-acids (NEFA)

Plasma triglyceride and NEFA concentrations were measured using a L-Type TG M Assay kit (WAKO Diagnostics, Mountain view, CA) and a NEFA kit (HR Series NEFA-HR (2)) (WAKO Diagnostics), respectively. To determine triglyceride and NEFA levels in liver samples, 25-50 mg of liver tissue was homogenized in TPER buffer (50 mg liver/mL TPER) (ThermoFisher Scientific) containing 1x protease and phosphatase inhibitor (ThermoFisher Scientific) using a Geno/grinder® (SPEX SamplePrep, Metuchen, NJ, USA). Five microliters of lysate were used for determining triglyceride (TG) and NEFA concentrations. Protein concentrations in these samples were determined by a BCA Protein Assay kit (ThermoFisher Scientific).

Measurement of glycogen

Liver tissue (5-10 mg) was homogenized in 400 µL of 30% KOH using a Geno/grinder® according to the manufacturer's instruction (SPEX SamplePrep). The homogenized liver tissue was transferred to a 2.0 mL Eppendorf™ Safe-Lock™ tube and incubated for 40 min in boiling water. After incubation, samples were cooled to RT and then kept at 4°C. Next, samples were mixed with 1.25 mL of 95% ethanol, incubated for 5 min in boiling water, cooled to RT, and centrifuged at 10,000x g for 5 min. The pellet was dissolved in 200 µL of sterilized double distilled water (ddH_2O) followed by adding 630 µL of 95% ethanol. The sample was then incubated for 5 min in boiling water, cooled to RT, and centrifuged at 10,000x g for 5 min. The pellet was then dissolved in 400 µL of ddH_2O followed by adding 800 µL ice-cold 0.2% anthrone reagent made in 98% sulphuric acid (ThermoFisher Scientific) to the sample, incubating for 10 min in boiling water, and then immediately cooled on ice. A hundred microliter sample was transferred into a 96-well plate and glycogen contents were measured by a spectrophotometer (Bioteck, Winooski, VT) at

680 nm along with dextrose standards (0.25-15 mg/mL, ThermoFisher Scientific). Glycogen contents were calculated by a standard curve method (27, 28).

Statistical analysis

Results are presented as mean±S.E.M. Student's *t*-test was used for analyzing statistical significance based on the distribution of the data. Pearson correlation coefficient was used to calculate *p* value for correlation between two test groups. Differences were considered to be significant at $p<0.05$ with one tailed distribution. All data analysis was blinded with genotype information by mouse number.

Results

Generation of *Znt8* allelic insufficient mice

The *Slc30a8*$^{tm1a(KOMP)Wtsi}$ (*Znt8*$^{+/-}$) knockout mouse was cryo-recovered by the KOMP (Knockout Mouse Project) Repository at the University of California Davis. In the *Znt8* knockout genome, a bacterial *LacZ* gene cassette was placed in the intron between exons 1 and 2 of the mouse *Znt8* gene. Thus, a *LacZ* transcript was expressed under the control of the *Znt8* promoter (Fig. 1A). The experimental mice (*Znt8*$^{+/-}$ and WT littermates,) were obtained by either *Znt8*$^{+/-}$ x *Znt8*$^{+/+}$ or *Znt8*$^{+/-}$ x *Znt8*$^{+/-}$ breeding. The progenies from both mating strategies produced *Znt8*$^{+/-}$, *Znt8*$^{-/-}$, and *Znt8*$^{+/+}$ mice in the expected Mendelian ratio (data not shown). Mice of both genders with a null allele of *Znt8* were viable, fertile, and displayed no obvious morphological abnormalities (data not shown). PCR using purified genomic DNA confirmed the presence of the *LacZ* gene in the *Znt8*$^{+/-}$ and *Znt8*$^{-/-}$genomes, but not in WT (Fig. 1B). Moreover, β-galactosidase staining demonstrated the expression of β-galactosidase in the pancreatic islet of *Znt8*$^{+/-}$ mice, but not in WT confirming the

results from PCR genotyping (Fig. 1C). ZnT8 protein could be detected in the islets of both *Znt8*$^{+/-}$ and WT mice. However, it was not detectable in the islet of *Znt8*$^{-/-}$ mice (Fig. 1D).

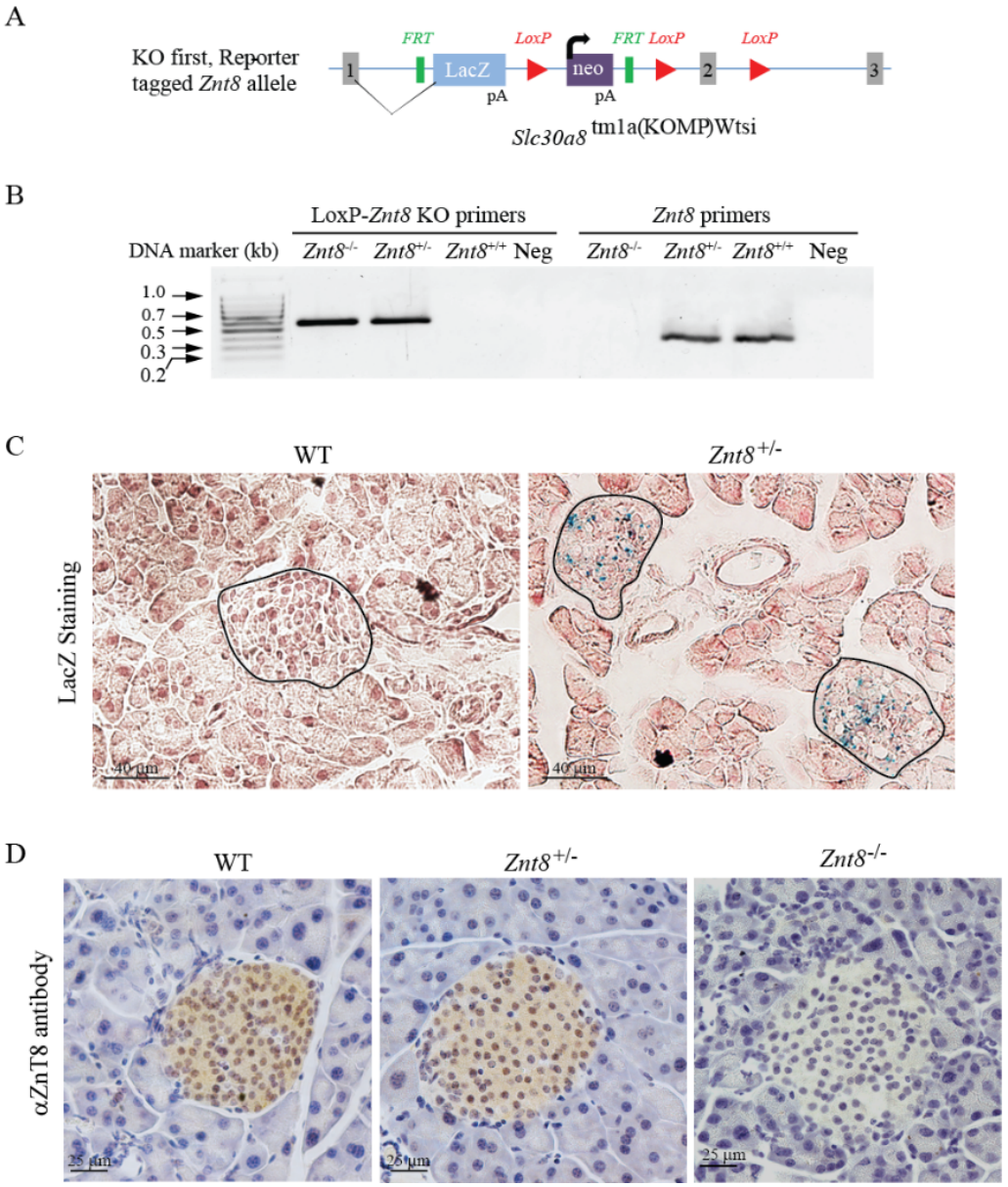

Figure 1. Generation of *Znt8*$^{+/-}$ (*Slc30a8*$^{tm1a(komp)wtsi}$) mice. A. The construct. A promoter-driven targeting cassette was inserted into the mouse *Znt8* gene between the exons 1 and 2. Thus, the amino acids encoded from exon 1 (MEFLERTYLVNDQATKMYAFPLDRWTRCWESGYPH) was fused in frame with the reporter LacZ sequence followed by a poly A signal in the *Znt8* knockout mice. Gray boxes, *Znt8* exons; FRT, flippase recognition target; LoxP, *Lox* sequences (short target sequences recognized by the Cre recombinase) derived from bacteriophage P1; LacZ, the bacterial β-galactosidase gene; Neo, the neomycin resistant gene. Arrow indicates the transcription start site for the neomycin resistant gene. B. The image of genotyping results for *Znt8*$^{+/+}$, *Znt8*$^{+/-}$, and *Znt8*$^{-/-}$. Genomic DNA was genotyped by 2 sets of primer pairs, LoxP-*Znt8* KO and *Znt8* primer pairs that detected the mouse genomic DNA with or without the targeting cassette, respectively. If only a DNA fragment (573-bp) was amplified by PCR using the LoxP-*Znt8* KO primer pair, it indicated the *Znt8*$^{-/-}$ genotype. If only a 376-bp DNA fragment was detected using the

Znt8 primer pair, it indicated *Znt8*$^{+/+}$ genotype. Lastly, if two DNA bands were detected (573- and 376-bp), it indicated *Znt8*$^{+/-}$ genotype. Negative controls (Neg) for PCR is shown (PCR reactions without the genomic DNA templates). DNA marker is shown on the left. C. LacZ staining in the mouse pancreas. Cryosectioned pancreas (*Znt8*$^{+/-}$) was stained with X-gal. The LacZ activity (blue) was only detected in the islets of *Znt8*$^{+/-}$ mice. No LacZ activity was detected in the WT islets. D. Immunohistochemical staining of ZnT8 in the mouse pancreases. Representative images of ZnT8 staining are shown. ZnT8 protein (brown color) was detected in the islets of WT and *Znt8*$^{+/-}$ mice. It was absent in the islets of *Znt8*$^{-/-}$ mice. The scale bar = 25 μm.

Effects of *Znt8* allelic insufficiency on body weight, insulin secretion, and glucose metabolism

To assess the role of *Znt8* allelic insufficiency in insulin secretion and glucose control during diet-induced obesity and insulin resistance, *Znt8*$^{+/-}$ and *Znt8*$^{+/+}$ mice were fed a high-fat diet (45% kcal fat) for 17 weeks. The high-fat diet was introduced when the experimental mice were at weaning age (3 weeks old). The progress of diet-induced obesity and insulin resistance was monitored by body weight, fasting and non-fasting blood glucose levels, insulin tolerance, and glucose tolerance (Fig. 2A). At 3 weeks of age, no significant difference in body weight was observed between *Znt8*$^{+/-}$ and WT mice (female *Znt8*$^{+/-}$, 6.8±1.1 g vs female WT, 7.0±1.0 g and male *Znt8*$^{+/-}$, 7.6±1.1 g vs male WT, 7.2±1.0 g). After 8 weeks on the high-fat diet, female *Znt8*$^{+/-}$ mice appeared to gain less weight than the WT control. After 14 weeks, the body weight difference was statistically significant in female mice between the two genotypes (*Znt8*$^{+/-}$, 23.9±3.5 g vs WT, 27.0±4.8 g; $p<0.05$; Fig. 2B). Unlike the female counterpart, male mice had no obvious weight difference between the two genotypes (Fig. 2C).

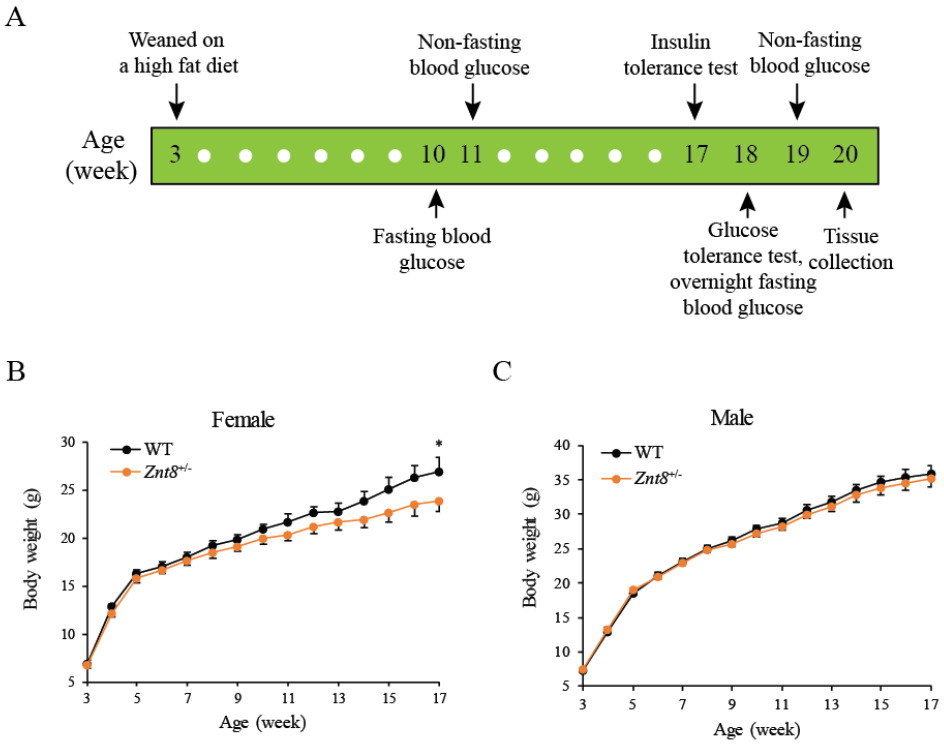

Figure 2. Study design and growth curves. A. Study design. Mice were weaned at 3 weeks of age and fed the high-fat diet *ad libitum.* The time points for fasting and non-fasting blood collections are indicated. Intraperitoneal insulin and glucose tolerance tests were performed at 17 and 18 weeks of age, respectively. Mice were euthanized at 20 weeks of age. B. Growth curve of female mice. C. Growth curve of male mice. Body weight (gram) was measured weekly after introduction of the high-fat diet. All values are expressed as mean±S.E.M. (*error bars*), n=8-12/genotype/sex. *, $p<0.05$.

To gain further insight into the impact of *Znt8* allelic insufficiency on glucose metabolism during diet-induced insulin resistance, we examined blood glucose levels in both fasting and non-fasting conditions. As shown in Fig 3A, after 7 weeks on the high-fat diet, male *Znt8*$^{+/-}$ mice presented a slightly higher 6-h fasting blood glucose level than the control mice (*Znt8*$^{+/-}$, 188±9.3 mg/dL, n=12 vs WT, 155±11.2 mg/dL, n=8; $p<0.05$). However, this difference was not detected in the fasting blood samples (overnight) after 15 weeks on the diet in male mice (*Znt8*$^{+/-}$, 98±6.9 mg/dL, n=12 vs WT, 107±17.3 mg/dL, n=8). On the other hand, no differences were observed in male mice for non-fasting blood glucose levels between genotypes after high-fat diet intake (Fig. 3B). Furthermore, differences in levels of either fasting or non-fasting blood glucose were not

observed in female mice between genotypes after consumption of the high-fat diet (Fig. 3A & B). Taken together, *Znt8* allelic insufficiency might be associated with an increased 6-h fasting blood glucose level at early age after exposure to the high-fat diet in male mice. However, this effect was not seen in female mice.

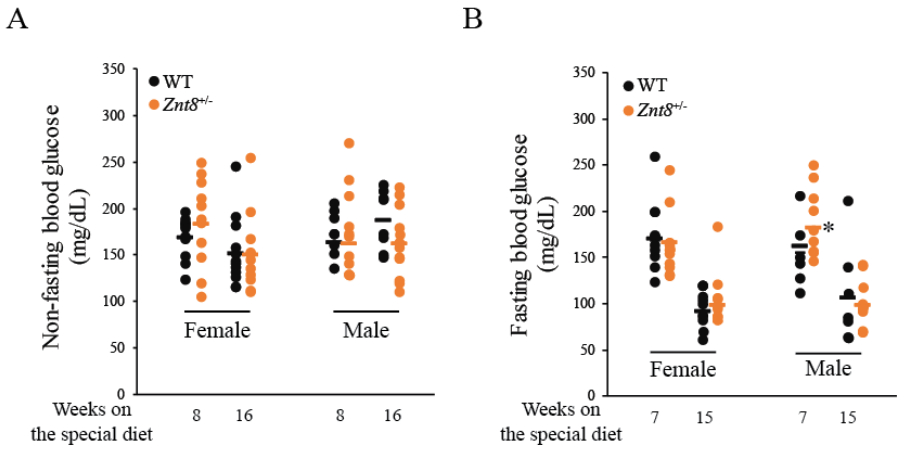

Figure 3. Blood glucose levels. A. Non-fasting blood glucose levels. Blood glucose concentrations were measured at 8 and 16 weeks after introduction of the high-fat diet. B. Fasting blood glucose concentrations. Six-hour and overnight fasting blood glucose levels were determined at 7 and 15 weeks after consumption of the high-fat diet, respectively. All data points are plotted. −represents the mean. n=8-12/genotype/sex. *, $p<0.05$.

A major function of ZnT8 in the pancreatic islets is to sequester zinc from the cytoplasm into insulin-containing granules for insulin crystallization in β-cells (19). To investigate whether *Znt8* allelic insufficiency affected insulin secretion and glucose handling, glucose-stimulated insulin secretion was assessed after 15 weeks on the high-fat diet. As shown in Fig. 4A & B, plasma insulin levels were lower in *Znt8*$^{+/-}$ mice of both genders than the controls after an intraperitoneal glucose load (1.5 g/kg body weight). The difference was more obvious in males than females at 30- and 60-min timepoints. Notably though, plasma insulin level in female *Znt8*$^{+/-}$ mice remained lower (0.54±0.10 ng/mL, n=10) than the control (0.81±0.06 ng/mL, n=12) at the 120-min time point whereas no difference was seen between genotypes in male mice at this time point (*Znt8*$^{+/-}$, 98±0.14 ng/mL, n=10 vs WT, 1.09±0.14 ng/mL, n=8). It is worth nothing that

although glucose-stimulated insulin secretion was reduced in female *Znt8*$^{+/-}$ mice, there was no change in blood glucose levels compared to the control (Fig. 4C). On the other hand, male *Znt8*$^{+/-}$ mice had a less striking blood glucose surge (283.6±20.0 mg/dL, n=10) than the control (368.1±7.5 mg/dL, n=8; p<0.01) at 15 min after glucose stimulation (Fig. 4D), indicating that male *Znt8*$^{+/-}$ mice had a better glucose control shortly after a glucose load. Finally, insulin tolerance tests suggested that *Znt8* allelic insufficiency had no evident impact on peripheral insulin sensitivity in mice of both genders (Fig. 4E & F).

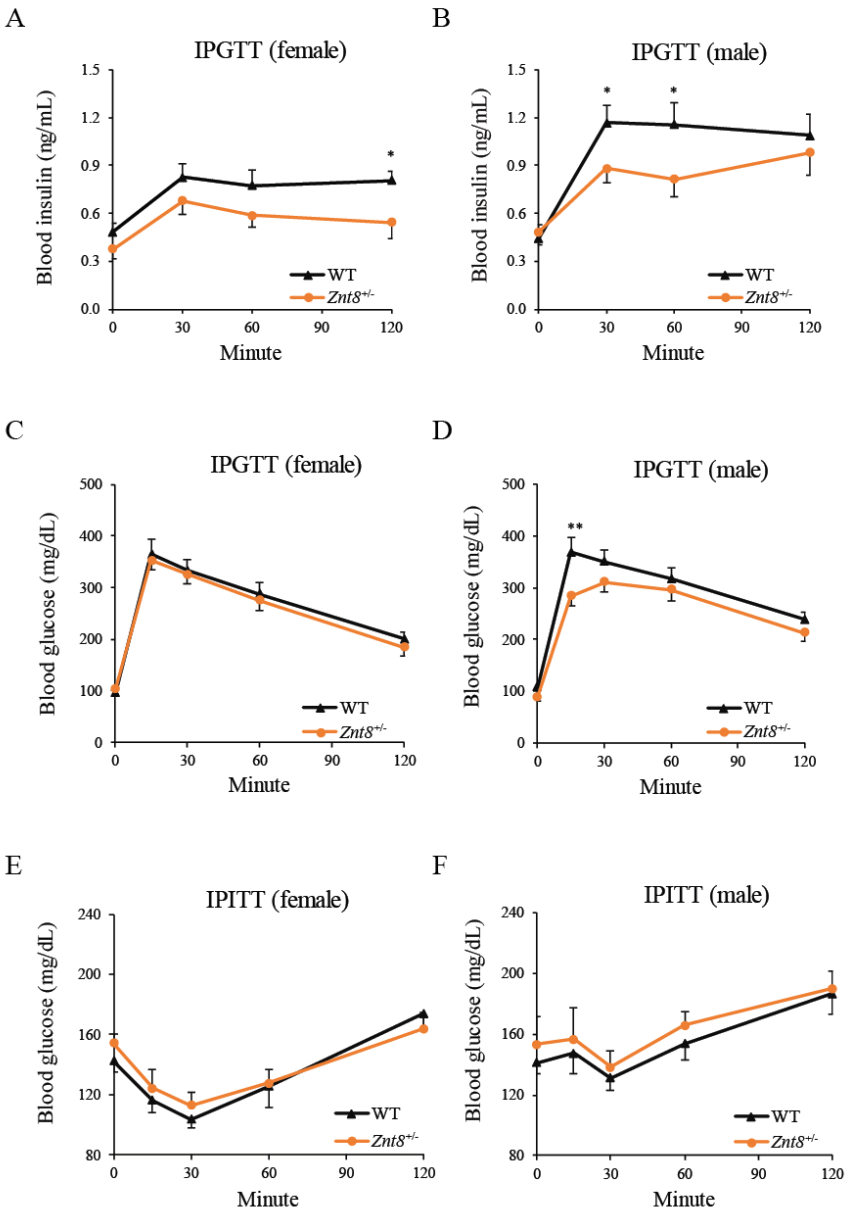

Figure 4. Intraperitoneal glucose (IPGTT) and insulin (IPITT) tolerance tests. A. Blood insulin levels in female mice during IPGTT. B. Blood insulin levels in male mice during IPGTT. C. Blood glucose levels in female mice during IPGTT. D. Blood glucose levels in male mice during IPGTT. Intraperitoneal GTT (glucose: 1.5 mg/kg) was performed at 18-week-old fasted overnight. E. Blood glucose levels in female mice during IPITT. F. Blood glucose levels in male mice during IPITT. Intraperitoneal ITT (insulin: 100 mU/mL, 5.5 U/kg of body weight) was performed at 17-week-old. Each data point represents the mean±S.E.M., n=8-12/genotype/sex. *, $p<0.05$; **, $p<0.01$.

Reductions in fat pad weight, adipocyte size, and fasting triglyceride levels in female *Znt8*$^{+/-}$ mice

After 17 weeks on the high-fat diet, mice were euthanized and fat pads (gonadal, posterior subcutaneous, and retroperitoneal) were dissected and weighed. As shown in Fig. 5A, the total weight of these fat pads from female *Znt8*$^{+/-}$ mice was decreased to ~50% of the control (*Znt8*$^{+/-}$, 542.7±146.9 mg, n=11 vs WT, 1061.1±217.4 mg; n=12; $p<0.05$) whereas there was no difference between genotypes in male *Znt8*$^{+/-}$ mice (Fig. 5A). To investigate whether fat deposits were different in adipocytes between genotypes, we quantified adipose cell numbers and sizes in gonadal adipose sections and correlated the results to the wet weights of the gonadal fat pad. The results showed that the fat cell sizes were significantly smaller in female *Znt8*$^{+/-}$ mice than in the control (*Znt8*$^{+/-}$, 2448.2±340.8 pixel/cell vs WT, 4763.8±549.9 pixel/cell; n=3-4; $p<0.01$) (Fig. 5B). However, this difference was not noted between genotypes in male mice. Correlation analysis of fat cell sizes with fat pad weights demonstrated a positive relationship between two variables in both *Znt8*$^{+/-}$ and WT mice ($R^2=0.6709$, $p<0.0001$), suggesting that the decreased fat pad weights in female *Znt8*$^{+/-}$ mice was at least partly due to fat deposit reductions rather than adipocyte number reductions.

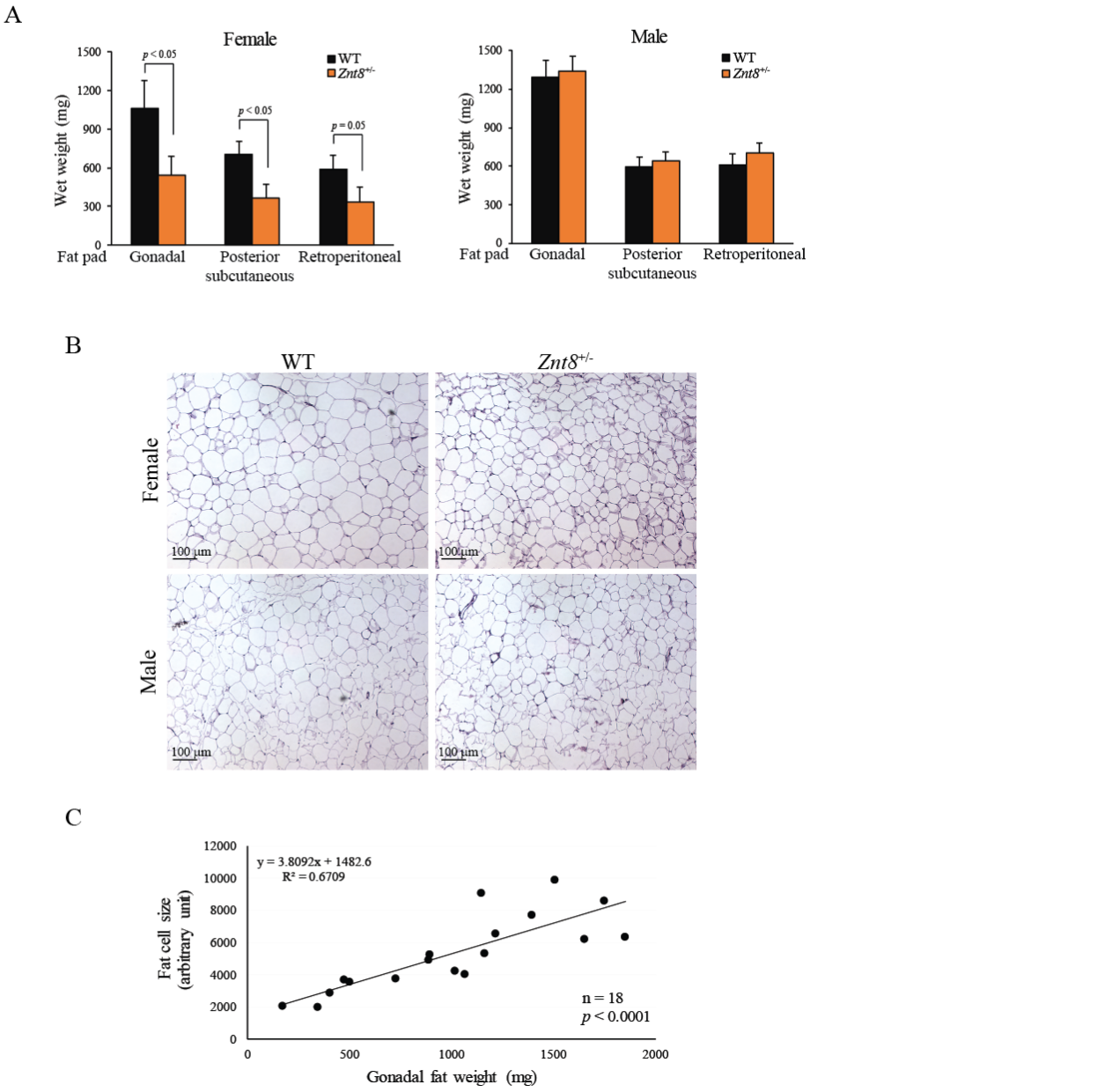

Figure 5. Changes in the adipose tissue. A. Fat pad weights. Mice were euthanized after 17-weeks on the high-fat diet. Indicated fat pads were dissected and weighed at necropsy. Each data point represents the mean±S.E.M. n=8-12/genotype/sex. B. H&E staining of gonadal fat pads. Scale bar=100 µm. C. Regression analysis of adipocyte sizes with gonadal fat weights. Fat cell sizes were measured using the Adiposoft plugin in ImageJ software.

Reduced fat deposits in female *Znt8*$^{+/-}$ mice suggested the presence of an alteration in triglyceride or fatty acid metabolism induced by *Znt8* allelic insufficiency. Therefore, we quantified levels of fasting plasma triglycerides (TG), liver TG, and non-esterified free fatty acids

(NEFA) after 17-weeks of high-fat consumption. As shown in Fig. 6A, female *Znt8*$^{+/-}$ mice had a significantly lower level of fasting TG than the control (*Znt8*$^{+/-}$, 25.7±1.8 mg/dL, n=9 vs WT, 38.3±4.1 mg/dL; n=10; $p<0.05$), whereas male *Znt8*$^{+/-}$ mice showed a comparable level of fasting TG with the control (*Znt8*$^{+/-}$, 43.1±3.8 mg/dL, n=11 vs WT, 40.0±6.2 mg/dL; n=7; $p>0.05$). Moreover, the average of fasting NEFA level in male *Znt8*$^{+/-}$ was reduced by 40% compared to WT (*Znt8*$^{+/-}$, 15.8±2.7 μmol/dL, n=11 vs WT, 26.4±5.9 μmol/dL; n=7; $p<0.05$). This difference in the fasting NEFA concentrations was not seen between genotypes in female mice (*Znt8*$^{+/-}$, 10.7±3.2 μmol/dL, n=10 vs WT, 10.6±3.0 μmol/dL; n=9; $p>0.05$) (Fig. 6B). Next, we examined TG and NEFA contents in the livers of *Znt8*$^{+/-}$ and WT mice. As shown in Fig. 6C, after 17-weeks on the high-fat diet, fat accumulation was apparent in the livers of both genotypes. However, no obvious anatomical abnormalities of the liver were observed in the two genotypes. Moreover, both TG and NEFA contents in the livers of the two genotypes in both genders were similar (Fig. 6D & E). Taken together, the results demonstrated that *Znt8*$^{+/-}$ mice had better blood TG (female) and NEFA (male) profiles than the controls after 17-weeks of high-fat consumption.

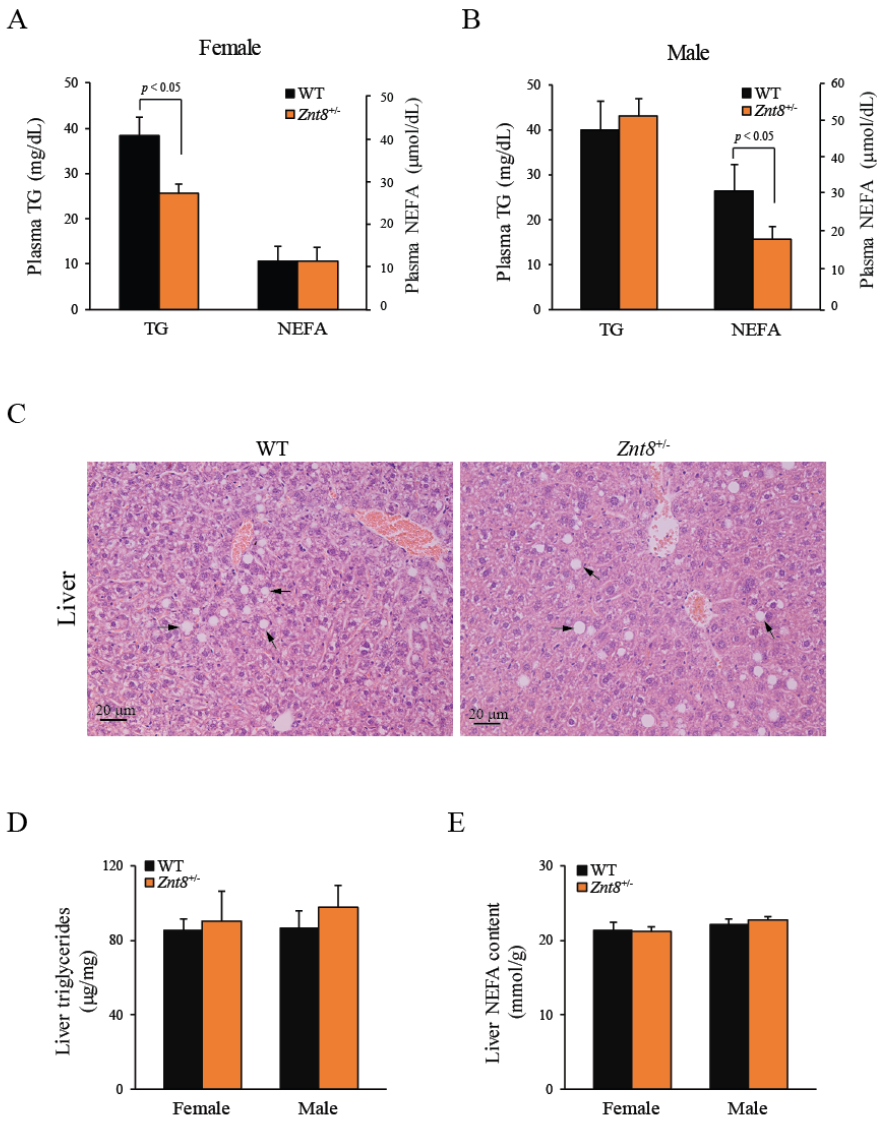

Figure 6. Plasma and liver triglyceride (TG) and non-esterified fatty acid (NEFA) levels. Mice were fasted 4-6 h after 17-weeks on the high-fat diet. Blood and livers were collected at necropsy. A & B. TG levels in the plasma samples from female and male mice, respectively. The y- axis to the left and right of the graph represents the plasma TG (mg/dL) and NEFA (μmole/dL) levels, respectively. (C) H&E staining of the liver. Scale bar=20 μm. Arrows indicate lipid drops in hepatocytes. (D) Liver TG. E. Liver NEFA. Each data point represents the mean±S.E.M. n=7-11/genotype/sex. *p*-values are displayed in the graphs.

Changes in liver glycogen levels in *Znt8*$^{+/-}$ mice

In addition to the pancreas, the liver plays critical roles in glucose control and lipid metabolism (29). During the fed state, excess glucose is converted and stored in the liver as glycogen or fat. In the fasted state, the liver regulates glucose metabolism by glycogenolysis and gluconeogenesis

(30). We showed that *Znt8* allelic insufficiency had no significant effect on the liver TG and NEFA levels after 17-weeks of high-fat intake (Fig. 6D & E). Thus, we investigated liver glycogen contents in $Znt8^{+/-}$ and WT mice. Remarkably, we found that the average of liver glycogen levels was significantly lower in female $Znt8^{+/-}$ mice (13.1±4.8 µg/mg liver, n=9, $p<0.05$) than the control (26.6±5.2 µg/mg liver, n=10) while the liver weights between the two genotypes were similar ($Znt8^{+/-}$, 837.4±61.1 mg, n=9; WT, 883.0±26.7 mg, n=10) (Fig. 7). On the other hand, the average of glycogen levels in the liver of male $Znt8^{+/-}$ mice was higher (45.5±13.1 µg/mg liver, n=11) than the control (20.0±10.3 µg/mg liver, n=7) (Fig. 7) although it was not significantly different (p=0.09). Interestingly, the liver of male $Znt8^{+/-}$ mice was slightly heavier (1184.9±61.0 mg, n=9) than the control (964.6±74.9 mg, n=7; $p<0.05$), consistent with the result of increased glycogen contents in the $Znt8^{+/-}$ liver.

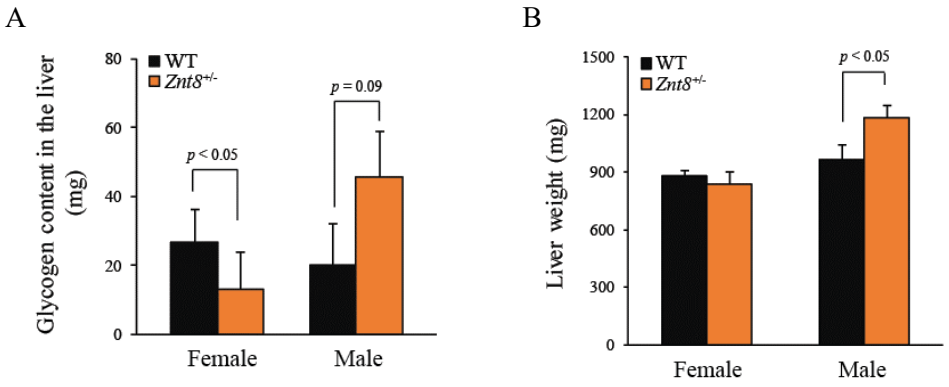

Figure 7. Liver glycogen contents and liver weights. Mice were fasted 4-6 h after 17-weeks on the high-fat diet. Livers were dissected at necropsy. A. Liver glycogen contents. B. Liver weights. The wet weight of the whole liver was determined (mg). Glycogen contents were measured as described in Materials and Methods. Each data point represents the mean±S.E.M. n=7- 11. *p*-values are displayed in the graphs.

Decreased glucagon secretion in male $Znt8^{+/-}$ mice

In addition to β-cells, ZnT8 is also expressed in other endocrine cells albeit much lower than the β-cells (31, 32), such as glucagon-secreting α-cells (33). Therefore, we examined circulating glucagon levels during glucose challenge after 15-weeks of high-fat consumption. We found that

blood glucagon levels in female *Znt8*$^{+/-}$ mice were comparable to the control during glucose challenge (Fig. 8A). However, male *Znt8*$^{+/-}$ mice displayed lower blood glucagon concentrations than WT at all five time points examined (0, 15, 30, 60, and 120 min) (Fig. 8B). The area under the curve (AUC) for the circulating glucagon concentration (pg/mL x 120 min) during glucose challenge in male *Znt8*$^{+/-}$ mice was ~40% of the control (Fig. 8C). The most striking difference was in the overnight fasting glucagon level between the two genotypes of male mice with male *Znt8*$^{+/-}$ mice having only half amount of the circulating glucagon concentration of WT mice (Fig. 8B), These data suggest that glucagon secretion in α-cells was negatively affected by *Znt8*$^{+/-}$ allelic insufficiency in male mice.

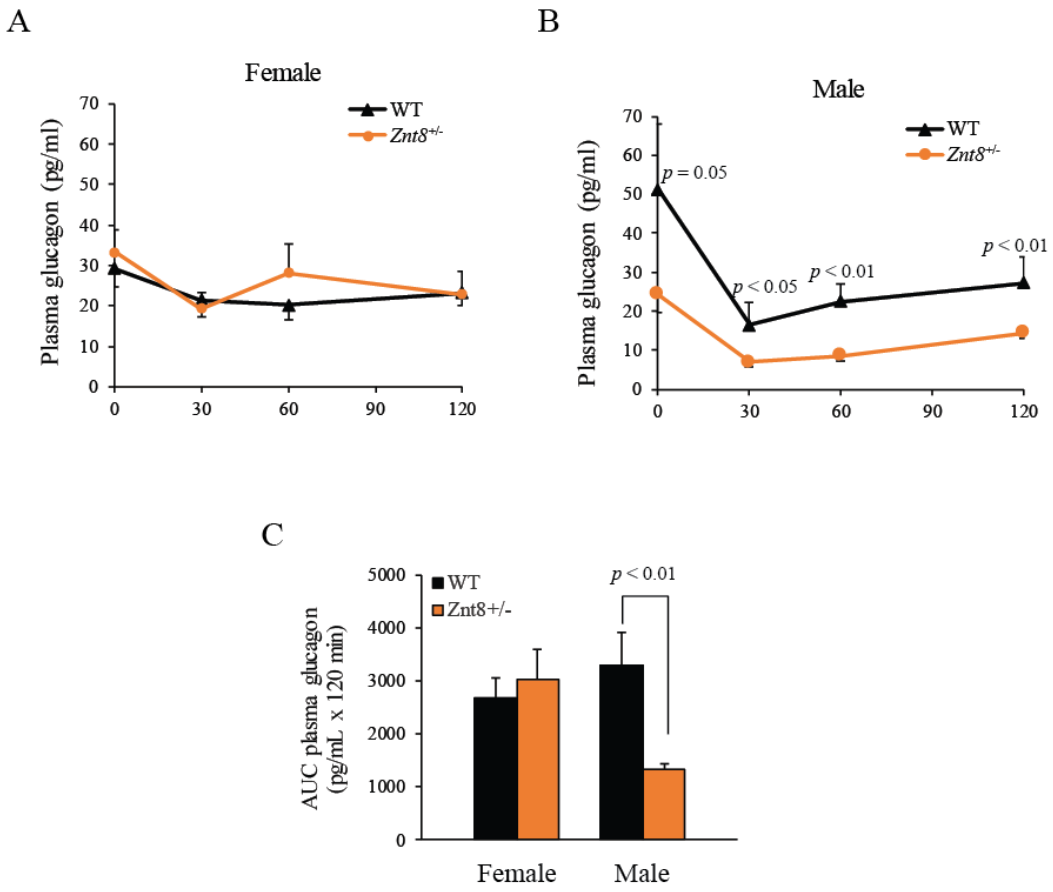

Figure 8. Circulating glucagon levels during intraperitoneal glucose tolerance test (IPGTT). A. Females. B. Males. C. Area under the curve of plasma glucagon concentrations. Mice were fasted for 16-18 h 15 weeks after the introduction of the high-fat diet. IPGTT was performed as described in Materials and Methods. Each data point represents the mean±S.E.M. n=7-12/genotype/sex. *p*-values are displayed in the graphs.

Discussion

The primary goal of this study was to determine whether *Znt8* allelic insufficiency in mice had a protective effect on diet-induced glucose intolerance and if so, to try to understand the mechanisms underlying this beneficial phenotype. The results from the current study showed that *Znt8* allelic insufficiency could reduce glucose-induced insulin secretion in mice of both genders on a pure C57Bl/6N genetic background fed a high-fat diet, which is in line with a previous finding in mice with a global *Znt8*KO (19). However, we demonstrated that this deleterious effect on the glucose-induced insulin secretion induced by *Znt8* allelic insufficiency had limited impact on the whole-body glucose utilization in mice. Instead, we observed an improved glucose tolerance in male *Znt8*$^{+/-}$ mice after a long period of high-fat intake. In addition, female *Znt8*$^{+/-}$ mice had less fat depositions in fat cells after high-fat consumption without obvious alterations in glucose metabolism. In a recently published paper, Syring et al. also found improved glucose tolerance in *Znt8*$^{+/-}$ male mice with a high-fat diet challenge. Together, the results from the current study suggest that both glucose and lipid metabolisms were influenced by *Znt8* allelic insufficiency after a period of high-fat intake, and it was sex-dependent. Besides, ZNT8 plays an important role in insulin and glucagon secretion from β- and α-cells, respectively. Finally, we found that the average of liver glycogen levels was significantly lower in female *Znt8*$^{+/-}$ mice. On the other hand, the liver of male *Znt8*$^{+/-}$ mice was slightly heavier, consistent with the result of increased glycogen contents in the *Znt8*$^{+/-}$ liver. Therefore, the interplay between the pancreas and the liver may be essential for the protective function of *Znt8* allelic insufficiency in mice and possibly in humans. Nevertheless, the metabolic pathways involved in the protective effect of *Znt8* allelic insufficiency appear different between females and males which warrants further investigations.

A sex-differential response to diet-induced obesity and insulin resistance has been reported in humans and animals (34, 35). Female mice are less prone to diet-induced insulin resistance and glucose intolerance than males. One of the proposed mechanisms is that female mice tend to have higher capacity in adipocyte expansiveness leading to a good insulin sensitivity and glucose responsiveness in adipocytes (36). The results from this study showed that *Znt8* allelic insufficiency significantly decreased fat depots of female mice after a prolonged time of high-fat intake. However, this reduction in adipocyte expansion in female *Znt8*$^{+/-}$ mice appeared to have limited influence on glucose metabolism. A plausible mechanism is that *Znt8* allelic insufficiency may affect the responsiveness of the adipose tissue and liver to glucagon in mice. Glucagon, a counter-regulatory hormone to insulin, is able to stimulate energy expenditure resulting in lower body adiposity along with restoring glucose homeostasis during hypoglycemic states through increased hepatic glycogenolysis and gluconeogenesis (37, 38). Animal studies have shown that increased glucagon signaling suppresses triglyceride synthesis and increases triglyceride removal rates in the liver, therefore, leading to lower plasma triglyceride concentrations with no apparent effect on the total hepatic triglyceride levels (39, 40). Given the fact that female *Znt8*$^{+/-}$ mice had lower fat depots and reduced fasting circulating triglyceride concentrations without changes in the hepatic total triglycerides together with decreased hepatic glycogen contents, these indicated that female *Znt8*$^{+/-}$ mice had enhanced lipid catabolism and improved glycogenolysis. Moreover, it is known that an increase in diet-induced fat mass triggers glucose intolerance because of increased release of cytokines and free fatty acids (41–43). Therefore, an inhibition of diet-induced fat mass expansion by *Znt8* allelic insufficiency might allow female *Znt8*$^{+/-}$ mice to remain normoglycemia in the state of reduced insulin secretion caused by the loss of a functional allele of *Znt8*. Further

investigations are warranted to elucidate the signaling molecules that contribute to proper glucose and lipid controls in *Znt8*$^{+/-}$ mice.

In contrast, male *Znt8*$^{+/-}$ mice had a decreased fasting circulating glucagon level accompanied by a higher liver glycogen concentration, suggesting that *Znt8* allelic insufficiency may adversely influence glucagon secretion and its downstream function in male mice. The biological effect of *Znt8* on glucagon secretion has been studied using *Znt8* knockout mice, including α-cell-specific and global KO models, as well as transgenic mice with *Znt8* being over-expressed globally or α-cells specifically. Solomou et. al. reported that mice with a fractional α-cell-specific depletion of *Znt8* expression (~15%, α*Znt8*KO) had normal glucose tolerance when maintained on a regular laboratory chow diet. However, an enhanced glucagon secretion was observed during hypoglycemic clamps (33). An elevation of glucagon secretion, but not a concurrent increase in the total α-cell-associated glucagon content, was also observed in the α*Znt8*KO islets maintained in a lower glucose level (1 mM) (33). Conversely, mice over-expressing human *ZNT8* in α-cells (αZnT8Tg) secreted less glucagon during hypoglycemia. Again, the α-cell-associated glucagon concentration was unchanged in these islets (44). These results highlight an important physiological role of ZnT8 in regulation of glucagon secretion from α-cells during fasting.

We showed that glucagon secretion during hypoglycemia in male *Znt8*$^{+/-}$ mice was reduced 50% compared to WT. This secreting pattern could be explained by the interplay between insulin and glucagon. Insulin secretion is increased in response to elevated blood glucose. In turn, increased intra-islet insulin effectively inhibits glucagon secretion from α-cells (45). During the fasting state, insulin levels are greatly reduced, and the inhibition of glucagon secretion is lifted. One of the key elements in determining the triggering level of glucagon secretion is the percentage

decrement (delta glucagon secretion) in the local insulin concentration from the fed to fasting state (46). The more the insulin concentration drops, the stronger the signal for glucagon secretion. Thus, a smaller difference in the insulin concentrations between the fed and fasted conditions in *Znt8*$^{+/-}$ islets might be responsible for less glucagon secretion during hypoglycemia. This hypothesis is further supported by *in vitro* studies conducted by Hardy et. al. (47). The authors showed that glucagon secretion from the islets of *Znt8*KO mice fed a 45% high-fat diet was ~50% less than the control 2 h after glucose stimulation at 11.1 mM. Moreover, López-Soldado et. al. demonstrated an improved glucose tolerance in mice fed a high-fat diet when the liver glycogen storage was increased (48). Taken together, we conclude that reduce glucagon secretion levels in both fed and fasting states in mice with *Znt8* allelic insufficiency could be the key in reducing the risk of T2D as hyperglucagonemia is thought to be a causal factor in the pathophysiological development of T2D (49, 50).

In summary, we demonstrated that *Znt8* allelic insufficiency presented a protective effect on lipid metabolism in female mice and had improved glucose metabolism in male mice during high-fat intake despite the presence of reduced levels of glucose-induced insulin secretion. Moreover, fasting and fed blood glucagon levels remained significantly lower in male *Znt8*$^{+/-}$ mice. Our data suggests that *Znt8* allelic insufficiency could provide protective effects on diet-induced glucose intolerance, possibly through regulation of glucagon secretion in males and lipid metabolism in females.

References

1. Type 2 Diabetes | National Institutes of Health (NIH) [online] https://www.nih.gov/research-training/accelerating-medicines-partnership-amp/type-2-diabetes (Accessed February 8, 2020)
2. Lebovitz, H. E. (1999) Type 2 diabetes: An overview. in *Clinical Chemistry*, pp. 1339–1345, American Association for Clinical Chemistry Inc., **45**, 1339–1345
3. Wajchenberg, B. L. (2007) β-cell failure in diabetes and preservation by clinical treatment. *Endocr. Rev.* **28**, 187–218
4. Søndergaard, L. G., Stoltenberg, M., Doering, P., Flyvbjerg, A., and Rungby, J. (2006) Zinc ions in the endocrine and exocrine pancreas of zinc deficient rats. *Histol. Histopathol.* **21**, 619–625
5. Dunn, M. F. (2005) Zinc-ligand interactions modulate assembly and stability of the insulin hexamer - A review. in *BioMetals*, pp. 295–303, Springer, **18**, 295–303
6. PD, Z., SH, M., IJ, F., O, K., A, S., WH, B., AD, W., SF, L., and I, M. (1994) Video image analysis of labile zinc in viable pancreatic islet cells using a specific fluorescent probe for zinc. *J. Histochem. Cytochem.* **42**, 877–884
7. Chimienti, F., Devergnas, S., Favier, A., and Seve, M. (2004) Identification and cloning of a β-cell-specific zinc transporter, ZnT-8, localized into insulin secretory granules. *Diabetes*. **53**, 2330–2337
8. Huang, L., and Tepaamorndech, S. (2013) The SLC30 family of zinc transporters-A review of current understanding of their biological and pathophysiological roles. *Mol. Aspects Med.* **34**, 548–560
9. Lemaire, K., Chimienti, F., and Schuit, F. (2012) Zinc transporters and their role in the

pancreatic β-cell. *J. Diabetes Investig.* **3**, 202

10. Sladek, R., Rocheleau, G., Rung, J., Dina, C., Shen, L., Serre, D., Boutin, P., Vincent, D., Belisle, A., Hadjadj, S., Balkau, B., Heude, B., Charpentier, G., Hudson, T. J., Montpetit, A., Pshezhetsky, A. V., Prentki, M., Posner, B. I., Balding, D. J., Meyre, D., Polychronakos, C., and Froguel, P. (2007) A genome-wide association study identifies novel risk loci for type 2 diabetes. *Nature*. **445**, 881–885
11. Huang, L. (2014) Zinc and its transporters, pancreatic β-cells, and insulin metabolism. in *Vitamins and Hormones*, pp. 365–390, Academic Press Inc., **95**, 365–390
12. Cauchi, S., Proença, C., Choquet, H., Gaget, S., De Graeve, F., Marre, M., Balkau, B., Tichet, J., Meyre, D., Vaxillaire, M., Froguel, P., Balkau, B., Ducimetière, P., Eschwège, E., Alhenc-Gelas, F., Gallois, Y., Girault, A., Fumeron, F., Marre, M., Cogneau, J., Born, C., Caces, E., Cailleau, M., Moreau, J. G., Rakotozafy, F., Tichet, J., and Vol, S. (2008) Analysis of novel risk loci for type 2 diabetes in a general French population: The D.E.S.I.R. study. *J. Mol. Med.* **86**, 341–348
13. Staiger, H., Machicao, F., Stefan, N., Tschritter, O., Thamer, C., Kantartzis, K., Schäfer, S. A., Kirchhoff, K., Fritsche, A., and Häring, H. U. (2007) Polymorphisms within novel risk loci for type 2 diabetes determine β-cell function. *PLoS One*. 10.1371/journal.pone.0000832
14. Ruchat, S. M., Elks, C. E., Loos, R. J. F., Vohl, M. C., Weisnagel, S. J., Rankinen, T., Bouchard, C., and Pérusse, L. (2009) Association between insulin secretion, insulin sensitivity and type 2 diabetes susceptibility variants identified in genome-wide association studies. *Acta Diabetol.* **46**, 217–226
15. Wenzlau, J. M., Juhl, K., Yu, L., Moua, O., Sarkar, S. A., Gottlieb, P., Rewers, M., Eisenbarth, G. S., Jensen, J., Davidson, H. W., and Hutton, J. C. (2007) The cation efflux

transporter ZnT8 (Slc30A8) is a major autoantigen in human type 1 diabetes. *Proc. Natl. Acad. Sci. U. S. A.* **104**, 17040–17045

16. De Grijse, J., Asanghanwa, M., Nouthe, B., Albrecher, N., Goubert, P., Vermeulen, I., Van Der Meeren, S., Decochez, K., Weets, I., Keymeulen, B., Lampasona, V., Wenzlau, J., Hutton, J. C., Pipeleers, D., and Gorus, F. K. (2010) Predictive power of screening for antibodies against insulinoma-associated protein 2 beta (IA-2β) and zinc transporter-8 to select first-degree relatives of type 1 diabetic patients with risk of rapid progression to clinical onset of the disease: Implicat. *Diabetologia*. **53**, 517–524

17. Huang, L., and Kirschke, C. P. (2016) Down-Regulation of Zinc Transporter 8 (SLC30A8) in Pancreatic Beta-Cells Promotes Cell Survival. *Austin J Endocrinol Diabetes*. **3**, 1037

18. Flannick, J., Thorleifsson, G., Beer, N. L., Jacobs, S. B. R., Grarup, N., Burtt, N. P., Mahajan, A., Fuchsberger, C., Atzmon, G., Benediktsson, R., Blangero, J., Bowden, D. W., Brandslund, I., Brosnan, J., Burslem, F., Chambers, J., Cho, Y. S., Christensen, C., Douglas, D. A., Duggirala, R., Dymek, Z., Farjoun, Y., Fennell, T., Fontanillas, P., Forsén, T., Gabriel, S., Glaser, B., Gudbjartsson, D. F., Hanis, C., Hansen, T., Hreidarsson, A. B., Hveem, K., Ingelsson, E., Isomaa, B., Johansson, S., Jørgensen, T., Jørgensen, M. E., Kathiresan, S., Kong, A., Kooner, J., Kravic, J., Laakso, M., Lee, J.-Y., Lind, L., Lindgren, C. M., Linneberg, A., Masson, G., Meitinger, T., Mohlke, K. L., Molven, A., Morris, A. P., Potluri, S., Rauramaa, R., Ribel-Madsen, R., Richard, A.-M., Rolph, T., Salomaa, V., Segrè, A. V, Skärstrand, H., Steinthorsdottir, V., Stringham, H. M., Sulem, P., Tai, E. S., Teo, Y. Y., Teslovich, T., Thorsteinsdottir, U., Trimmer, J. K., Tuomi, T., Tuomilehto, J., Vaziri-Sani, F., Voight, B. F., Wilson, J. G., Boehnke, M., McCarthy, M. I., Njølstad, P. R., Pedersen, O., Groop, L., Cox, D. R., Stefansson, K., and Altshuler, D. (2014) Loss-of-

function mutations in SLC30A8 protect against type 2 diabetes. *Nat. Genet. 2014 464*. **46**, 357–363

19. Lemaire, K., Ravier, M. A., Schraenen, A., Creemers, J. W. M., Van De Plas, R., Granvik, M., Van Lommel, L., Waelkens, E., Chimienti, F., Rutter, G. A., Gilon, P., In't Veld, P. A., and Schuit, F. C. (2009) Insulin crystallization depends on zinc transporter ZnT8 expression, but is not required for normal glucose homeostasis in mice. *Proc. Natl. Acad. Sci. U. S. A.* **106**, 14872–14877

20. Wijesekara, N., Dai, F. F., Hardy, A. B., Giglou, P. R., Bhattacharjee, A., Koshkin, V., et al. (2010) Beta cell-specific Znt8 deletion in mice causes marked defects in insulin processing, crystallisation and secretion. *Diabetologia*. **53**, 1656–1668

21. Tamaki, M., Fujitani, Y., Hara, A., Uchida, T., Tamura, Y., Takeno, K., Kawaguchi, M., Watanabe, T., Ogihara, T., Fukunaka, A., Shimizu, T., Mita, T., Kanazawa, A., Imaizumi, M. O., Abe, T., Kiyonari, H., Hojyo, S., Fukada, T., Kawauchi, T., Nagamatsu, S., Hirano, T., Kawamori, R., and Watada, H. (2013) The diabetes-susceptible gene SLC30A8/ZnT8 regulates hepatic insulin clearance. *J. Clin. Invest.* **123**, 4513–4524

22. Davidson, H. W., Wenzlau, J. M., and O'Brien, R. M. (2014) Zinc transporter 8 (ZnT8) and β cell function. *Trends Endocrinol. Metab.* **25**, 415–424

23. Yu, Y. Y., Kirschke, C. P., and Huang, L. (2007) Immunohistochemical analysis of ZnT1, 4, 5, 6, and 7 in the mouse gastrointestinal tract. *J. Histochem. Cytochem.* **55**, 223–234

24. Kirschke, C. P., and Huang, L. (2008) Expression of the ZNT (SLC30) family members in the epithelium of the mouse prostate during sexual maturation. *J. Mol. Histol.* **39**, 359–370

25. Haematoxylin Eosin (H&E) staining | Protocols Online [online] https://www.protocolsonline.com/histology/dyes-and-stains/haematoxylin-eosin-he-

staining/ (Accessed July 21, 2021)

26. Galarraga, M., Campión, J., Muñoz-Barrutia, A., Boqué, N., Moreno, H., Martínez, J. A., Milagro, F., and Ortiz-de-Solórzano, C. (2012) Adiposoft: automated software for the analysis of white adipose tissue cellularity in histological sections. *J. Lipid Res.* **53**, 2791–2796

27. Krisman, C. R. (1962) A method for the colorimetric estimation of glycogen with Iodine. *Anal. Biochem.* **4**, 17–23

28. Hassid, W. Z., and Abraham, S. (1957) [7] Chemical procedures for analysis of polysaccharides. in *Methods in Enzymology*, pp. 34–50, Academic Press, **3**, 34–50

29. Trefts, E., Gannon, M., and Wasserman, D. H. (2017) The liver. *Curr. Biol.* **27**, R1147–R1151

30. Ward, C. (2014) Glycogenolysis and glycogenesis. *Diapedia*. [online] http://dx.doi.org/10.14496/dia.51040851111.13 (Accessed July 21, 2021)

31. Zhong, M. L., Chi, Z. H., Shan, Z. Y., Teng, W. P., and Wang, Z. Y. (2012) Widespread expression of zinc transporter ZnT (SLC30) family members in mouse endocrine cells. *Histochem. Cell Biol.* **138**, 605–616

32. Murgia, C., Devirgiliis, C., Mancini, E., Donadel, G., Zalewski, P., and Perozzi, G. (2009) Diabetes-linked zinc transporter ZnT8 is a homodimeric protein expressed by distinct rodent endocrine cell types in the pancreas and other glands. *Nutr. Metab. Cardiovasc. Dis.* **19**, 431–439

33. Solomou, A., Meur, G., Bellomo, E., Hodson, D. J., Tomas, A., Migrenne Li, S., Philippe, E., Herrera, P. L., Magnan, C., and Rutter, G. A. (2015) The Zinc Transporter Slc30a8/ZnT8 Is Required in a Subpopulation of Pancreatic α-Cells for Hypoglycemia-induced Glucagon

Secretion. *J. Biol. Chem.* **290**, 21432–21442

34. Macotela, Y., Boucher, J., Tran, T. T., and Kahn, C. R. (2009) Sex and depot differences in adipocyte insulin sensitivity and glucose. *Diabetes*. **58**, 803–812

35. Kautzky-Willer, A., Harreiter, J., and Pacini, G. (2016) Sex and gender differences in risk, pathophysiology and complications of type 2 diabetes mellitus. *Endocr. Rev.* **37**, 278–316

36. Medrikova, D., Jilkova, Z. M., Bardova, K., Janovska, P., Rossmeisl, M., and Kopecky, J. (2012) Sex differences during the course of diet-induced obesity in mice: Adipose tissue expandability and glycemic control. *Int. J. Obes.* **36**, 262–272

37. Claus, T. H., Park, C. R., and Pilkis, S. J. (1983) Glucagon and Gluconeogenesis. 10.1007/978-3-642-68866-9_15

38. Petersen, M. C., Vatner, D. F., and Shulman, G. I. (2017) Regulation of hepatic glucose metabolism in health and disease. *Nat. Rev. Endocrinol. 2017 1310*. **13**, 572–587

39. Eaton, R. P. (1973) Hypolipemic action of glucagon in experimental endogenous lipemia in the rat. *J. Lipid Res.* **14**, 312–318

40. Guettet, C., Rostaqui, N., Navarro, N., Lecuyer, B., and Mathe, D. (1991) Effect of Chronic Glucagon Administration on the Metabolism of Triacylglycerol-Rich Lipoproteins in Rats Fed a High Sucrose Diet. *J. Nutr.* **121**, 24–30

41. Boden, G. (2011) Obesity, insulin resistance and free fatty acids. *Curr. Opin. Endocrinol. Diabetes Obes.* **18**, 139–143

42. Wieser, V., Moschen, A. R., and Tilg, H. (2013) Inflammation, Cytokines and Insulin Resistance: A Clinical Perspective. *Arch. Immunol. Ther. Exp. 2013 612*. **61**, 119–125

43. Luca, C. de, and Olefsky, J. M. (2008) Inflammation and insulin resistance. *FEBS Lett.* **582**, 97–105

44. Solomou, A., Philippe, E., Chabosseau, P., Migrenne-Li, S., Gaitan, J., Lang, J., Magnan, C., and Rutter, G. A. (2016) Over-expression of Slc30a8/ZnT8 selectively in the mouse α cell impairs glucagon release and responses to hypoglycemia. *Nutr. Metab. (Lond).* **13**, 46

45. Franklin, I., Gromada, J., Gjinovci, A., Theander, S., and Wollheim, C. B. (2005) β-Cell Secretory Products Activate α-Cell ATP-Dependent Potassium Channels to Inhibit Glucagon Release. *Diabetes*. **54**, 1808–1815

46. Raju, B., and Cryer, P. E. (2005) Loss of the decrement in intraislet insulin plausibly explains loss of the glucagon response to hypoglycemia in insulin-deficient diabetes: Documentation of the intraislet insulin hypothesis in humans. *Diabetes*. **54**, 757–764

47. Hardy, A. B., Wijesekara, N., Genkin, I., Prentice, K. J., Bhattacharjee, A., Kong, D., Chimienti, F., and Wheeler, M. B. (2012) Effects of high-fat diet feeding on Znt8-null mice: differences between β-cell and global knockout of Znt8. *Am. J. Physiol. Endocrinol. Metab.* **302**, E1084–E1096

48. López-Soldado, I., Zafra, D., Duran, J., Adrover, A., Calbó, J., and Guinovart, J. J. (2015) Liver Glycogen Reduces Food Intake and Attenuates Obesity in a High-Fat Diet–Fed Mouse Model. *Diabetes*. **64**, 796–807

49. Godoy-Matos, A. F. (2014) The role of glucagon on type 2 diabetes at a glance. *Diabetol. Metab. Syndr.* **6**, 91

50. Unger, R. H., and Orci, L. (1975) THE ESSENTIAL ROLE OF GLUCAGON IN THE PATHOGENESIS OF DIABETES MELLITUS. *Lancet*. **305**, 14–16

Chapter 4 - The interplay of ZNT8 and somatostatin in the gastrointestinal tract and its impact on glucose metabolism

Abstract

Aims/hypothesis

ZNT8 is responsible for zinc delivery to secretory vesicles for insulin crystallization in pancreatic beta-cells. However, enhanced zinc transporter activity of ZNT8 is related to inceased risk for type 2 diabetes (T2D). On the other hand, *ZNT8* allelic insufficiency is associated with reduction in risk of T2D by ~65%. Yet, the underlying mechanisms for these observations are not fully understood. Co-expression of ZNT8 in other endocrine cells that produce and secrete hormones involved in regulation of glucose metabolism has been reported. The aim of this study was to explore the role of ZNT8 in regulating select metabolic hormones, such as somatostatin, ghrelin, gastric inhibitory polypeptide (GIP), and glucagon-like peptide-1 (GLP1) during insulin resistance induced by dietary high-fat (HFD) intake.

Methods

Znt8-null homozygote (KO), *Znt8*-heterozygote (het), and wild type (wt) mice were fed a high-fat diet (60% kcal fat, HFD) from 5 to 13 weeks age. Body weight was monitored weekly. Oral glucose tolerance test (OGTT) was performed after 8 weeks on the diet. Blood was collected during OGTT for determining glucose metabolism-relevant hormone levels, such as insulin and glucagon. To examine the correlation of *Znt8* mRNA expression with *Sst* and glucagon in the pancreatic islets, islets from *Znt8* het and wt mice were isolated at necropsy and pelleted for total RNA isolation. Mouse stomach and duodenum tissues were embedded and sectioned. Immunofluorescent staining was performed to detect the co-expression of ZNT8 with

metabolically relevant hormones, including somatostatin (SST), ghrelin, GIP, GLP1, cholecystokinin (CCK).

Results

Consumption of a HFD for 8 weeks induced glucose intolerance in all three genotypes of mice as indicated by OGTT. After adjustment of the data obtained from the oral saline challenge, which was performed to control for stress- induced change on glucose metabolism stimulated by experimental procedures, *Znt8* het mice showed lower glucagon levels at 30-min after the glucose administration than wt mice (p=0.012). *Znt8* KO mice had the most suppressed glucagon levels at the 2-h time point among all three genotypes (KO vs. het: p=0.048; KO vs. wt: p=0.00036). In addition, compared to both *Znt8* het and wt mice, *Znt8* KO mice had the lowest insulin level at 30-min after the glucose load (KO vs. het: p=0.084; KO vs. wt: p=0.018 after adjusting for the saline treatment or KO vs. het: p=0.044; KO vs. wt: p=0.028 without adjusting for the saline treatment). Furthermore, quantitative RT-PCR results suggested that *Znt8* mRNA expression was strongly and positively correlated with the expression of glucagon (R^2=0.75, p=2.43*10^{-4}) and *Sst* (R^2=0.8788, p=6.78*10^{-6}) in pancreatic islets. Most importantly, ZNT8 was found to colocalize with somatostatin in the mouse pylorus mucosa, but not with ghrelin, GIP, GLP1, and CCK.

Conclusion/interpretation

Znt8 heterozygotes may be protected from high-fat-induced glucose intolerance or type 2 diabetes due to enhanced suppression of glucagon levels leading to better glycemic control. Colocalized expression of ZNT8 and somatostatin suggest a role of ZNT8 in regulating SST production and secretion, which may have an indirect impact on the rate of digestion and absorption of foods in the gut as well as the secretions of pancreatic hormones after meals. These findings would provide new research targets to uncover the role of ZNT8 in T2D development.

Introduction

SLC30A8 (ZNT8) is dominantly expressed in pancreatic beta-cells for transporting zinc from the cytoplasm to insulin-containing secretory vesicles to form insulin crystals (1). Insulin crystallization in secretory vesicles is important for insulin storage and stability (2). Genome-wide association studies (GWAS) have revealed that individuals with a single nucleotide polymorphism (SNP, rs13266634; R325W) in *ZNT8* have increased risk for type-2 diabetes (T2D) by 12-23% depending on races (3–5). A cellular study revealed that the R325 allele increased the zinc transporter activity of ZNT8. Thus, zinc is more enriched in secretory vesicles of beta-cells with the R325 allele of ZNT8 compared to that with W325 (6). However, how does the enrichment of zinc in the insulin-containing secretory vesicles affect the risk of T2D is not fully understood. Later, a GWAS study reported that *ZNT8* allelic insufficiency was associated with a decreased risk of T2D by 65% (7). This observation is consistent with the findings of the SNP rs13266634 R325 variant, which is associated with a higher zinc activity of ZNT8 and the risk of developing T2D. How could a reduced expression of *ZNT8* have a beneficial effect on T2D prevention? To answer this question, I hypothesized that ZNT8 might also be expressed in endocrine cells other than the beta-cell (insulin) or alpha cell (glucagon) (8) and regulate hormone secretion in these endocrine cells, especially those involved in the regulation of glucose metabolism in the gastrointestinal tract. I further hypothesized that reduced glucose-induced insulin secretion due to *ZNT8* allelic insufficiency might trigger compensatory responses of other hormones in regulation of glucose metabolism. Thus, these hormones act in concert to affect changes in the utilization of glucose leading to reduced risk of developing T2D in individuals with *ZNT8* allelic insufficiency.

My research included two parts. The objective of part 1 was to find if any of the glucose metabolism-related hormones, other than insulin and glucagon, be affected by ZNT8. For this

purpose, I performed a feeding trial in mice having different genotypes of *Znt8*, including *Znt8* knockout (KO), heterozygote (het), and the wild-type control (wt). Male mice were fed a high-fat diet (60% kcal fat) for 8 weeks to induce insulin resistance (from 5-13 weeks of age). By doing so, I argued whether *Znt8* heterozygotes would have better glucose tolerance than the control (wt) mice. In addition, blood levels of glucose metabolism-relevant hormones during oral glucose tolerance test would be determined to illustrate which hormone interplayed with *Znt8* allelic insufficiency in mice. As there is no report for *ZNT8*-null mutations in humans, the data obtained from *Znt8* KO mice would also be interesting and useful for understanding the mechanism of zinc action in the body and its association with chronic diseases. I anticipated that the null-mutation of *Znt8* would not trigger a compensatory effect as glucose-induced insulin secretion was largely impaired due to lack of ZNT8 function in beta-cells. Thus, *Znt8* KO mice would be glucose intolerant after 8 weeks in a high-fat diet. On the other hand, *Znt8* het mice would have a better control of glucose levels due to *Znt8* allelic insufficient-induced compensatory reactions, which might lead to a reduction of diabetes' risk. The aim of part 2 was to find out if any of the select hormones involved in glucose metabolism, other than insulin and glucagon in pancreatic islets, would be colocalized with ZNT8. For this purpose, I performed immunofluorescent staining of metabolically relevant endocrine cells in the mouse stomach and duodenum. The results would provide clues for which hormone(s) might be the compensatory target for *Znt8* allelic insufficiency in mice.

Materials and Methods

Study Part 1

Animals and diets

To generate mice with *Znt8*$^{-/-}$, *Znt8*$^{+/-}$ and *Znt8*$^{+/+}$, mice (*Slc30a8*$^{tm1a(KOMP)Wtsi}$, herein *Znt8*$^{+/-}$, and *Znt8*$^{+/+}$ littermates in a mixed background of C57BL/6N and C57BL/6J) were cryo-recovered from the KOMP Repository at the University of California, Davis, California, USA. *Znt8*$^{+/-}$ male mice were crossed to *Znt8*$^{+/+}$ female littermates to produce *Znt8*$^{+/-}$ mice. Brother-sister mating of *Znt8*$^{+/-}$ mice was carried out to generate experimental male mice. Offspring were genotyped as described below. Weaned mice (3 weeks old) were fed a standard laboratory chow diet for 2 weeks. At 5-week-old, mice were fed a high-fat diet (60% kcal fat, lard 91%; soybean oil 9%, D12492, Research Diets, New Brunswick, NJ) and double-distilled water *ad libitum* for two months. All mice were raised in a temperature-controlled room at 22-24^{o}C with a 12 h light-dark cycle. All animal experiments were conducted in accordance with National Institutes of Health Guidelines for the Care and Use of Experimental Animals and were approved by the Institutional Animal Care and Use Committee of the University of California, Davis.

Isolation of genomic DNA and genotyping

Genomic DNA was isolated from mouse tail clips or ear clips using a DNeasy Tissue Kit (Qiagen, Valencia, CA). PCR was used for genotyping according to the protocol provided by the KOMP repository at the University of California, Davis. Primers were as follows: LoxP-forward: 5'-GAGATGGCGCAACGCAATTAAT-3' and *Znt8* KO-reverse: 5'-TGAATGTATGTGTGTGCATGTGTGGG-3'; *Znt8*-forward: 5'-TCAAGATTCAGAATCAGTGTCATCTGG-3' and *Znt8*-tt-reverse: 5'-AGACACCTGATCATGCATTTGCACC-3'. PCR products were visualized by agarose-gel electrophoresis. PCR products yielded from the *Znt8*$^{-/-}$ genomic DNA was 573-bp long while it was 376-bp in size from the wt genome. *Znt8*$^{+/-}$ mice have both size bands.

Oral glucose tolerance test (OGTT) and tissue collection

After 8 weeks on the high-fat diet, mice were fasted overnight before performing the oral glucose tolerance test. Mice were weighed and fasting glucose levels were measured. Mice (from the three *Znt8*$^{-/-}$, *Znt8*$^{+/-}$ and *Znt8*$^{+/+}$ groups) were randomly divided into 2 additional study groups: glucose challenge (test) and saline control. Mice in the test group were gavage-fed glucose solution at the 1.5 g/kg body weight dose. An equal volume of saline was gavage-fed to mice in the control group. Blood glucose levels were determined at 30, 60, and 120 min after glucose administration. Blood (~150 µL) was taken from the submandibular vein at each time point. Saline (150 µL) was injected via the peritoneal cavity right after each blood draw at 0, 30 and 60 min time points to replenish the loss of the blood volume. Insulin and glucagon levels were also determined during OGTT using a mouse Ultra-Sensitive mouse insulin Elisa kit (Crystal Chem. Elk Grove village, IL, USA) and a mouse glucagon ELISA kit (Crystal Chem. Elk Grove village, IL, USA), respectively. Mice were anesthetized right after OGTT. A final blood collection was performed. The stomach and the first centimeter of the duodenum were dissected and snap-frozen in liquid nitrogen or fixed in 4% paraformaldehyde until use. Visceral fat pads and the liver were dissected and weighed. The pancreas was isolated for islet isolation (described below) (9).

Pancreatic islet isolation

Pancreas was put in a 35 mm petri dish on ice and the pancreas was inflated by injection of 3 mL ice-cold collagenase type XI (Sigma, St. Louis, MO) made in 1x HBSS (1.4 mg/mL; 1000 U/mL, Gibco, ThermoFisher Scientific) using an insulin syringe. After incubation of 5 min on ice, the pancreas was minced and transferred into a 50 mL conical tube containing 2 mL collagenase type XI (1.4 mg/mL). The tube was then placed in a water bath at 37^{o}C for ~25 min. The digestion was

shaken by hands every 5 min during incubation until all tissue chunks disappeared. The digestion was terminated by placing the tube on ice and adding 25 mL ice-cold buffer solution (1 mM $CaCl_2$ in 1x HBSS). The digested pancreas was then centrifuged at 290x g (ThermoFisher Scientific Multifuge X1R Refrigerated Centrifuge) for 30 min at 4°C. The supernatant was then discarded. The pellet was washed with 20 mL the same buffer solution as mentioned above by centrifugation. The pellet was resuspended in 15 mL buffer solution again and filtered through a pre-wetted 70 μm cell strainer. The tube was washed with another 20 mL buffer solution and the resulting washing solution passed through the cell strainer again. Finally, the strainer was washed with 25 mL buffer solution. The strainer was turned upside down over a 100 mm petri dish and the captured islets were rinsed off into the petri dish by applying 15 mL cell culture medium (RPMI 1640 medium with 20 mM L-glutamine, 100 U/mL penicillin, 1000 μg/mL streptomycin and 10% fetal bovine serum (FBS)). Islets were then hand-picked under a microscope using a 1000 μL pipette with a wide-open tip. About 10-20 islets were put into a 15 mL conical tube containing 5 mL culture medium and pelleted by centrifugation at 246x g for 2 min at 4°C. The supernatant was discarded. Islets were lysed in 800 μL Trizol solution (ThermoFisher Scientific) and incubated for 5 min on ice. The lysed islets were stored at -80°C until use.

RNA purification, cDNA synthesis, and quantitative RT-PCR

RNA purification

After being defrosted on ice, Trizol solution was spun at 12,000x g at 4°C for 10 min. Supernatant was then transferred to a new Eppendorf tube and 200 μL chloroform was added. Samples were then shaken vigorously for 15 s, incubated at room temperature (RT) for 5 min, and then centrifuged at 12,000x g at 4°C for 15 min. The colorless upper aqueous phase containing RNA

was transferred to a new Eppendorf tube containing 500 µL RNA-grade isopropanol and glycogen (1.5 µl of 15 mg/mL, GlycoBlue™ Coprecipitant, ThermoFisher Scientific). The tube was inverted two times and incubated at RT for 10 min. Samples were then centrifuged at 12,000x g at 4ºC for 10 min. The supernatant was discarded. The pellet was washed with 1 mL 75% ethanol in DEPC water and centrifuged at 12,000x g at 4ºC for 5 min. The supernatant was removed with a micropipette and the pellet was air-dried for 10-15 min with the lid open. The total RNA was dissolved by adding 50 µL DEPC water.

cDNA synthesis

The total RNA concentration was determined using a Thermo Scientific™ Invitrogen™ Nanodrop™ One Spectrophotometer (ThermoFisher Scientific). Total RNA (500 ng) was reverse-transcribed into cDNA using a Maxima first strand cDNA synthesis kit for RT-PCR (ThermoFisher Scientific) according to the manufacturer's instructions.

Quantitative PCR

cDNA was diluted to 5 ng/µL with Ultrapure™ distilled water (Invitrogen, ThermoFisher Scientific). The PCR reaction mix was made in a SsoAdvanced™ universal SYBR green mix (Bio-Rad, Hercules, CA) containing 2 µL of diluted cDNA sample and 1 µL of 5 pmol/ µL forward primer and 1 µL of 5 pmol/ µL reverse primer for a specific gene (see below for the primer sequences). PCR was performed on a Quantstudio™ 7 flex real-time PCR system (Applied biosystems, ThermoFisher Scientific). Primer sequences were as follows: m*Znt8*-RT-Forward: CAAAACTGGACAGCGCATCAA and m*Znt8*-RT-Reverse: GTGATAGATGCCTCCTGCCTC;

m*Sst*-RT-Forward: CTCTGCATCGTCCTGGCTTT and m*Sst*-RT-Reverse: GGCATCATTCTCTGTCTGGT; m*Gcg*-RT-Forward: GACAGAAGCGCATGAGGACC and m*Gcg*-RT-Reverse: TGGCAATGTTGTTCCGGTTC.

The primer sequences were designed using the Primer Design Tool (https://www.ncbi.nlm.nih.gov/tools/primerblast). Primer oligos were synthesized by ThermoFisher Scientific. Melting temperature for each primer pairs were analyzed. Quantitative PCR was run in triplicate and the average cycle number (Ct) was obtained. The amount of the target transcripts was then normalized to the amount of the *Actb* transcripts by subtracting the Ct of the target from the Ct of *Actb* (ΔCt).

Statistical analysis

Sample sizes for the study groups were calculated using G power analysis (Student *t*-test, a, 0.05; effect size, 0.3; power, 0.80; two tails). Results are presented as either mean ± standard deviation (S.D.) or mean ± standard error of the mean (S.E.M). Student's *t*-test was used for analyzing statistical significance. Pearson correlation coefficient was used to calculate p value for correlation analyses between two test groups. Differences were considered to be significant at $p<0.05$ with one tailed distribution.

Study Part 2

Animals and diets

Two male wt mice (C57BL/6N) obtained from the in-house breeding protocol of *Znt8*$^{+/-}$ colonies were maintained on a standard laboratory chow diet (Laboratory Rodent Diet 5001, LabDiet, Brentwood, MO) *ad libitum* and double-distilled water was always supplied. One was euthanized

for tissue collection at fed state and the other was fasted overnight for tissue embedding and conducting immunofluorescent staining to explore potential co-expression of ZNT8 with metabolic hormones and their expression patters in the gut in wt mice. Mice were maintained in a temperature-controlled room at 22-24ºC with a 12 h light-dark cycle. The animal experiment was conducted in accordance with National Institutes of Health Guidelines for the Care and Use of Experimental Animals and were approved by the Institutional Animal Care and Use Committee of the University of California, Davis.

Preparation of Mouse Pylorus and duodenum Tissue Sections

After euthanization, the stomach and the first centimeter of the duodenum were dissected. Pylorus of the stomach and the duodenum were then separated and rinsed with 1x DEPC-PBS. Tissues were fixed in 4% paraformaldehyde (ThermoFisher Scientific, Waltham, MA) overnight. Fixed tissues were then dehydrated in 70% FLEX (Richard-Allan Scientific, Kalamazoo, MI) and placed at 4ºC until further process (detailed method was described in Materials and Methods in Chapter 2). Tissues were embedded in Type 9 paraffin (Richard-Allan Scientific) as previously described (Chapter 2) and sectioned into a thickness of 5 μm sections and stored the sections at RT until further process for immunofluorescent staining.

Antibodies

Antibodies used in this study is summarized in Table 1. Briefly, the guinea pig polyclonal anti-ZNT8 antibody was generated against a synthetic peptide (ASPDSQVVRREIAKALSKSFTM) and has been previously validated (10). The rabbit monoclonal anti-GIP antibody (ab209792) and rabbit polyclonal anti-GLP1 antibody (ab22625) were purchased from Abcam (Waltham, MA).

The GIP antibody was generated against a synthetic human GIP from amino acids (aa) 50-150 while GLP1 antibody was generated against a synthetic human GLP1 from aa 1-19. The rat monoclonal anti-SST antibody (MAB2358) generated against a full-length peptide of human somatostatin was bought from R&D systems (Minneapolis, MN). The rabbit polyclonal anti-SST antibody (hpa019472) produced against a synthetic peptide of the human somatostatin from aa 25-107 was purchased from ATLAS ANTIBODIES (Bromma, Sweden). The rat monoclonal anti-ghrelin antibody (883622) generated against a recombinant mouse ghrelin peptide from aa 24-117 was bought from NOVUS Biologicals (Centennial, CO). Finally, the rabbit polyclonal anti-CCK antibody (ABIN617891) generated against sulfated CCK-8 (aa 26-33) was purchased from antibodies-online (Limerick, PA).

Antibody	Host	Type	Antigen	Company	Catalog No.
ZNT8	Guinea pig	Polyclonal	Synthetic peptide: ASPDSQ-VVRREIAKALSKSFTM	Generated from Huang Lab (10)	N/A
GIP	Rabbit	Polyclonal	Synthetic human GIP aa 50-150	Abcam	ab209792
GLP1	Rabbit	Polyclonal	Human GLP-1 aa 1-19	Abcam	ab22625
SST	Rat	Monoclonal	Human somatostatin	R&D systems	MAB2358
SST	Rabbit	Polyclonal	Human somatostatin aa 25-107	ATLAS ANTIBODIES	hpa019472
Ghrelin	Rat	Monoclonal	Recombinant mouse ghrelin peptide aa 24-117	NOVUS biologicals	883622
CCK	Rabbit	Polyclonal	Sulfated CCK-8 aa 26-33	Antibodies-online	ABIN617891

Table 1. Information for the antibodies used in the study

Immunofluorescent staining

The pylorus and duodenum were deparaffinized in Xylene and rehydrated sequentially using 100%, 70% and 50% FLEX alcohols. Tissue antigen retrieval was accomplished in 10 mM sodium citrate, pH 6.0 at the boiling temperature for 20 min. Cell membrane was permeabilized with 0.4% saponin in 1x PBS for 20 min. Non-specific binding to antibodies were blocked with 3% goat serum in 1x TBS (10 mM Tris-HCL, pH 7.4, containing 0.15 M NaCl with 1% bovine serum albumin (BSA) and 0.05% sodium azide) for 1 h. Primary antibodies were diluted in 1x TBS containing 1% goat serum as follows: ZNT8, 1:100; GIP, 1:100; GLP-1, 1:250; Ghrelin, 1:50; rat anti-SST, 1:25; rabbit anti-SST, 1:50; CCK, 1:100. Secondary goat anti-rabbit, anti-guinea pig, (ThermoFisher Scientific) were diluted at 1:200-250 and anti-rat was diluted at 1:1000 in 1x PBS containing 2% goat serum. The nucleus was stained with DAPI (Vector Laboratories, Burlingame, CA) and mounted with the mounting medium (Vector Laboratories). Stained sections were viewed using a EVOS AL Auto imaging system (ThermoFisher Scientific). Images were acquired using a built-in high-sensitivity CMOS color camera with 40X objectives. Confocal images were acquired using a Leica TCS SP8 STED 3X inverted microscope with a 63X/1.4 oil HC PL APO CS2 lens (Leica Microsystems, Buffalo Grove, IL).

Results

Male mice fed a 60 kcal% fat diet for 8 weeks developed severe glucose intolerance

My previous study (see Chapter 3) demonstrated that *Znt8* allelic insufficiency improves glucose tolerance in male mice fed a diet with 45% kcal from fat. Importantly, I found that decreased glucagon levels during intraperitoneal glucose tolerance test (IPGTT) in mice with *Znt8* allelic insufficiency might be an underlying mechanism for the better regulation of glucose metabolism

during high-fat-induced insulin resistance. To assess whether *Znt8* allelic insufficiency could still exert its beneficial effect on glucose regulation during severely impaired glucose tolerance induced by a very high-fat diet, such as a diet with 60% kcal fat, a cohort of male mice, including *Znt8* het and wt mice as well as *Znt8* KO mice were fed a high-fat diet with 60% kcal from fat (HFD) for 8 weeks starting at 5 weeks of age. I included *Znt8* KO mice in this study with the purpose of examining whether the presence of a functional allele of *Znt8* was essential for the protective effect on glucose control. In addition, I conducted this dietary feeding study only in male mice as it was shown that wt male mice are more prone to high-fat (45% kcal fat)-induced glucose intolerance while female mice were resistant (see Chapter 3, pages 19–20). Thus, it would be apparent if a protective effect was observed in *Znt8* het mice compared to the wt control. Body weights were recorded weekly after the specific diet was introduced. It is worth to note that there was no difference in body weights among three genotypes when mice were at 5 weeks of age. During 8 weeks of HFD feeding, mice were steadily gaining weights. However, all mice gained similar weights regardless of their genotypes (Fig. 1). Additionally, no difference in the weights of the liver and visceral fat pads were observed among the three genotypic groups of mice (Fig 1).

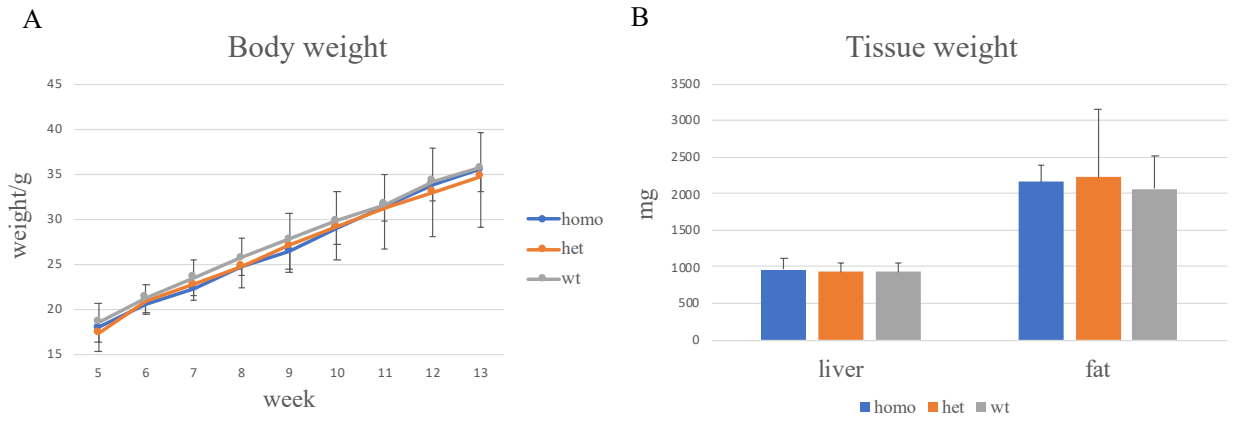

Figure 1. Growth curves and tissue weights at necropsy. A. Growth curves. Body weight (gram) was measured weekly after the introduction of the high-fat diet. B. Weights of the Liver and visceral fat pads. Mice were euthanized 2 h after OGTT at 13 weeks of age (8 weeks on the high-fat diet). Tissues were dissected and weighed at necropsy. Each data point represents the mean±S.D. n=10-12/genotype. homo=*Znt8* KO; het=*Znt8* heterozygote; wt=wild type.

My previous study (Chapter 3) showed that male *Znt8* het mice had a better glucose control after 15-week intake of a high-fat (45% kcal fat) diet than the wt control likely due to a decreased fasting blood glucagon level. Thus, glucagon levels at the fasting state as well as during OGTT were examined. Surprisingly, no difference was noticed in glucagon levels (both fasting and during OGTT) among *Znt8* KO, *Znt8* het and wt mice after 8 weeks on the HFD (60% kcal from fat). Glucagon levels in *Znt8* het mice remained relatively stable during OGTT and gradually reached to the peak 2 h after the glucose administration (Fig. 2A). On the other hand, glucagon levels fluctuated during OGTT in *Znt8* KO and wt mice at the 30 min and 60 min time points, respectively (Fig. 2A). However, no statistical significance was detected at the two time points (30 min, KO vs. wt: p=0.080, KO vs. het: p=0.14, het vs. wt: p=0.23; 60 min, KO vs. wt: p=0.41, KO vs. het: p=0.16, het vs. wt: p=0.074). The fluctuation of circulating glucagon concentrations during OGTT in wt and *Znt8* KO mice hinted that glucose-induced suppression of glucagon secretion was impaired in these mice. In addition, glucagon levels were almost unchanged after the saline load (vehicle) at all 4 time-points examined in all three genotypic groups (Fig. 2B). However, when the glucagon levels during OGTT were adjusted for the saline control, a significant glucose-mediated suppression of glucagon level was observed in *Znt8* het mice at the 30 min time point (p=0.012), which was consistent with our previous study (Chapter 3), whereas glucagon levels in *Znt8* KO and wt mice remained similar to the ones without being adjusted for the saline control (Fig. 2C). These results suggested that stress was a dependent variable for measuring the glucagon levels in *Znt8* het mice during glucose challenge. In this case, the inclusion of a saline control group is essential in order to observe the effect of *Znt8* het on glucagon levels during OGTT. Furthermore, glucagon levels in *Znt8* KO mice did not increase at 2 h after the glucose load as those in *Znt8* het

and wt mice (KO vs. het: p=0.048; KO vs. wt: p=0.00036), suggesting *Znt8* KO mice also had severe impaired glucagon metabolism besides of lack of insulin secretion (8).

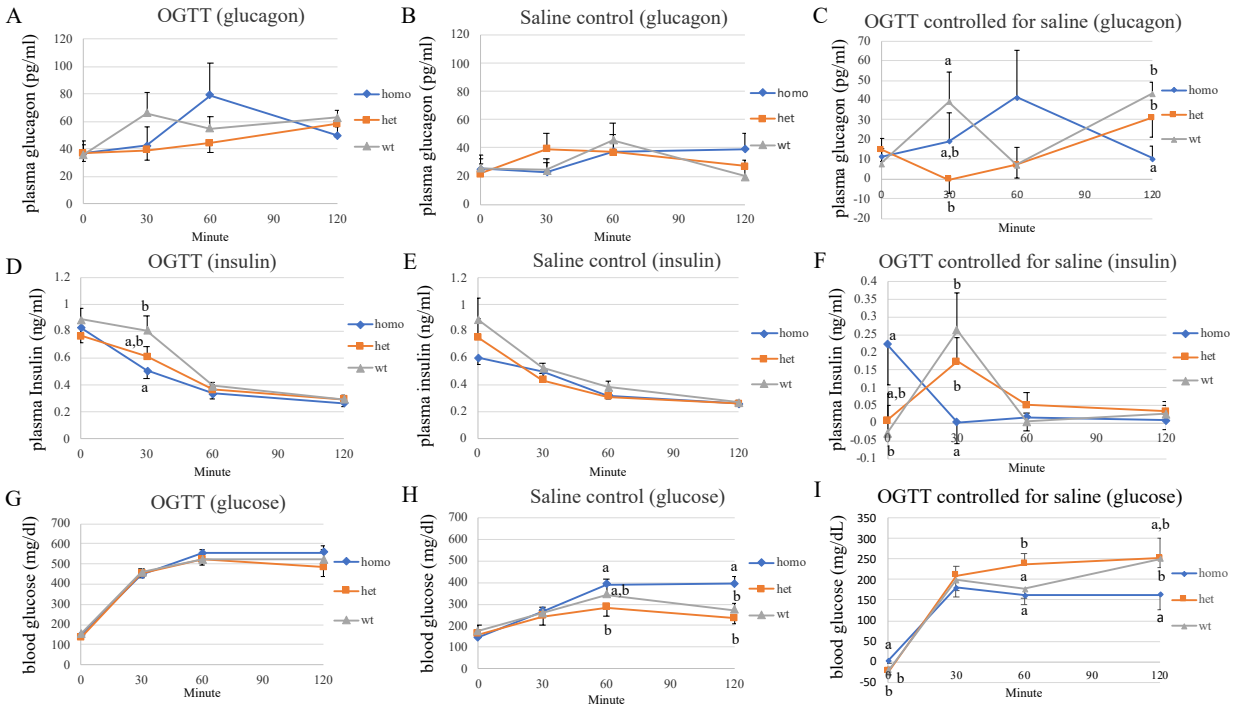

Figure 2. Plasma glucagon, insulin and blood glucose levels during glucose or saline vehicle challenge. A. Glucagon levels during OGTT without adjusting for the saline control. B. Glucagon levels during saline challenge. C. Glucagon levels during OGTT adjusted for the saline control. D. Insulin levels during OGTT without adjusting for the saline control. E. Insulin levels during saline challenge. F. Insulin levels during OGTT adjusted for the saline control. G. Glucose levels during OGTT without adjusting for the saline control. H. Glucose levels during saline challenge. I. Glucose levels during OGTT adjusted for the saline control. Each data point represents the mean±S.E.M. n=10-12/genotype for glucose challenge groups; n=5/genotype for saline groups. The OGTT adjusted for saline groups were calculated by using each value in OGTT per time point per mouse minus the mean value of the saline group per genotype of the corresponding time point. Different letters (a or b) indicate $p<0.05$.

Circulating insulin levels were also examined before and after the glucose challenge. Again, vehicle challenge was performed as a control for the OGTT procedure. As shown in Fig. 2F, after adjusting for the saline control, insulin levels were significantly increased in both *Znt8* het and wt mice in response to the oral glucose stimulation at 30 min ($p<0.05$). But it was not the case for *Znt8* KO mice which insulin levels failed to rise in response to the oral glucose load at 30 min. It is worth to note that the fasting insulin levels was higher in *Znt8* KO mice than wt mice (p=0.038), suggesting increased basal insulin secretion in *Znt8* KO mice likely due to the

compensation for the lack of insulin crystallization. Taken together, *Znt8* KO mice had increased fasting insulin levels, but failed to respond to glucose-induced insulin increase.

As expected, blood glucose levels increased after an oral glucose load during OGTT in all mice regardless of genotypes of *Znt8* (Fig. 2F-G). Interestingly, the average of glucose concentrations of *Znt8* het mice was significantly lower than that of *Znt8* KO at 60 min after the saline challenge ($p<0.040$). The glucose level of the wt control was between the levels of *Znt8* het and *Znt8* KO at the 60 min time point. Moreover, while post-saline glucose levels at 120 min recovered towards the baseline in both *Znt8* heterozygotes and wt mice, it remained on the peak level in *Znt8* KO mice (KO vs. het: $p=0.0026$; KO vs. wt: $p=0.020$), suggesting *Znt8* KO mice had the worst glycemic control during saline challenge than *Znt8* het and wt mice. After adjusting for the saline control, it was noted that *Znt8* KO mice had higher fasting glucose levels than *Znt8* het ($p=0.032$) and wt mice ($p=0.035$). However, during OGTT, *Znt8* KO mice had the lowest glucose levels at 60 min (KO vs. het: $p=0.018$) and 120 min (KO vs. wt: $p=0.017$). On the other hand, *Znt8* het mice had the highest glucose level than both the wt control and *Znt8* KO mice ($p<0.05$) at 60 min and remained significantly higher than *Znt8* KO mice at 120 min. Taken together, *Znt8* het mice had a blunted elevation of blood glucose levels at 60 min after glucose challenge compared to the wt control and *Znt8* KO mice (Fig. 2G), suggesting *Znt8* allelic insufficiency might play a role in control of stress-induced glucose release from tissues, such as the liver and muscle.

mRNA expression of *Znt8* is highly and positively correlated with the expression of glucagon and *Sst*

Insulin-mediated suppression of glucagon secretion is largely facilitated by a paracrine action of SST secreted from the delta-cell in the islet (14). Thus, it is plausible that ZNT8 may also play a

role in regulating SST expression or secretion in delta-cells similar to its action in control of insulin and glucagon secretion (15, 16). Thus, a correlation of *Znt8* mRNA expression with that of *Sst* and glucagon was investigated. As shown in Fig. 3, mRNA expression of both glucagon (R^2=0.75, p=2.43*10^{-4}) and *Sst* (R^2=0.8788, p=6.78*10^{-6}) were highly and positively correlated to the expression of *Znt8* mRNA in isolated islets, which provided the first evidence for a possible role of ZNT8 in regulation of SST production and secretion. Further research is needed for studying the functional link between them.

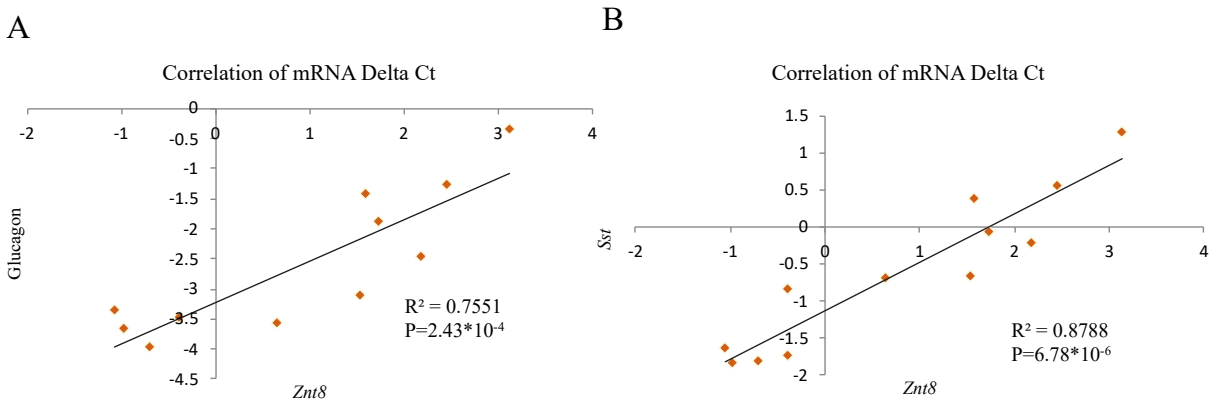

Figure 3. Correlation of mRNA expression of glucagon (A) and *Sst* (B) with *Znt8* in isolated islets. Mice were euthanized right after the OGTT was completed. Pancreas tissues were dissected, and islets were hand-picked for total RNA isolation. Quantitative RT-PCR was used for quantifying gene expression levels. The expression of mouse *Actb* was used as the housekeeping gene for the relative quantification. Delta Ct (ΔCt)=mean Ct of the target gene minus mean of *Actb*; n=12.

ZNT8 colocalizes with SST in delta-cells of the stomach

The positive correlation of *Znt8* and *Sst* mRNA expression was an interesting finding as it is well known that SST is an inhibitory peptide hormone for controlling the secretion of both insulin and glucagon which regulate glucose levels in the circulation (17, 18). SST is expressed in delta-cells located in the islet as well as in the stomach (18). A potential co-expression of ZNT8 protein with SST in the stomach was investigated using immunofluorescent staining. As shown in Fig. 4, ZNT8 was detected in the pylorus of the stomach. Interestingly, the ZNT8 fluorescent stain was co-

localized with the SST peptide in gastric delta cells when a monoclonal SST antibody raised against a full-length of the human SST (preprosomatostatin) was used (Fig. 4A). When a polyclonal SST antibody raised against the amino acids from 25 to 107 (preprosomatostatin without the first 24 and the last 9 amino acids) was used, no overlapping expression of ZNT8 and SST was detected in delta-cells (Fig. 4B). It is known that SST has two active cyclic forms produced by an alternative cleavage of the single preproprotein (19). The N-terminal end of SST (first 24 amino acids) is the signal peptide that directs SST precursors into the secretory pathway of the delta-cell. Then, the signal peptide is cleaved to form prosomatostatin which is further processed into SST28 (containing the last 28 amino acids) and SST14 (containing the last 14 amino acids). Based on the staining results obtained from 2 antibodies used in this study, it is likely that ZNT8 was co-expressed in the delta-cells that expressed either unprocessed preproSST or one of the two forms of matured SST, or both. At the present, I am not able to make a conclusion of which form of SST was co-expressed with ZNT8 in delta-cells. Further immunofluorescent staining is required for precisely determining which form of SST is co-expressed with ZNT8 when an antibody is available and suitable for immunofluorescent staining analysis.

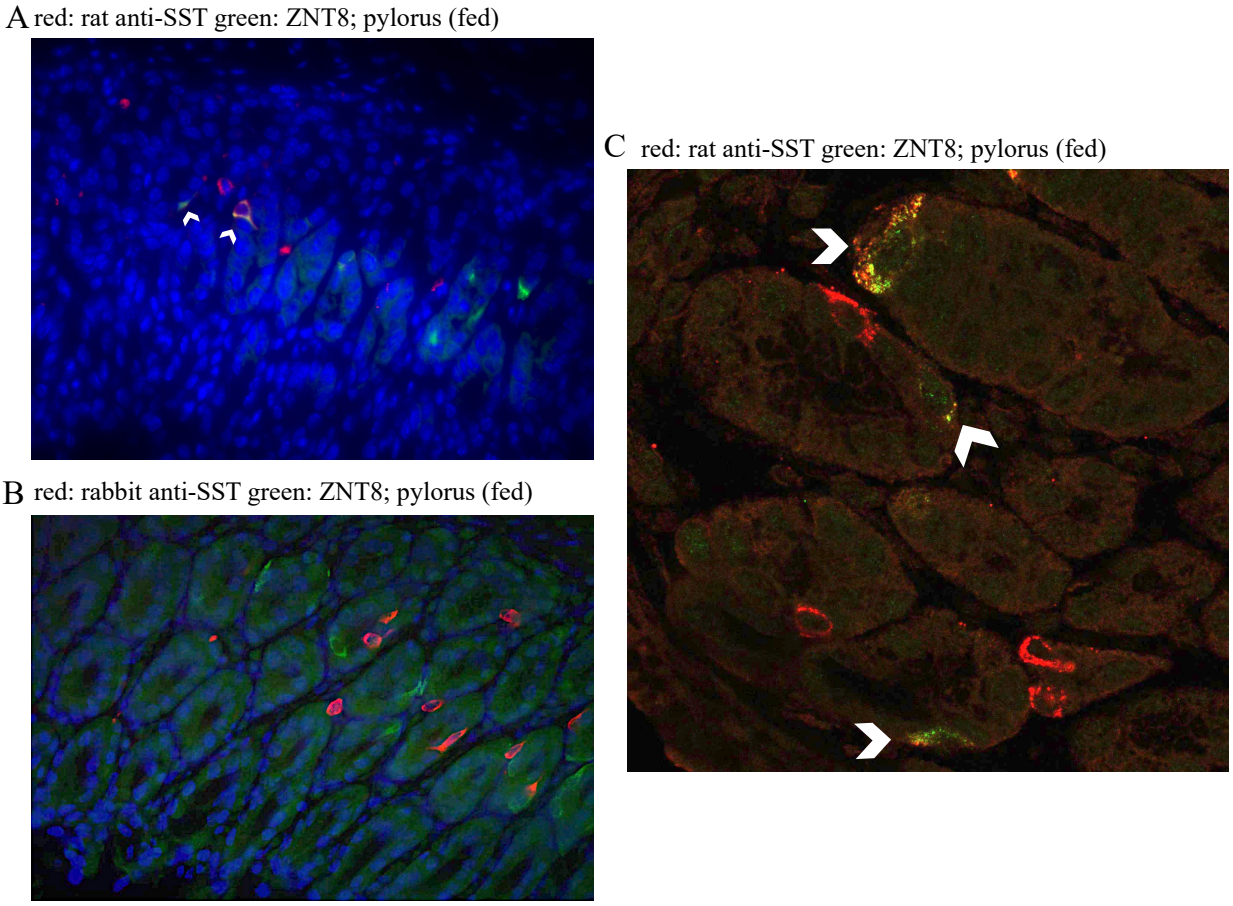

Figure 4. Immunofluorescent staining of SST (red) with ZNT8 (green). A. SST and ZNT8 expression in the delta-cells located in the pylorus of the stomach isolated from mice without fasting. The full length of the SST was detected by a rat monoclonal anti-SST antibody raised against a full length (amino acids 1-116) of the human SST. Both SST and ZNT8 were expressed and co-localized (yellow) in some of delta-cells. 40X. B. Staining of SST and ZNT8 in the pylorus of the stomach detected by a rabbit polyclonal anti-SST antibody raised against amino acids 25-107 of the human SST. This antibody did not detect the co-expression of SST with ZNT8. 40X. C. Confocal image of co-expression of SST with ZNT8. The rat monoclonal anti-SST antibody was used for detecting the full-length of SST. 63X. Open arrows pointed to cells expressed both SST and ZNT8. Yellow or orange indicates the overlapping expression of the two proteins in delta-cells. Again, the co-expression of SST and ZNT8 was only detected in part of delta-cells. Scale bar = 50μm.

Other hormones secreted from endocrine cells in the gut that are involved in controlling metabolic regulations, such as GIP, GLP1, ghrelin, and CCK, were also examined to explore whether co-expression of ZNT8 with these hormones exist in these endocrine cells. As shown in Fig. 5, ZNT8 was not co-expressed with any hormones examined in the mouse duodenum or the stomach.

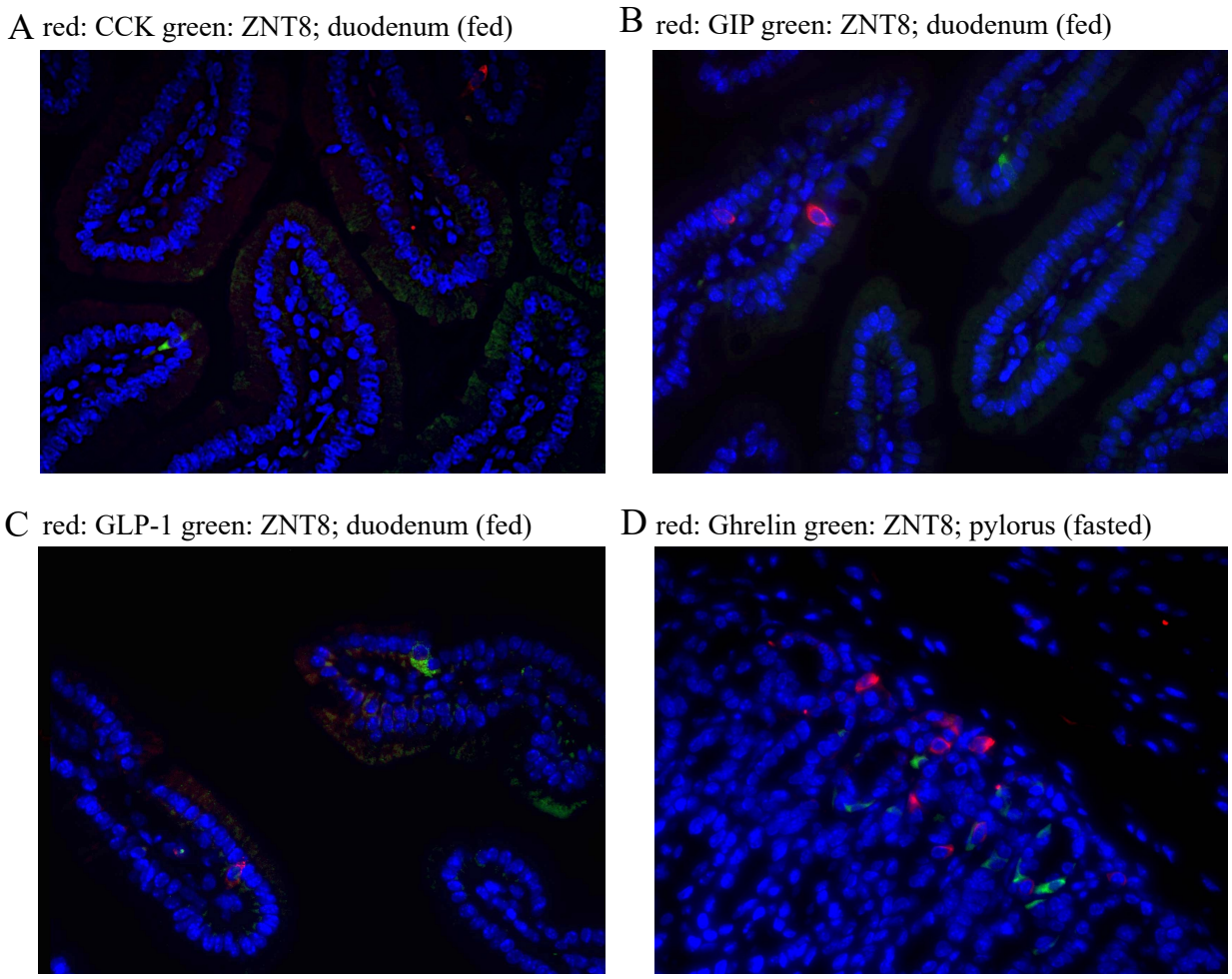

Figure 5. Immunofluorescent staining of hormones in the gut (red) with ZNT8 (green). A. CCK. 40X. B. GIP. 40X. C. GLP1. 40X. Scale bar = 50µm. D. Ghrelin. 40X. None of these hormones colocalized with ZNT8. 63X. Scale bar = 20µm.

Discussion

In this study, I investigated the effect of *Znt8* allelic deficiency and *Znt8*-null on glucose metabolism during HFD-induced insulin resistance. All mice regardless of *Znt8* genotypes had impaired glucose tolerance after 8 weeks on the specific diet. Glucose-induced stimulation of insulin secretion was severely impaired in *Znt8* KO. On the other hand, fasting insulin levels was increased in *Znt8* KO mice compared to the wt control and *Znt8* het. One interesting observation from this study was that the fasting glucagon level as well as glucose tolerance in *Znt8* het mice

remained the same as wt in this study, which is different from the observation where significantly decreased fasting glucagon levels accompanied with better glucose tolerance was detected in the *Znt8* het mice fed a 45% fat diet for 15 weeks (Chapter 3). The plausible reasons may be 1) the current study used a 60% kcal fat-diet to induce a severe glucose tolerance in mice; 2) due to severe insulin resistance, insulin compensation was severely impaired by the lack of insulin responses after the glucose administration in all three genotypic groups leading to no response of glucagon.

However, the het mice in the current study presented a much lower glucagon level at 30 min after oral glucose challenge with adjusting to saline treatment than wt. This finding was consistent with my previous study (Chapter 3) and the two feeding studies in *Znt8* het mice support that reduced glucagon secretion levels could be the key to decrease the risk of type 2 diabetes as hyperglucagonemia is thought to be a causal factor in the pathophysiological development of T2D (20, 21).

It has been shown that fasting insulin levels in *Znt8* KO mice fed a high-fat diet were 4 to 5-fold higher than that in the wt control (16, 22), indicating impaired insulin storage induced by the lack of ZNT8 expression stimulates basal insulin secretion. In the current study, compared to the wt control and *Znt8* het mice and after adjusting for the saline control, it showed that *Znt8* KO mice failed to respond to the glucose stimulator while both wt and *Znt8* het responded and reached to a peak at 30 min after the glucose load. This result suggested that ZNT8 is essential for glucose-stimulated insulin secretion, supported by Chimienti et al. They found that ZNT8-overexpressing INS-1E cells (rat pancreatic beta-cell line) stimulated cellular zinc accumulation accompanied by nearly doubled glucose-stimulated insulin secretion than control (23).

A strong and positive associations of mRNA *Znt8* expression with glucagon was revealed in this study (R^2=0.75, p=2.43*10^{-4}) in islets isolated from the three genotypic mice, suggesting

that ZNT8 is likely involved in glucagon synthesis or secretion in islets. This association is supported by the observation reported by Cauchi et al. in human islets (R^2=0.49, p=4.89*10^{-5}) (24). Most importantly, a significant and positive association between mRNA expression of *Znt8* and *Sst* was found (R^2=0.8788, p=6.78*10^{-6}). This novel finding may serve as the foundation for future studies that aim to investigate the interplays of ZNT8 with insulin, glucagon, and SST in regulation of glucose metabolism and its role in diabetes development or prevention, since SST is an inhibitory peptide hormone for regulating both insulin and glucagon activities during fasting and after meals.

Delta-cells in the islet of both humans and mice reside between alpha- and beta-cells and have extensive contacts with surrounding alpha- and beta-cells by projecting long filopodia-like processes (25). Increased glucose in the pancreas stimulates SST secretion, which in turn binds to SST receptors on the membrane of the beta-cell resulting in the suppression of glucose-induced insulin secretion as well as insulin-stimulated glucagon suppression (26). These paracrine signaling among the islet endocrine cells facilitate the regulation of blood glucose after meals. It is known that variance of interspecies in biology and of architecture of islets exist between rodents and humans. In mice, insulin-secreting beta-cells forming the core of the islet surrounded by other endocrine cells, such as alpha- and delta-cell in the periphery while, in humans, alpha-, beta-cells, and delta-cells are randomly distributed throughout the islet. (27). It is reported that zinc contents in the secretory granules of the delta-cells of mice are at least 10 times lower than the alpha-cells and at least 50 times lower than the beta-cells (28). Moreover, ZNT8 protein can be readily detected in both alpha-cells and beta-cells, but not the delta-cells in the mouse islets (28). On the other hand, in human islets, ZNT8 is expressed in the delta-cells and the granular zinc content in these cells is comparable with that in the beta-cells (28). In humans and rodents, besides of its

residence in the islet, delta-cells also reside in the gastrointestinal tract (GI), especially enriched in the pylorus of the stomach. Two forms of SST are produced in the delta-cells in the gut: SST-14 and SST-28, whereas SST-14 plays a paracrine function, SST-28 is the circulating form of SST and acts remotely, including the pancreatic islets.

The difference of ZNT8 expression between humans and rodents and a positive association of *Znt8* mRNA and *Sst* in the mouse islets (Fig. 3) prompted me to examine the expression of mouse ZNT8 protein expression in the delta-cells in the GI. As expected, ZNT8 could be detected in the delta-cells in the pylorus of the stomach and duodenum (Fig. 4). However, only part of the delta-cells co-expressed with ZNT8, suggesting a heterogeneity of the delta-cells in the gut. Currently, I am unable to distinguish which SST form was co-expressed with ZNT8 in the gastric delta-cells as the 2 commercially available antibodies that I used have some overlapping amino acids (aa) in the antigens that used to raise the antibodies, as shown in Fig 6. The secondary structure of SST-28 has two linkages, one is the bond between serine (aa 89) and phenylalanine (aa 109), the other one is the disulfide bond between two cysteines (aa 105 and aa 116), which may cover the amino acids AGCKN (aa 103-107) and make them undetectable by the rabbit anti-SST polyclonal antibody. In contrast, the amino acids AGCKN of SST-14 remain open to be detected by the rat anti-SST monoclonal antibody. Therefore, ZNT8 might be co-expressed with SST-28, but its co-expression with SST-14 could not be excluded now. Future studies are required for precisely determine which form of SST is co-expressed with ZNT8.

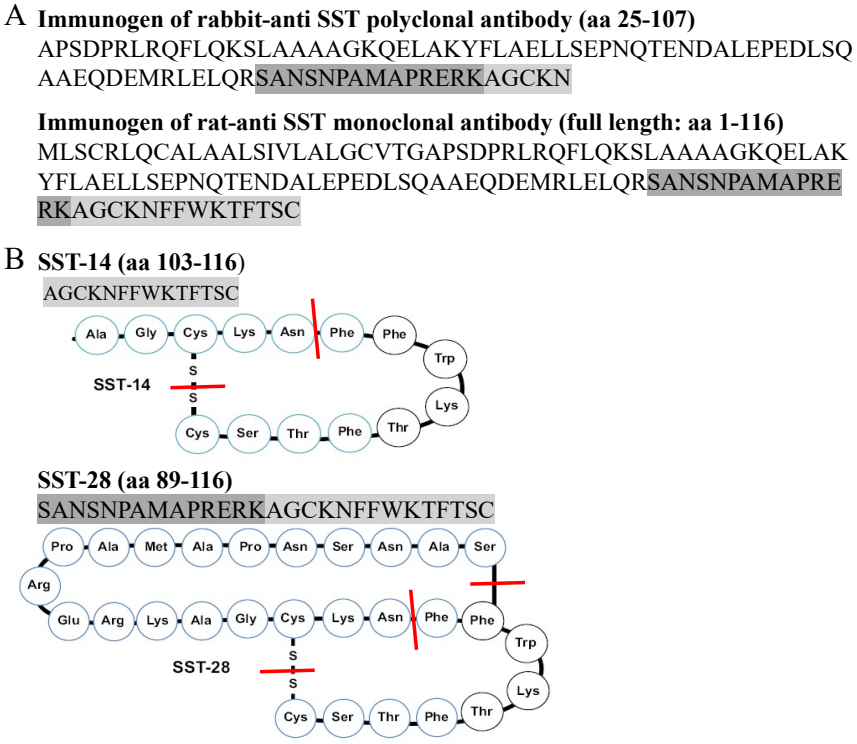

Figure 6. Amino acid (aa) sequences A. aa sequences of immunogens of the two different anti-SST antibodies. B. aa sequences of SST-14 and SST-28 and their cyclic structures. Light grey: aa sequence of SST-14; Dark grey: the first 14 aa of SST-28; Red lines indicate the structures or amino acids cannot be detected by the rabbit polyclonal antibody.

In the stomach, SST inhibits the secretion of an array of chemicals and endocrine hormones, including hydrochloric acid, intrinsic factor, gastrin, ghrelin, and histamine resulting in decreasing the rate of digestion and absorption (29, 30). Bolkent et al. reported that the SST-secreting cell density was higher in the stomach of diabetic rats than normal rats (31). Gavage feeding zinc for 60 days could reverse this effect in diabetic rats suggesting that zinc may play a role in the function of delta cells (31). It is interesting to find that ZNT8 may colocalize with only one type of delta cells, however, there's rarely any research done to relate ZNT8 with SST. Therefore, I made a hypothesis about how ZNT8 regulates only one type of delta cells based on existing evidence, which will be tested in further studies: prosomatostatin is independently cleaved into SST-14 and SST-28 by proprotein convertase PC1/PC2 and furin, respectively (32). Furin

activity can be inhibited by zinc (33), while no such association has been found between PC1/2 and zinc. Therefore, ZNT8 may play a role in regulating SST maturation by affecting the furin enzymatic activity leading to indirect regulation of SST-28 production. Furthermore, in humans, SST-14 was found to have 2-3 folds higher affinity than SST-28 to their receptors SSTR1-4, while SST-28 had 10-30 folds higher affinity to SSTR-5 than SST-14 (34). While all five SSTRs exist in the stomach and pancreas, their expression is cell type-specific (35). In pancreatic islets, SSTR-1 is specifically present in beta-cells and SSTR-2 is specifically expressed in alpha-cells while SSTR-5 is expressed in both beta- and delta-cells (35). Therefore, glucose-induced insulin secretion can be inhibited through SSTR-5 by circulating SST-28 secreted from the GI system. ZNT8 may be involved in this process by affecting the amount of SST-28 production or secretion.

In conclusion, the male *Znt8* KO, het, and wt mice fed a 60% kcal fat-diet for 8 weeks developed severely impaired glucose tolerance associated with greatly impaired glucose-stimulated insulin secretion and glucose-inhibited glucagon secretion. *Znt8* KO mice had the lowest glucose-stimulate insulin level than *Znt8* het and wt mice, consistent with ZNT8's role in crystallization in beta-cells. *Znt8* het had lower glucagon levels than wt 30 min after the oral glucose administration. *Znt8* KO mice, on the other hand, had the lowest adjusted blood glucagon levels than other two genotypic mice 2 h after the glucose load. In addition, *Znt8* het mice had better glycemic control under stress, indicating ZNT8 may play a role in stress-induced glucose release. The results from the current study support the notion that *Znt8* allelic deficiency has a beneficial influence in glucose control during high-fat diet-induced insulin resistance while *Znt8* KO did not. The mechanism underlying the protective effect of *Znt8* allelic insufficiency may lie in the interplay among insulin, glucagon, and somatostatin during insulin resistance.

Due to the influences of COVID-19, several experiments were remained undone, which were important to uncover 1) which SST form is co-expressed with ZNT8 in delta-cells in the gut; 2) whether *Znt8* het or *Znt8* KO influences maturation of SST-28 by affecting furin enzymatic activity; 3) to determine plasma levels of somatostatin, ghrelin, GIP and GLP1 during OGTT; and 4) mRNA levels of *Znt8*, *somatostatin*, *ghrelin*, *Gip*, *Glp1* in the pylorus and duodenum tissues. I believe more clear conclusions will be drawn upon the completion of these experiments.

References

1. Chimienti, F., Devergnas, S., Favier, A., and Seve, M. (2004) Identification and cloning of a β-cell-specific zinc transporter, ZnT-8, localized into insulin secretory granules. *Diabetes*. **53**, 2330–2337
2. Dunn, M. F. (2005) Zinc-ligand interactions modulate assembly and stability of the insulin hexamer - A review. in *BioMetals*, pp. 295–303, **18**, 295–303
3. rs13266634 - SNPedia [online] https://www.snpedia.com/index.php/Rs13266634 (Accessed February 4, 2021)
4. Sladek, R., Rocheleau, G., Rung, J., Dina, C., Shen, L., Serre, D., Boutin, P., Vincent, D., Belisle, A., Hadjadj, S., Balkau, B., Heude, B., Charpentier, G., Hudson, T. J., Montpetit, A., Pshezhetsky, A. V., Prentki, M., Posner, B. I., Balding, D. J., Meyre, D., Polychronakos, C., and Froguel, P. (2007) A genome-wide association study identifies novel risk loci for type 2 diabetes. *Nature*. **445**, 881–885
5. Scott, L. J., Mohlke, K. L., Bonnycastle, L. L., Willer, C. J., Li, Y., Duren, W. L., Erdos, M. R., Stringham, H. M., Chines, P. S., Jackson, A. U., Prokunina-Olsson, L., Ding, C. J., Swift, A. J., Narisu, Hu, T., Pruim, R., Xiao, R., Li, X. Y., Conneely, K. N., Riebow, N. L., Sprau, A. G., Tong, M., White, P. P., Hetrick, K. N., Barnhart, M. W., Bark, C. W., Goldstein, J. L., Watkins, L., Xiang, F., Saramies, J., Buchanan, T. A., Watanabe, R. M., Valle, T. T., Kinnunen, L., Abecasis, G. R., Pugh, E. W., Doheny, K. F., Bergman, R. N., Tuomilehto, J., Collins, F. S., and Boehnke, M. (2007) A genome-wide association study of type 2 diabetes in finns detects multiple susceptibility variants. *Science (80-.).* **316**, 1341–1345
6. Merriman, C., Huang, Q., Rutter, G. A., and Fu, D. (2016) Lipid-tuned Zinc Transport

Activity of Human ZnT8 Protein Correlates with Risk for Type-2 Diabetes. *J. Biol. Chem.* **291**, 26950–26957

7. Flannick, J., Thorleifsson, G., Beer, N. L., Jacobs, S. B. R., Grarup, N., Burtt, N. P., Mahajan, A., Fuchsberger, C., Atzmon, G., Benediktsson, R., Blangero, J., Bowden, D. W., Brandslund, I., Brosnan, J., Burslem, F., Chambers, J., Cho, Y. S., Christensen, C., Douglas, D. A., Duggirala, R., Dymek, Z., Farjoun, Y., Fennell, T., Fontanillas, P., Forsén, T., Gabriel, S., Glaser, B., Gudbjartsson, D. F., Hanis, C., Hansen, T., Hreidarsson, A. B., Hveem, K., Ingelsson, E., Isomaa, B., Johansson, S., Jørgensen, T., Jørgensen, M. E., Kathiresan, S., Kong, A., Kooner, J., Kravic, J., Laakso, M., Lee, J. Y., Lind, L., Lindgren, C. M., Linneberg, A., Masson, G., Meitinger, T., Mohlke, K. L., Molven, A., Morris, A. P., Potluri, S., Rauramaa, R., Ribel-Madsen, R., Richard, A. M., Rolph, T., Salomaa, V., Segrè, A. V., Skärstrand, H., Steinthorsdottir, V., Stringham, H. M., Sulem, P., Tai, E. S., Teo, Y. Y., Teslovich, T., Thorsteinsdottir, U., Trimmer, J. K., Tuomi, T., Tuomilehto, J., Vaziri-Sani, F., Voight, B. F., Wilson, J. G., Boehnke, M., McCarthy, M. I., Njølstad, P. R., Pedersen, O., Groop, L., Cox, D. R., Stefansson, K., and Altshuler, D. (2014) Loss-of-function mutations in SLC30A8 protect against type 2 diabetes. *Nat. Genet.* **46**, 357–363
8. Solomou, A., Meur, G., Bellomo, E., Hodson, D. J., Tomas, A., Migrenne Li, S., Philippe, E., Herrera, P. L., Magnan, C., and Rutter, G. A. (2015) The Zinc Transporter Slc30a8/ZnT8 Is Required in a Subpopulation of Pancreatic α-Cells for Hypoglycemia-induced Glucagon Secretion. *J. Biol. Chem.* **290**, 21432–21442
9. Li, D. S., Yuan, Y. H., Tu, H. J., Liang, Q. Le, and Dail, L. J. (2009) A protocol for islet isolation from mouse pancreas. *Nat. Protoc.* **4**, 1649–1652
10. Huang, L., and Kirschke, C. P. (2016) Down-Regulation of Zinc Transporter 8 (SLC30A8)

in Pancreatic Beta-Cells Promotes Cell Survival. *Austin J Endocrinol Diabetes*. **3**, 1037

11. Macotela, Y., Boucher, J., Tran, T. T., and Kahn, C. R. (2009) Sex and Depot Differences in Adipocyte Insulin Sensitivity and Glucose Metabolism. *Diabetes*. **58**, 803–812
12. Teppala, S., and Shankar, A. (2010) Association between serum IGF-1 and diabetes among U.S. adults. *Diabetes Care*. **33**, 2257–2259
13. Kautzky-Willer, A., Harreiter, J., and Pacini, G. (2016) Sex and gender differences in risk, pathophysiology and complications of type 2 diabetes mellitus. *Endocr. Rev.* **37**, 278–316
14. Elliott, A. D., Ustione, A., and Piston, D. W. (2014) Somatostatin and insulin mediate glucose-inhibited glucagon secretion in the pancreatic α-cell by lowering cAMP. *Am. J. Physiol. Metab.* **308**, E130–E143
15. Hardy, A. B., Serino, A. S., Wijesekara, N., Chimienti, F., and Wheeler, M. B. (2011) Regulation of glucagon secretion by zinc: lessons from the β cell-specific Znt8 knockout mouse model. *Diabetes, Obes. Metab.* **13**, 112–117
16. Nicolson, T. J., Bellomo, E. A., Wijesekara, N., Loder, M. K., Baldwin, J. M., Gyulkhandanyan, A. V., Koshkin, V., Tarasov, A. I., Carzaniga, R., Kronenberger, K., Taneja, T. K., Da Silva Xavier, G., Libert, S., Froguel, P., Scharfmann, R., Stetsyuk, V., Ravassard, P., Parker, H., Gribble, F. M., Reimann, F., Sladek, R., Hughes, S. J., Johnson, P. R. V., Masseboeuf, M., Burcelin, R., Baldwin, S. A., Liu, M., Lara-Lemus, R., Arvan, P., Schuit, F. C., Wheeler, M. B., Chimienti, F., and Rutter, G. A. (2009) Insulin storage and glucose homeostasis in mice null for the granule zinc transporter ZnT8 and studies of the type 2 diabetes-associated variants. *Diabetes*. **58**, 2070–2083
17. Koerker, D. J., Ruch, W., Chideckel, E., Palmer, J., Goodner, C. J., Ensinck, J., and Gale, C. C. (1974) Somatostatin: Hypothalamic inhibitor of the endocrine pancreas. *Science*

(80-.). **184**, 482–484

18. Arimura, A., Sato, H., Dupont, A., Nishi, N., and Schally, A. V. (1975) Somatostatin: Abundance of immunoreactive hormone in rat stomach and pancreas. *Science (80-.).* **189**, 1007–1009

19. Mouchantaf, R., Patel, Y. C., and Kumar, U. (2004) SOMATOSTATIN. in *somatostatin* (Srikant, C. B. ed), pp. 17–28, Montreal, Quebec

20. Godoy-Matos, A. F. (2014) The role of glucagon on type 2 diabetes at a glance. *Diabetol. Metab. Syndr.* **6**, 91

21. Unger, R. H., and Orci, L. (1975) THE ESSENTIAL ROLE OF GLUCAGON IN THE PATHOGENESIS OF DIABETES MELLITUS. *Lancet*. **305**, 14–16

22. Hardy, A. B., Wijesekara, N., Genkin, I., Prentice, K. J., Bhattacharjee, A., Kong, D., Chimienti, F., and Wheeler, M. B. (2012) Effects of high-fat diet feeding on Znt8-null mice: Differences between β-cell and global knockout of Znt8. *Am. J. Physiol. - Endocrinol. Metab.* **302**, E1084-96

23. Chimienti, F., Devergnas, S., Pattou, F., Schuit, F., Garcia-Cuenca, R., Vandewalle, B., Kerr-Conte, J., Van Lommel, L., Grunwald, D., Favier, A., and Seve, M. (2006) In vivo expression and functional characterization of the zinc transporter ZnT8 in glucose-induced insulin secretion. *J. Cell Sci.* **119**, 4199–4206

24. Cauchi, S., Guerra, S. Del, Choquet, H., D'Aleo, V., Groves, C. J., Lupi, R., McCarthy, M. I., Froguel, P., and Marchetti, P. (2010) Meta-analysis and functional effects of the SLC30A8 rs13266634 polymorphism on isolated human pancreatic islets. *Mol. Genet. Metab.* **100**, 77–82

25. Drigo, R. A. e, Jacob, S., García-Prieto, C. F., Zheng, X., Fukuda, M., Nhu, H. T. T.,

Stelmashenko, O., Peçanha, F. L. M., Rodriguez-Diaz, R., Bushong, E., Deerinck, T., Phan, S., Ali, Y., Leibiger, I., Chua, M., Boudier, T., Song, S.-H., Graf, M., Augustine, G. J., Ellisman, M. H., and Berggren, P.-O. (2019) Structural basis for delta cell paracrine regulation in pancreatic islets. *Nat. Commun. 2019 101*. **10**, 1–12

26. Rorsman, P., and Huising, M. O. (2018) The somatostatin-secreting pancreatic δ-cell in health and disease. *Nat. Rev. Endocrinol.* **14**, 404

27. DJ, S., A, K., K, M., and M, H. (2010) Pancreatic islet plasticity: interspecies comparison of islet architecture and composition. *Islets*. 10.4161/ISL.2.3.11815

28. Ghazvini Zadeh, E. H., Huang, Z. J., Xia, J., Li, D., Davidson, H. W., and Li, W. hong (2020) ZIGIR, a Granule-Specific Zn2+ Indicator, Reveals Human Islet α Cell Heterogeneity. *Cell Rep.* **32**, 107904

29. Mani, B. K., and Zigman, J. M. (2015) A strong stomach for somatostatin. *Endocrinology*. **156**, 3876–3879

30. Krejs, G. J. (1986) Physiological role of somatostatin in the digestive tract: Gastric acid secretion, intestinal absorption, and motility. *Scand. J. Gastroenterol.* **21**, 47–53

31. Bolkent, S., Bolkent, S., Yanardag, R., Mutlu, O., and Yildirim, S. (2006) Alterations in somatostatin cells and biochemical parameters following zinc supplementation in gastrointestinal tissue of streptozotocin-induced diabetic rats. *Acta Histochem. Cytochem.* **39**, 9–15

32. YC, P., and A, G. (1995) Processing and intracellular targeting of prosomatostatin-derived peptides: the role of mammalian endoproteases. *Ciba Found. Symp.* 10.1002/9780470514733.CH3

33. P, P., T, K., RS, F., and O, B. (2004) Furin inhibition by compounds of copper and zinc. *J.*

Biol. Chem. **279**, 36219–36227

34. Patel, Y. C., Greenwood, M. T., Panetta, R., Demchyshyn, L., Niznik, H., and Srikant, C. B. (1995) The somatostatin receptor family. *Life Sci.* **57**, 1249–1265

35. Barnett, P. (2003) Somatostatin and Somatostatin Receptor Physiology. *Endocrine*. **20**, 255–264